Electronic Supplementary Material (ESI) for ChemComm.

Electronic Supplementary Information

Switching enzyme specificity from phosphate to resveratrol glucosylation

Michael Kraus, Clemens Grimm, Jürgen Seibel

Correspondence to: seibel@chemie.uni-wuerzburg

clemens.grimm@biozentrum.uni-wuerzburg.de

This PDF file includes:

Electronic Supplementary Information outline

1. Materials and Methods

1.1 Materials

Resveratrol-3-α-D-glucoside was produced and purified following the previously reported method.[1] Nigerose was produced and purified following the previously reported method.[2] All other chemicals were purchased from Sigma-Aldrich or VWR. Ni-NTA resin was a product of Sigma Aldrich, PCR primers were ordered from Sigma-Aldrich. Mutagenesis was performed applying the QuikChange II Site-Directed Mutagenesis Kit from Agilent.

1.2 Production of nigerose (as previously described)[2]

In a total volume of 10 ml, sucrose (400 mM) was supplemented with glucose (200 mM) in MOPS-NaOH buffer (20 mM, pH 7) and 30% (v/v) DMSO. 1.0 mL of BaSP Q345F (5 mg/mL, activity: 62 U/g) was added and the reaction was incubated at 37 °C under slow agitation. After 4 d (90% sucrose consumption) the reaction was stopped by the addition of 20 mL MeOH. The occurring precipitate was removed by centrifugation (10 min, 6000 g). After evaporation of the solvent and freeze-drying, the residual syrup was supplemented with 50 mL water and baker's yeast (immobilized on calcium alginate beads, 20 beads). The consumption of sugars at 20 °C was monitored by HPAEC After reaction completion, the baker's yeast was removed by filtration and the solvent was removed by freeze-drying. Silica gel chromatography (0.063-0.200 mm, MeCN/MeOH = 4:1) yielded pure nigerose (430 mg, 24%).

1.3 Production, isolation and characterization of glucosylated polyphenols

Ca. 1.66 – 4.38 mmol polyphenol were dissolved in 20 mL 30% (v/v) DMSO containing 100 mM MOPS-NaOH-buffer pH = 7 and 1.1 M sucrose and 40 mg BaSP Q345F. After 64 h at 50 °C the reaction was stopped by incubating the reaction mixture at 95 °C for 15 min. The solvent was removed under reduced pressure and the crude product was purified by column chromatography (silica, ethyl-acetate : methanol 12:1 -> water : isopropanol : ethyl-acetate 1:3:6). These reactions were performed to obtain sufficient amounts of glucosylated product for characterization, and not optimized for maximum conversion.

Yields:

233 mg naringenin-7-α-D-glucoside (27%)

323 mg fisetin-3'-α-D-glucoside (42%)

400 mg glucosylated quercetin (mixture of quercetin-3'-α-D-glucoside, quercetin-7'-α-D-glucoside and quercetin-3',7-α-D-diglucoside, 48%)

936 mg catechin-3'-α-D-glucoside (53%) 236 mg catechin-3',5-α-D-diglucoside (10%)

103 mg epicatechin-3'-α-D-glucoside (12%) 274 mg mixture of epicatechin-3'-α-D-glucoside and epicatechin-5'-α-D-glucoside (31%), epicatechin-3',5-α-D-diglucoside (20%)

1.19 g resveratrol-3-α-D-glucoside (70%)

1.4 Acetylation of Quercetin-3',7-α-D-diglucoside

12.5 mg (20 μmol) of Quercetin-3',7-α-D-diglucoside and 50.1 mg (0.490 mmol) acetic anhydride were dissolved in 1.0 mL pyridine and stirred overnight at room temperature. Then 10 mL of water was added, and after 30 minutes of stirring the reaction mixture was extracted 3x with 10 mL ethylacetate. The combined organic layers were washed (3x 10 mL 1M HCl, 2x 10 mL saturated $CuSO_4$-solution, 1x 10 mL brine) and the solvent removed under reduced pressure to yield 22.1 mg (17.4 μmol, 87%) Quercetin-3',7-α-D-diglucoside-undecaacetate.

1.5 Cloning expression and purification of BaSP wt, BaSP Q345F and BaSP D192N/ Q345F

Freeze-dried cultures of *B. adolescentis* (DSMZ 20083) were obtained from DSMZ (Deutsche Sammlung von Mikroorgansimen und Zellkulturen GmbH), and grown under anaerobic conditions in DSMZ medium Nr.58 without resazurin. Cells were harvested and the genomic DNA isolated, using a GenJet Genomic DNA purification Kit (Thermo Fisher). The BaSP gene was amplified from genomic DNA using the primers

5'-ATAACCATGGCTATGAAAAACAAGGTGCAGCTCATCAC-3' and 5'-CAATCCGCCTGTCGTCGCCCTCGAGTAAT-3'. The amplicon was inserted into pET-28b(+) using the NcoI and XhoI restriction sites yielding plasmid pET-28b(+)-BaSP-wt.

1.6 Construction of BaSP Q345F

The Q345F mutation was constructed applying the Megaprimer method. The mutagenic primers 5'-CCAATCTCGACCTCTACTTCGTCAACAGCACCTAC-3', and 5'-CAATCCGCCTGTCGTCGCCCTCGAGTAAT-3' were used for the creation of the megaprimer and 5'-ATAACCATGGCTATGAAAAACAAGGTGCAGCTCATCAC-3' was used for the second PCR. Cloning and purification of the variant followed the procedure described for the wildtype.

1.7 Construction of BaSP D192N/Q345F

The D192N exchange was achieved with the QuikChange II Site-Directed Mutagenesis Kit from Agilent following the manufacturer's protocol. The mutagenic primers were 5'-CTACATCCGCCTCAACGCCGTCGGC-3' and 5'-CCGACGGCGTTGAGGCGGATGTAG-3'.

1.8 Cloning Expression and Purification BaSP variants

E. coli Bl21 star™ cells were heat shock transformed with plasmid pET-28b(+)-BaSP-wt. Overnight cultures of the transformed host in LB-medium containing 50 mg/L kanamycin sulfate were grown and 1.8 mL was used to inoculate 250 mL of LB-medium (50 mg/L kanamycin sulfate). The cultures were incubated at 37 °C and 180 rpm until they reached an OD600 of 0.6, at which point the temperature was adjusted to 19 °C and IPTG was added to a final concentration of 0.5 mM. The cells were grown for additional 18 hours after which they were harvested by centrifugation (4000 g for 10 min). The sediment was resuspended in lysis buffer (60 mM phosphate, 250 mM NaCl, 11 mM imidazol, 5 mM β-mercaptoethanol pH=8 pH was adjusted before the addition of β-mercaptoethanol and imidazole via NaOH). Cells were lysed using a sonicator and centrifuged at 17000 g for 10 min at 4 °C. The lysate was loaded onto 0.5 mL Ni-NTA columns equilibrated with lysis buffer and incubated at 4 °C and slow rotation for a minimum of 2 hours. The column was washed with 2.5 mL of lysis buffer and the protein was eluted with 1.5 mL of elution buffer (60 mM phosphate, 250 mM NaCl, 230 mM imidazol, 5 mM β-

mercaptoethanol pH=8, pH was adjusted before the addition of β-mercaptoethanol and imidazole via NaOH). The buffer was exchanged to 20 mM MOPS-NaOH-buffer (pH=7) using 5 mL Hi-Trap columns from GE Healthcare.

1.9 Crystallization, soaking data collection

Crystals were grown using the hanging drop method. 4-20 g/L Protein solution were mixed with precipitant solution containing PEG 8000 (20-30% (w/v)), NaCl (200 mM) and Tris-HCl-buffer (pH= 7-8, 100 mM). Crystals were grown for 10 weeks at 16 °C up to a size of 0.05x0.04x0.08 mm. Crystals were then transferred to cryo solution containing PEG 1500 (30%(w/v)), glycerol (20%(w/v)) NaCl (200mM) Tris-HCl-buffer (100 mM pH=8) and resveratrol-3-α-D-glucoside or nigerose (100 g/L) and soaked over night, mounted in cryo loops and plunged into liquid nitrogen. At beamline ID30B of the ESRF Grenoble the mounted crystals were placed within a 100K nitrogen gas stream and datasets were collected over 180° oscillation range. The datasets were auto indexed, integrated and scaled with XDS.

1.10 Structure determination and -refinement

The structures of apo SP and the two complexes were solved by molecular replacement using chain B of PDB entry 2GDV as a search model within PHASER.[3] After initial refinement within Phenix,[4] regions with distinct conformational changes were manually rebuilt within COOT[5] and the appropriate ligands were modelled into the active site. After three more rounds of automated refinement and manual rebuilding including water and ligand placement, the R and R_{free} factors converged. Two conformations were modeled for Glu232 in PDB 5M9X as it displays a degree of flexibility. This is likely due to a subpopulation of ligand free protein molecules. Of note, several residues residing in β-turn regions appeared close to the border of or within the disallowed region of the Ramachandran plot. After inspection of the surrounding electron density we conclude that these are true outliers, most likely in a stressed conformation.

1.11 Data collection and refinement statistics

Table S 1 Data collection and refinement statistics.

	Resveratrol	*Nigerose*	*Apo*
PDB ID	5M9X	5MAN	5MB2
Wavelength [Å]	0.97625	0.97625	0.97625
Resolution range	47.06 - 2.349	43.75 - 2.04	43.57 - 1.752
Space group	P 43 21 2	P 43 21 2	P 43 21 2
Unit cell (a, b, c, α, β, γ) [Å, Å, Å, °, °, °]	83.1, 83.1, 157.2, 90.0. 90.0. 90.0	82.4, 82.4, 154.9, 90.0. 90.0. 90.0	82.9, 82.9, 153.6, 90.0. 90.0. 90.0
Total reflections	157373 (14977)	277167 (26255)	692483 (67202)
Unique reflections	23334 (2273)	34768 (3400)	54566 (5326)
Multiplicity	6.7 (6.6)	8.0 (7.7)	12.7 (12.6)
Completeness [%]	98.0 (97.0)	99.9 (99.9)	99.9 (99.0)
Mean I/sigma(I)	20.88 (0.96)	23.69 (1.60)	24.36 (1.69)
Wilson B-factor	67.88	48.91	30.56
R-merge	0.05327 (1.945)	0.04394 (1.366)	0.06463 (1.619)
Reflections used in refinement	23328 (2273)	34766 (3400)	54556 (5323)
R-work	0.2575 (0.4161)	0.2349 (0.3726)	0.1974 (0.3375)
R-free	0.2847 (0.4017)	0.2616 (0.3764)	0.2323 (0.3679)
Number of non-hydrogen atoms	4038	4103	4309
macromolecules	3975	3966	3983
Ligands	28	23	6
Solvent	35	114	320
Protein residues	504	504	504
RMS(bonds) [Å]	0.003	0.003	0.004
RMS(angles) [°]	0.61	0.56	0.63
Ramachandran			
favoured [%]	97.0	96.2	97.4
allowed [%]	2.6	3.6	2
outliers [%]	0.4	0.2	0.6
Clashscore	2.2	1.2	4.0
Average B-factor [Å^2]	99.8	60.4	49.4
Macromolecules	100.1	60.6	49.8
Ligands	80.4	75.1	60.7
Solvent	88.6	49.9	44.5

Statistics for the highest-resolution shell are shown in parentheses.

1.12 Determination of the active site volume

The active site volume was determined with CAVER-Analyst 1.0 using the settings:

Outer Probe Radius: 2.29 Å

Inner Probe Radius: 1.80 Å

1.13 Determination of kinetic parameters

Activity assays were performed at 37 °C in 50 mM MOPS-NaOH-buffer at pH=7 in at total volume of 100 µL containing 30% (v/v) DMSO, 50 mM of sucrose and 0.219 g/L BaSP Q345F or 0.307 mg/L (sucrose parameters) and 1.22 mg/L (phosphate parameters) BaSP wild type respectively. The acceptor molecules were added to obtain appropriate concentrations and samples of either 10 or 20 µL were taken at the appropriate timepoints, diluted with 230 to 490 µL water and the reaction was stopped by heating the samples at 95 °C for 6 minutes. Product formation was determined via HPAEC-PAD (High performance anion exchange chromatography with pulsed amperometric detection) by comparing the amount of glucose and fructose released, in the case of aromatic acceptors and phosphate and direct determination in the case of glucose used as an acceptor. This was necessary, since the glucosylated aromats cannot be directly detected at the concentrations occurring in the applied assay. All experiments were performed in triplicates.

1.14 Determination of yields

Reactions were performed in triplicates at 50 °C and contained 600 mM sucrose 100 mM MOPS-NaOH-buffer at pH=7, 30% (v/v) DMSO and 4.0 g/L BaSP Q345F in a final volume of 200 µL. Acceptor concentrations were 100 mM (-)-epicatechin and (+)-catechin, 75 mM resveratrol. 50 mM fisetin and quercetin and 25 mM ((rac)-naringenin). 10 µL samples were diluted with 190 µL of water and inactivated at 95 °C for 5 minutes and diluted in 1 mL MeOH:water (final concentration 50% (v/v) MeOH), and subjected to HPLC-Analysis. Yields were calculated using the total area under all peaks to include trace products that cannot be isolated.

1.15 HPLC-Methods

Conversions of polyphenols were determined on analytical scale using a YMC-ODS-AQ column (C_{18} column; 5 µm, 4.6×250 mm) and a Sykam S3345 detector for resveratrol separation.

(-)-Epicatechin, (+)-catechin and its glucosylated derivatives were resolved using a linear ternary gradient programmed as follows: solvent A: 0.1% (v/v) TFA, B: acetonitrile, C: 20 mM $NH_4H_2PO_4$: 0 to 10 min 4% B 50% C, 25 min 28% B, 50% C, 27to 35 min 4% B 50% C. The flow rate was set to 1.0 mL/min and the detection wavelength to 220 nm.
(+)-Catechin-5-glucoside and catechin-3'-5-diglucoside were resolved using a linear ternary gradient programmed as follows: solvent A: 0.1 % (v/v) TFA, B: acetonitrile, C: 20 mM $NH_4H_2PO_4$: 0 to 1 min 4% B 50% C, 12 min 31% B, 50% C, 12 to 13 min 31% B, 50% C 14 to 21 min 4% B 50% C. The flow rate was set to 1.0 mL/min and the detection wavelength to 220 nm.

(rac)-naringenin and its glucosylated compound were resolved using a linear binary gradient programmed as follows: solvent A: 0.1% (v/v) TFA, B: MeOH with 0.1% (v/v) TFA 0 to 3 min

40% B, 18 min 65% B, 19 to 25 min 40% B The flow rate was set to 1.0 mL/min and the detection wavelength to 220 nm.

Quercetin, Fisetin and their glucosylated compounds using a linear binary gradient programmed as follows: Solvent A: 20 mM $NH_4H_2PO_4$, Solvent B Acetonitrile. 0 to 5 min 10% B, 20 min 25% B, 21 to 25 min 50% B, 26 to 35 min 10%B. The flow rate was set to 1.0 mL/min and the detection wavelength to 320 nm.

Resveratrol and its glucosylated derivatives were resolved during 20 minutes using 65% of 0.1% TFA and 65% Acetonitrile for B, 20 min. The flow rate was set to 0.8 mL/min and the detection wavelength to 250 nm.

1.16 HPAEC-PAD Methods

HPAEC-PAD analysis was performed with a Dionex ICS-5000+ SP system utilizing a Carbopac PA10 column. Eluents were 100 mM NaOH (A), 100mM NaOH, 1 M NaOAc (B), 10 mM NaOH (C) and 250 mM NaOH (D).

Samples containing (+)-catechin and (-)-epicatechin and their glucosylated derivatives were resolved using a multistep gradient programmed as follows: 0 min to 9 min 100% A, flow = 0.25 mL/min, 10 min 100% B flow = 0.25, 11 min 100% B flow = 0.40. 11 min to 25 min 100% B flow = 0.4 mL/min, 25 min to 35 min 100% D flow = 0.4 mL/min, 35 min to 41 min 100% A flow = 0.4 mL/min, 41 min to 42 min 100% A flow = 0.25 mL/min, 42 min to 45 min 100% A flow = 0.25 mL/min.

Samples containing phosphate and glucose-1-α-D-phosphate were resolved using a multistep gradient programmed as follows: 0 to 5 min 100 A flow = 0.25 mL/min, 20 to 20.5 min 70% A, 30 % B flow = 0.25 mL/min, 21 min to 23 min 100% D flow = 0.5 mL/min, 23 min to 27.5 min 100% A flow = 0.5 mL/min, 28 min to 30 min 100% A flow = 0.25 mL/min.

Glucose concentration of samples containing fisetin or quercetin were resolved using a multistep gradient programmed as follows: the amount of solution A was raised nonlinear, using curve 9 from 5% A and 95% C to 100% A 20 minutes. 20 to 26 min 100% A, 26 to 32 min 5% A and 95% C. The flow was set to 0.25 mL/min.

Fructose concentrations of samples containing fisetin and quercetin and fructose and glucose concentrations of samples containing naringenin and resveratrol were determined under isocratic conditions with 100% A and a flow of 0.25 mL/min for 16 min.

Maltose and nigerose concentrations were determined under isocratic conditions with 97% A 3% B and a flow of 0.25 mL/min for 16 min.

1.17 Determination of the resveratrol-enzyme interface

The area of the interface between the resveratrol moiety and BaSP Q345F was determined using the PISA-server. For this purpose all atoms of the carbohydrate moiety were manually deleted before submitting the pdb-file.

2 Additional Figures

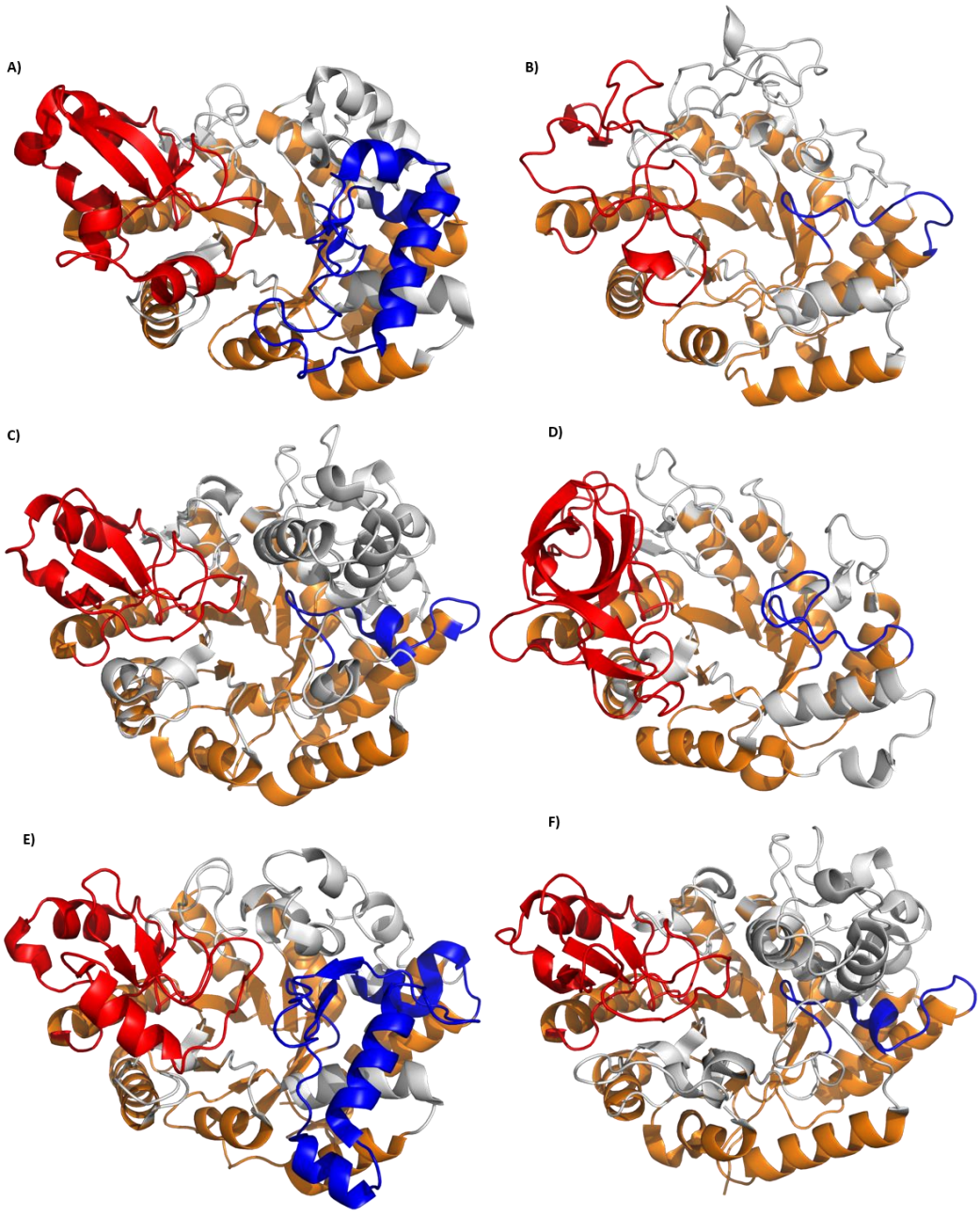

Fig. S 1

Alignment of various GH13 enzymes, viewing on top of the C-terminal end of the TIM barrel (orange); The domain/loop between β-sheet3 and α-helix3 is coloured in red. This domain/loop is domain b in BaSP. The domain/loop between β-sheet7 and α-helix7 is coloured in blue. This domain/loop is domain b' in BaSP. The remaining domains/loops between β-sheet and α-helix are shown in grey. The five selected GH13 enzymes contain a large domain in place of BaSP's domain b. While only the amylosucrase contains a structurally related b'-domain the remaining biocatalysts contain large domains that are possible subjects to a domain shift. For clarity reasons N-

and C-terminal domains located at the N-terminal end of the TIM-barrel are not shown, as they are not part of the active site.

A) 2gdv, Sucrose Phosphorylase from *Bifidobacterium adolsecentis*
B) 1a47, CGTase from *Thermoanaerobacterium thermosulfurigenes*
C) 2zid, Dextran glucosidase from *Streptococcus mutans*
D) 3bh4 Alpha-amylase from *Bacillus amyloliquefaciens*
E) 3ueq Amylosucrase from *Neisseria polysaccharea*
F) 4how: Isomaltulose synthase from *Erwinia rhapontici*

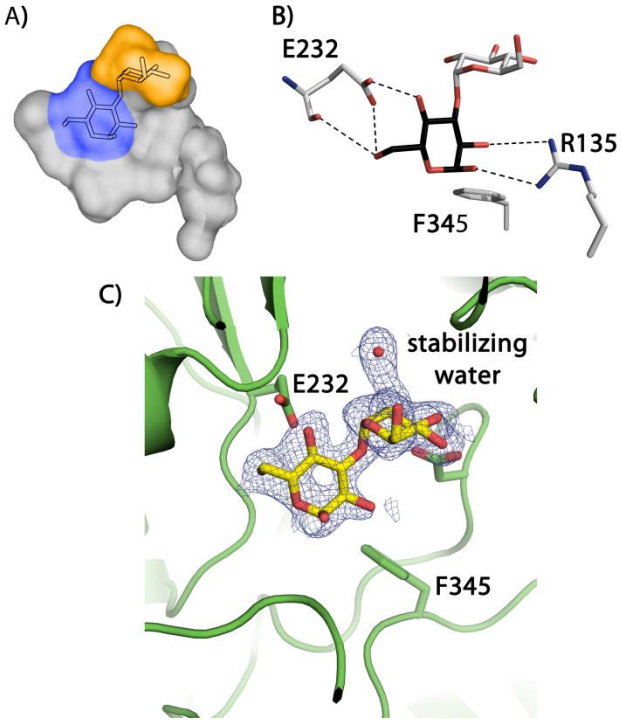

Fig. S2 Nigerose coordination in BaSP Q345F A) active site dimensions and acceptor glucose positioning; B) Hydrogen bonds between the acceptor glucose of nigerose and BaSP D192N/Q345F; C) Electron density of bound nigerose 1.0 σ.

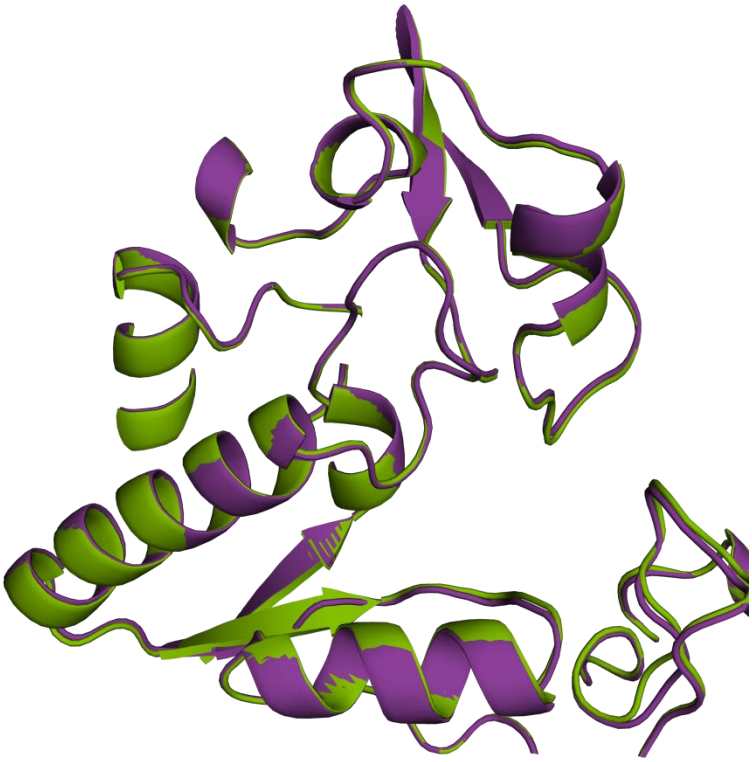

Fig. S 3

Alignment of BaSP Q345F binding resveratrol-3-α-D-glucoside (green) and the ligand free form (purple). This shows that the domain shift is ligand independent

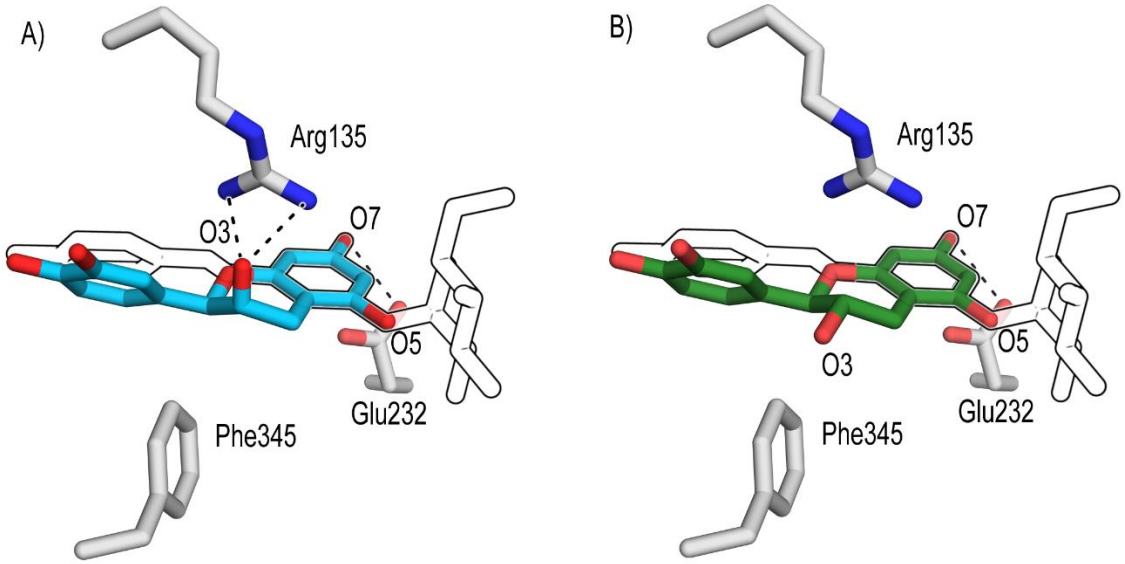

Fig. S 4 Investigation of the O5-glucosylatoion of (-)-epicatechin and (+)-catechin by BaSP Q345F

(-)-Epicatechin (A, light blue) and (+)-catechin (B, green) were superpositioned with the resveratrol moiety complexed by the D192N/Q345F-variant, which comprises the most likely productive binding mode, leading to (-)-epicatechin-5-glucosid and (+)-catechin-5-glucosid. The A ring of the flavanol is able to perfectly mimic resveratrol. The key difference is found at the 3-OH moiety which is oriented towardsArg^{135} in epicatechin in a distance and orientation suitable for a hydrogen bond. In the case of (+)-catechin the 3-OH group faces the nonpolar sidechain of F345. This observations are in accordance with the fact that glucosylation in 5-position is a slow side reaction for (+)-catechin, while glucosylation (-)-epicatechin is equally distributed between 3'-OH and 5'OH.

3 Additional Results

3.1 Kinetic Data

General Considerations:

The experiments required for determination of the activities at the lower acceptor substrate concentrations were challenging due to the detection limit of HPAEC-PAD and the presence of an excess of sucrose. This leads to relative high experimental errors, especially at the lower substrate concentrations.

(-)-epicatechin and (+)-catechin interfere with the pulsed amperometric detection resulting large experimental inaccuracies. These experiments where nonetheless included as the K_M-values are comparable with those of the other substrates. In addition previous experiments have shown that for catechin concentrations above 10 mM saturation was already reached.

The error-bars indicate the average of three repeats ± one standard deviation.

The direct linear plot follows the procedure described by Eisenthal and Cornish-Bowden.[6] The intersections were calculated and ranced using the algorythm included in chapter 6 of this supplementary information.

3.1.1 Resveratrol BaSP Q345F

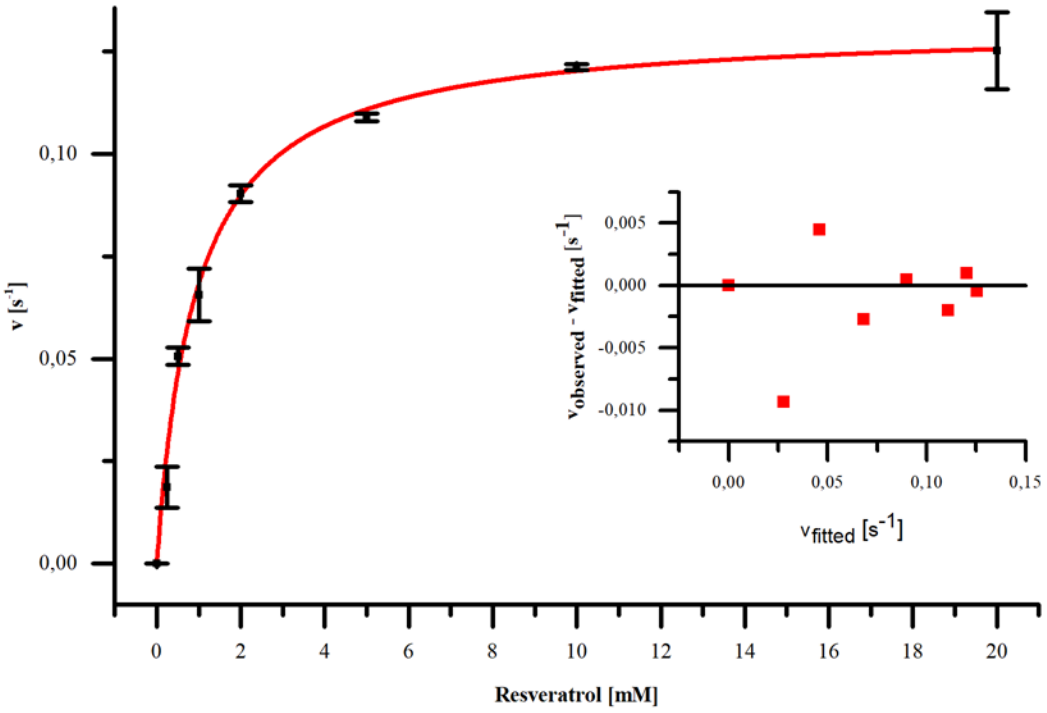

Fig. S 5 Michaelis Menten Fit and and residual analysis of BaSP Q345F transfer to resveratrol

Table S 2 Kinetic Parameters of BaSP Q345F, transfer to resveratrol derived via Michaelis-Menten fit

k_{cat} [s^{-1}]	standard deviation k_{cat} [s^{-1}]	K_M [mM]	standard deviation K_M [mM]	Kor. R^2
0.131	0.00179	0.924	0.08541	0.9996

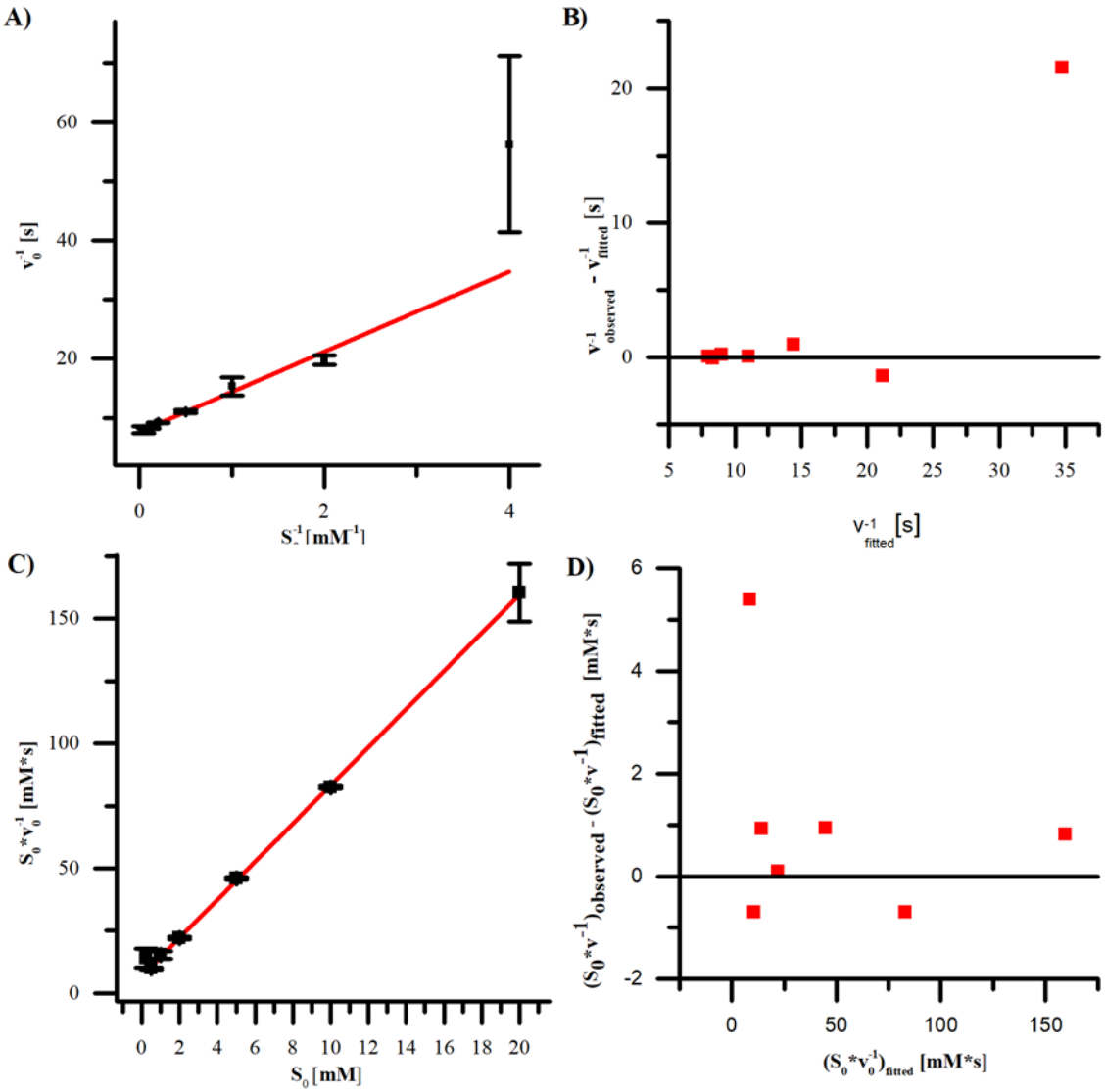

Fig. S 6 Linear plots of BaSP Q345F transfer to resveratrol A) Lineweaver-Burk plot B) residual analysis of the Lineweaver Burk plot C) Hanes-Woolf Plot D) residual analysis of the Hanes-Woolf plot

Table S 3 Kinetic Parameters of BaSP Q345F, transfer to resveratrol, linear plots

Method	k_{cat} [s^{-1}]	K_M [mM]
direct linear plot	0.131	0.989
Lineweaver-Burk plot	0.131	0.888
Hanes-Woolf plot	0.131	0.888

3.1.2 Quercetin BaSP Q345F

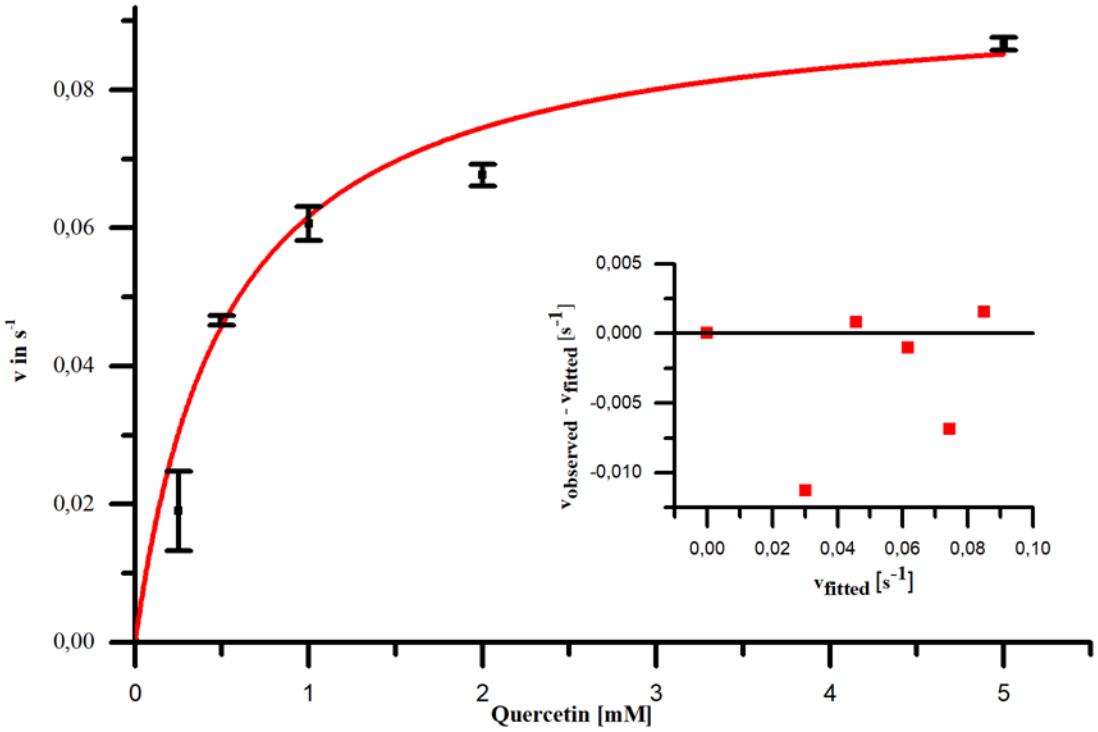

Fig. S 7 Michaelis Menten Fit and and residual analysis of BaSP Q345F transfer to quercetin

Table S 4 Kinetic Parameters of BaSP Q345F, transfer to quercetin derived via Michaelis-Menten fit

k_{cat} [s^{-1}]	standard deviation k_{cat} [s^{-1}]	K_M [mM]	standard deviation K_M [mM]	Kor. R^2
0.0941	0.00325	0.526	0.0603	0.9978

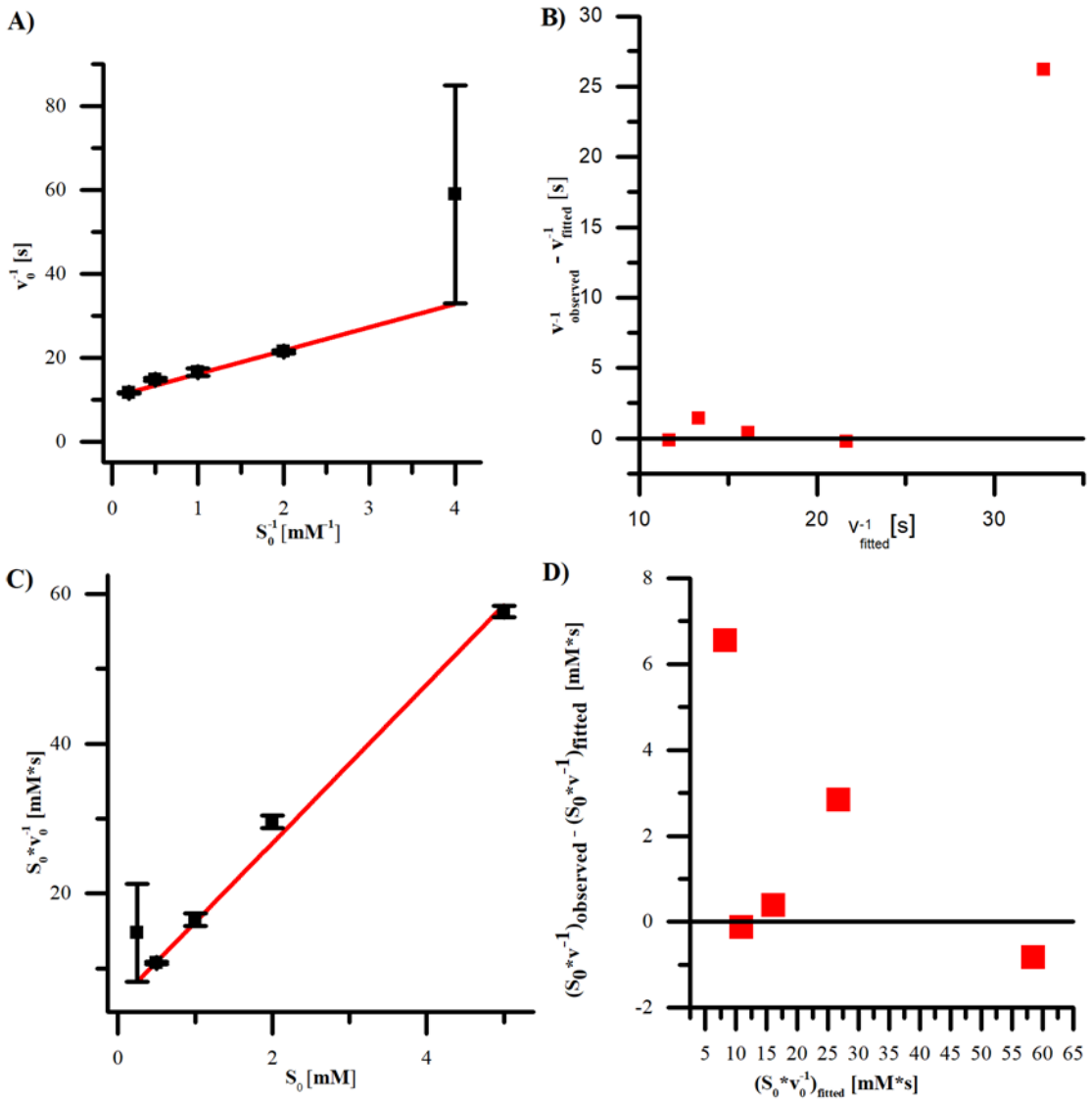

Fig. S 8 Linear plots of BaSP Q345F transfer to quercetin A) Lineweaver-Burk lot B) residual analysis of the Lineweaver Burk plot C) Hanes-Woolf Plot D) residual analysis of the Hanes-Woolf plot

Table S 5 Kinetic Parameters of BaSP Q345F, transfer to quercetin, linear plots

Method	k_{cat} [s^{-1}]	K_M [mM]
direct linear plot	0.096	0.564
Lineweaver-Burk plot	0.094	0.524
Hanes-Woolf plot	0.094	0.524

3.1.3 Fisetin BaSP Q345F

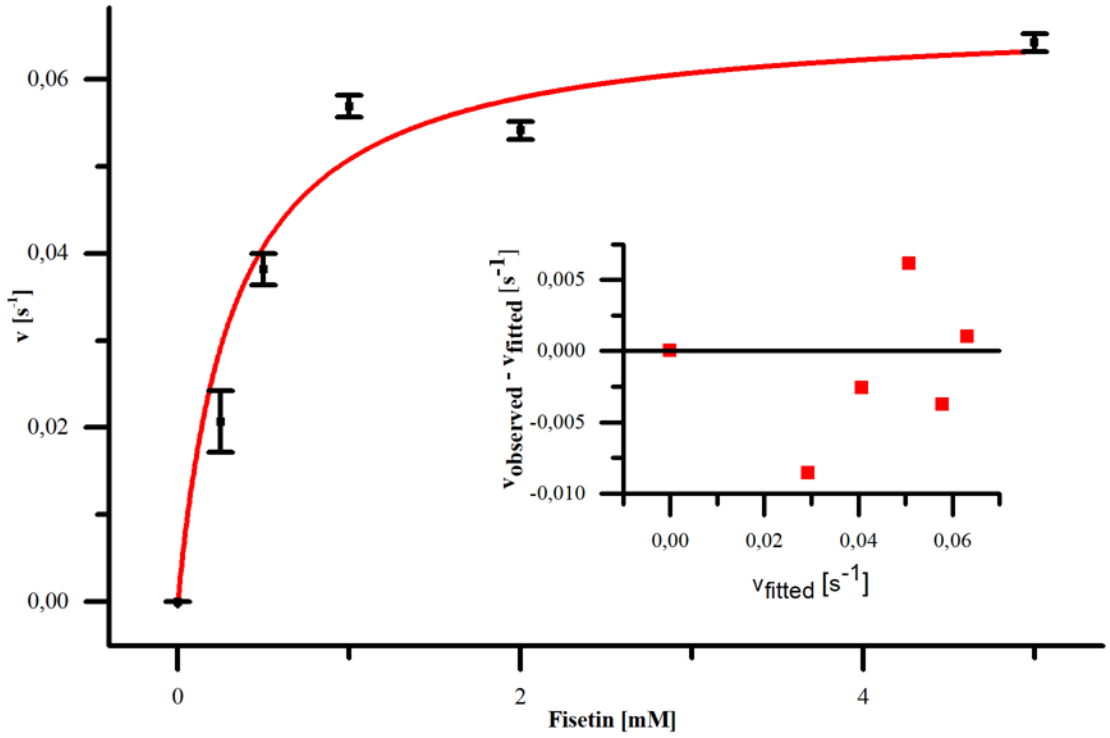

Fig. S 9 Michaelis Menten Fit and and residual analysis of BaSP Q345F transfer to fisetin

Table S 6 Kinetic Parameters of BaSP Q345F, transfer to fisetin derived via Michaelis-Menten fit

k_{cat} [s^{-1}]	standard deviation k_{cat} [s^{-1}]	K_M [mM]	standard deviation K_M [mM]	Kor. R^2
0.0673	0.00433	0.32491	0.1202	0.99362

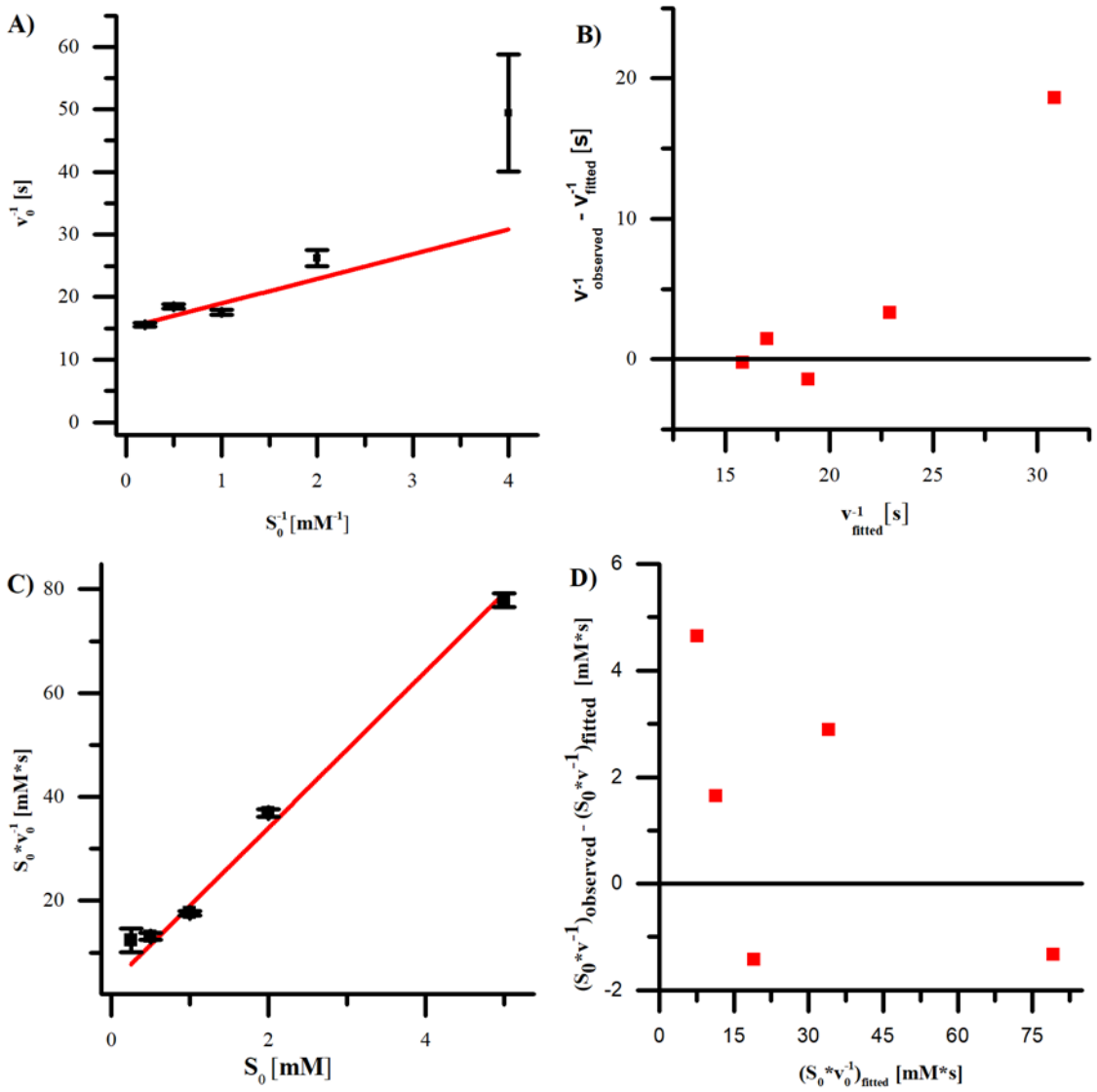

Fig. S 10 Linear plots of BaSP Q345F transfer to fiestin A) Lineweaver-Burk lot B) residual analysis of the Lineweaver Burk plot C) Hanes-Woolf Plot D) residual analysis of the Hanes-Woolf plot

Table S 7 Kinetic Parameters of BaSP Q345F, transfer to fisetin, linear plots

Method	k_{cat} [s^{-1}]	K_M [mM]
direct linear plot	0.071	0.612
Lineweaver-Burk	0.066	0.262
Hanes-Woolf plot plot	0.066	0.262

3.1.4 (-)-Epicatechin BaSP Q345F

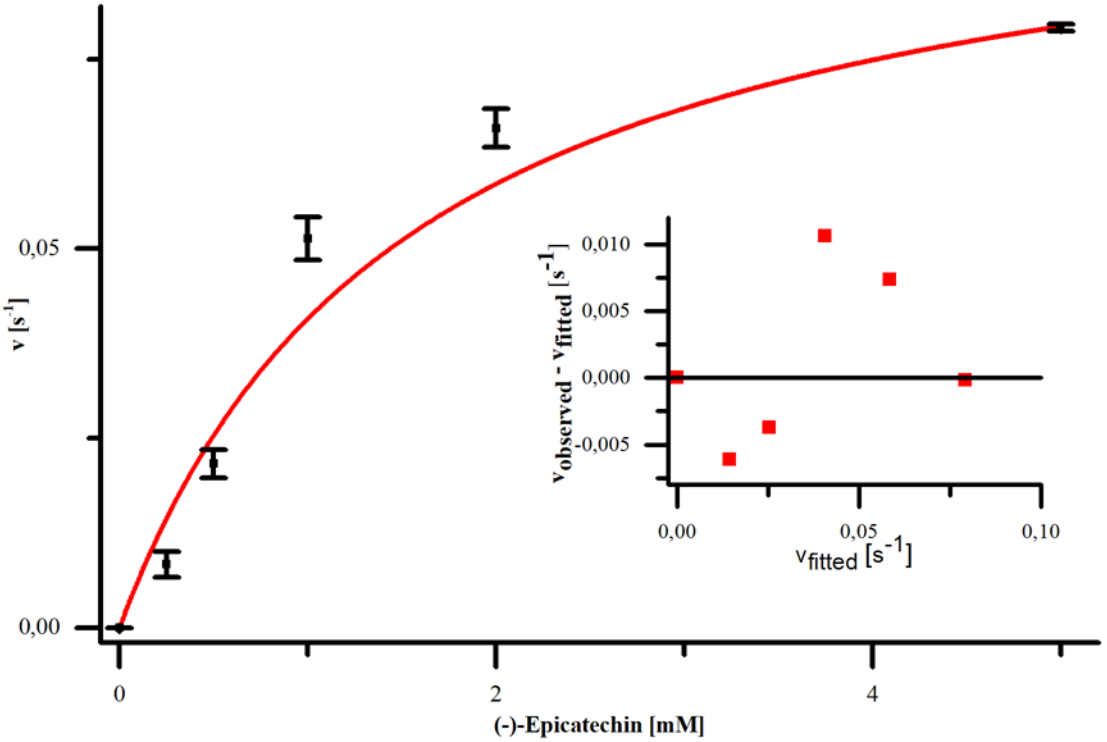

Fig. S 11 Michaelis Menten Fit and and residual analysis of BaSP Q345F transfer to (-)-Epicatechin

Table S 8 Kinetic Parameters of BaSP Q345F, transfer to (-)-epicatechin derived via Michaelis-Menten fit

k_{cat} [s^{-1}]	standard deviation k_{cat} [s^{-1}]	K_M [mM]	standard deviation K_M [mM]	Kor. R^2
0.10385	0.00739	1,54824	0.43356	0.99849

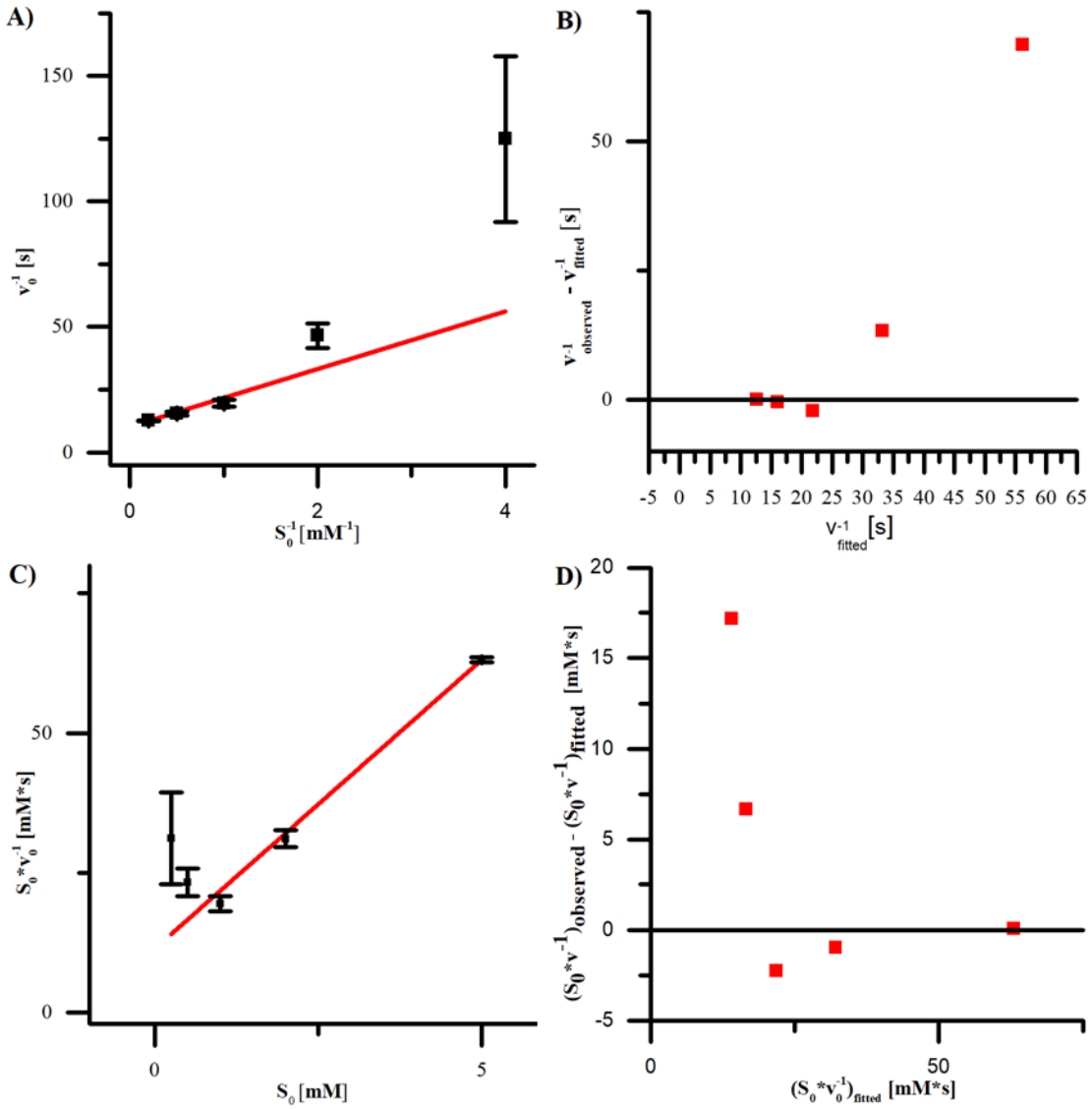

Fig. S 12 Linear plots of BaSP Q345F transfer to (-)-epicatechin A) Lineweaver-Burk lot B) residual analysis of the Lineweaver Burk plot C) Hanes-Woolf Plot D) residual analysis of the Hanes-Woolf plot

Table S 9 Kinetic Parameters of BaSP Q345F, transfer to (-)-epicatechin, linear plots

Method	k_{cat} [s^{-1}]	K_M [mM]
direct linear plot	0.092	0.787
Lineweaver-Burk plot	0.097	1.11
Hanes-Woolf plot	0.097	1.11

3.1.5 (+)-Catechin BaSP Q345F

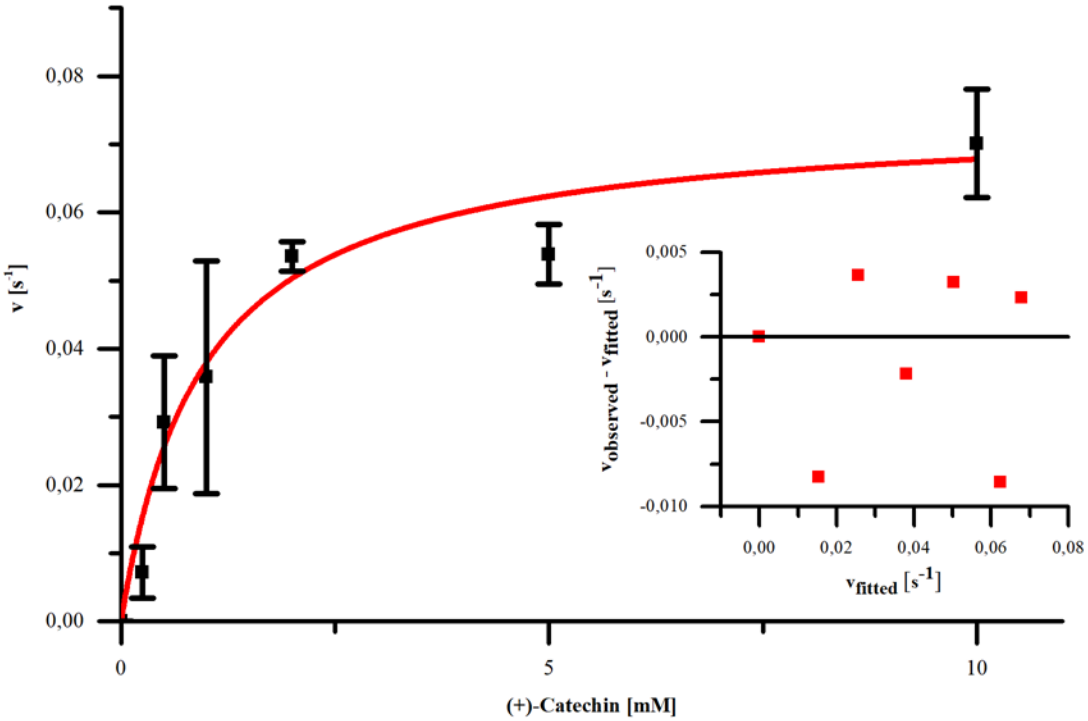

Fig. S 13 Michaelis Menten Fit and and residual analysis of BaSP Q345F transfer to (+)-Catechin

Table S 10 Kinetic Parameters of BaSP Q345F, transfer to (+)-Catechin derived via Michaelis-Menten fit

k_{cat} [s^{-1}]	standard deviation k_{cat} [s^{-1}]	K_M [mM]	standard deviation K_M [mM]	Kor. R^2
0.07427	0.00953	0.95265	0.40613	0.9842

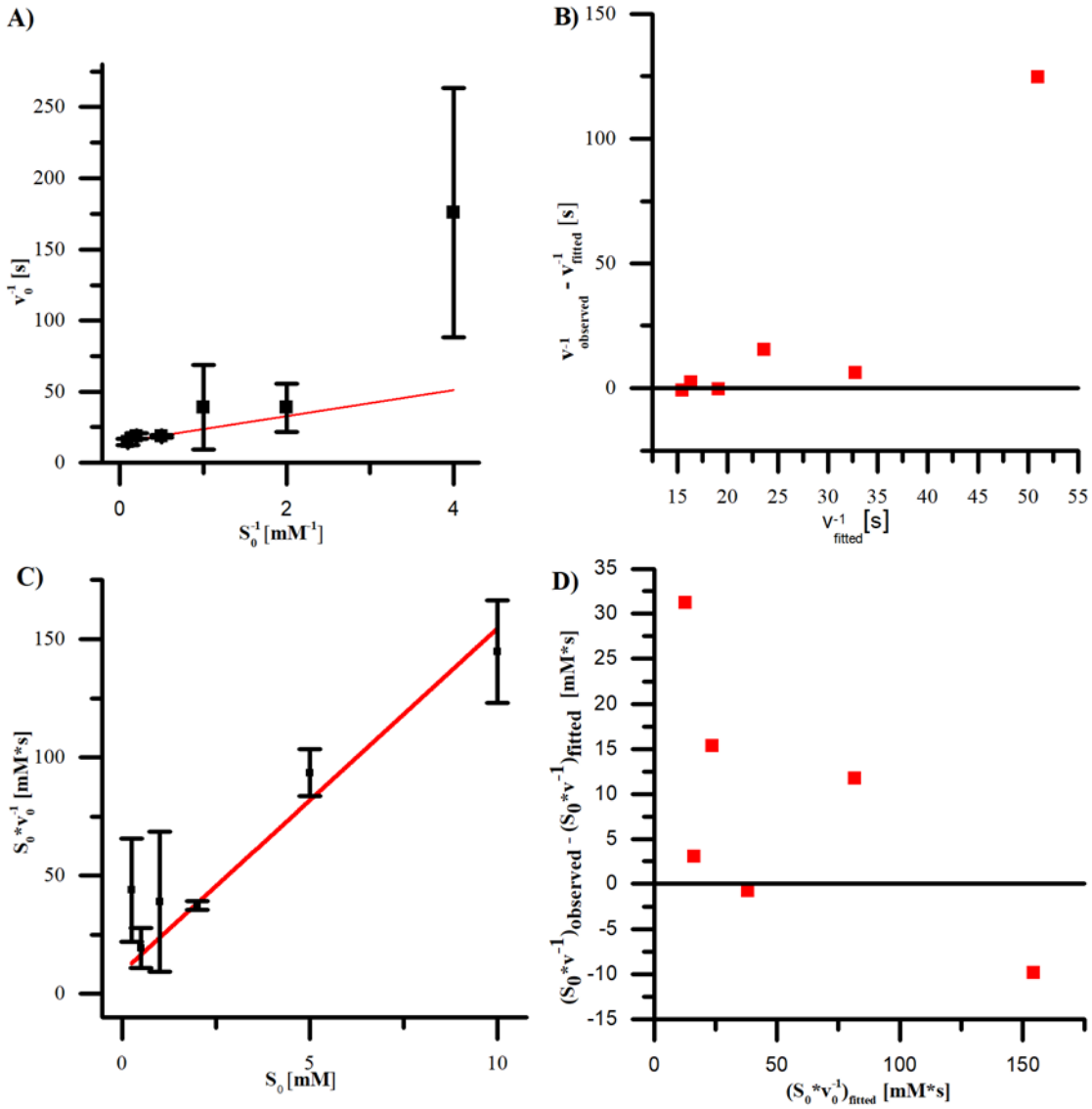

Fig. S 14 Linear plots of BaSP Q345F transfer to (+)-catechin A) Lineweaver-Burk lot B) residual analysis of the Lineweaver Burk plot C) Hanes-Woolf Plot D) residual analysis of the Hanes-Woolf plot

Table S 11 Kinetic Parameters of BaSP Q345F, transfer to (+)-catechin, linear plots

Method	k_{cat} [s^{-1}]	K_M [mM]
direct linear plot	0.074	0.770
Lineweaver-Burk plot	0.069	0.626
Hanes-Woolf plot	0.069	0.626

3.1.6 (rac)-Naringenin BaSP Q345F

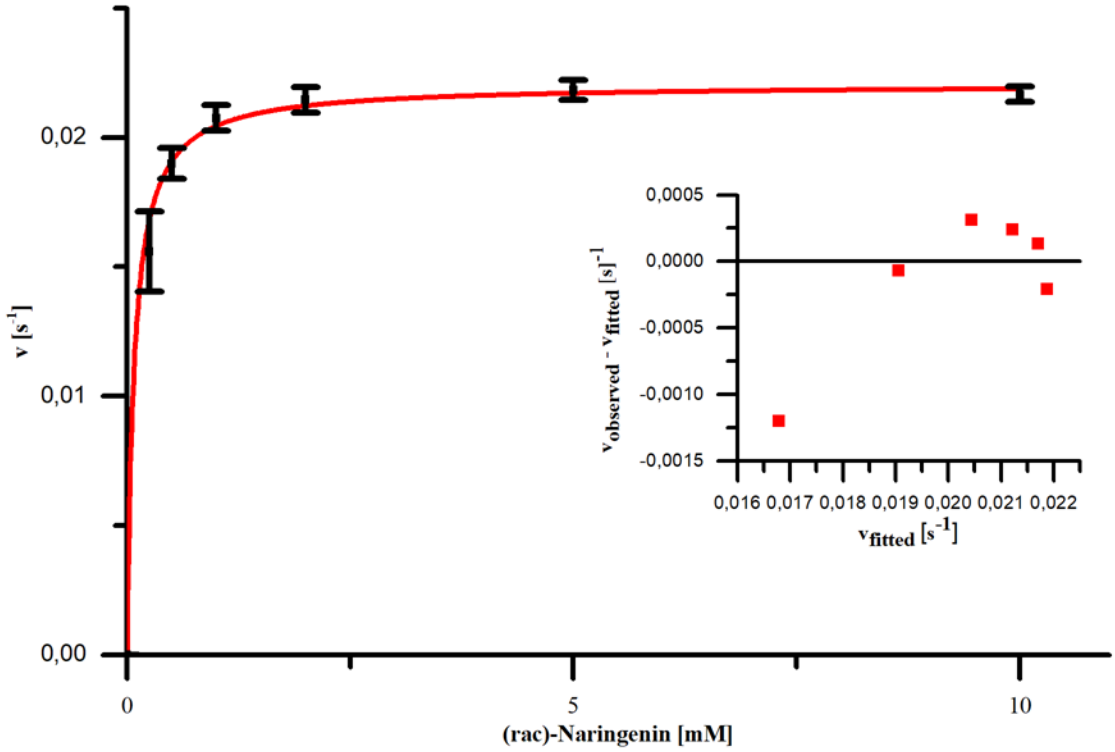

Fig. S 15 Michaelis Menten Fit and and residual analysis of BaSP Q345F transfer to (rac)-Naringenin

Table S 12 Kinetic Parameters of BaSP Q345F, transfer to (rac)-naringehin derived via Michaelis-Menten fit

k_{cat} [s^{-1}]	standard deviation k_{cat} [s^{-1}]	K_M [mM]	standard deviation K_M [mM]	Kor. R^2
0.0221	0.000149	0.0782	0.0099	0.99983

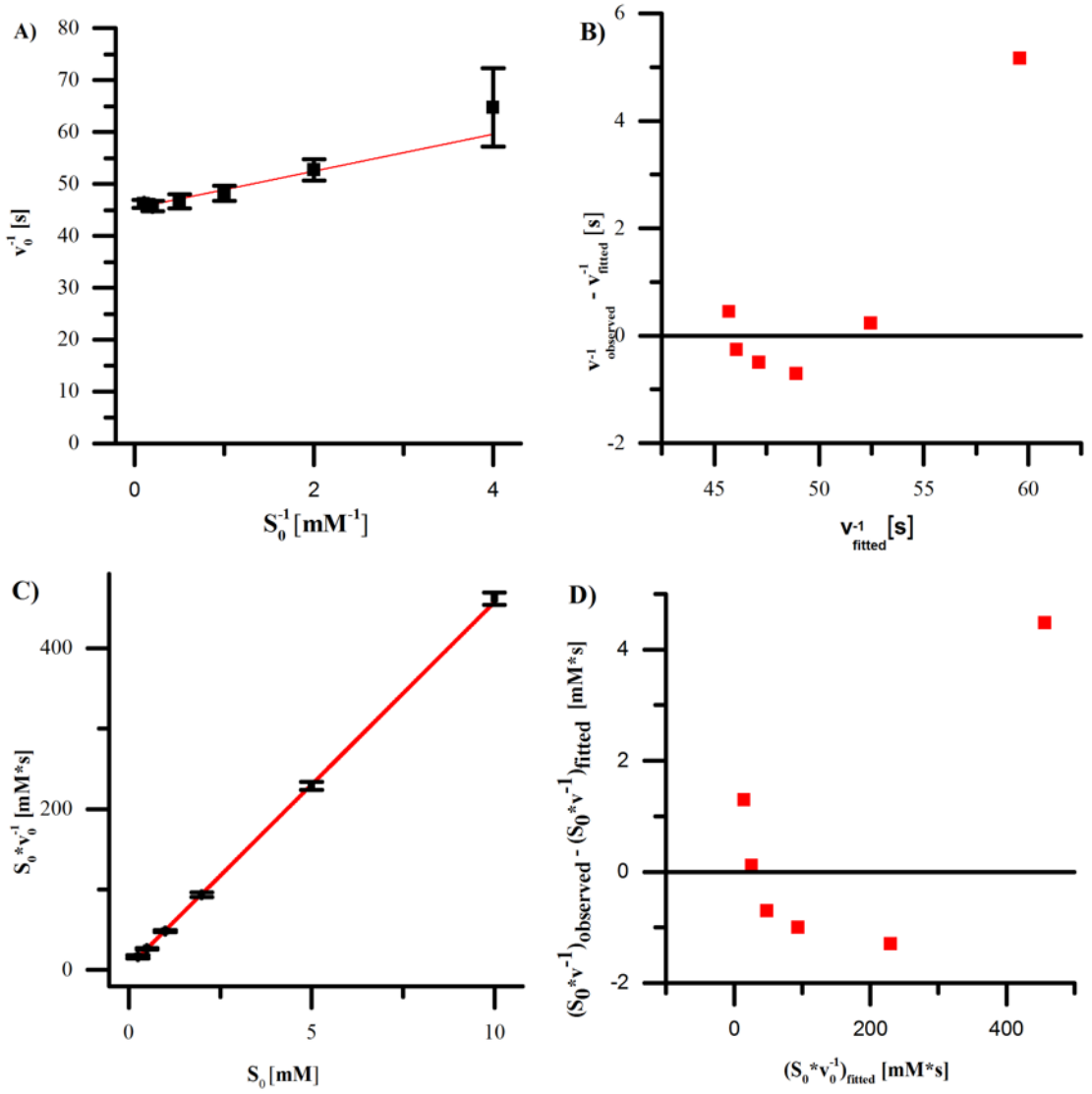

Fig. S 16 Linear plots of BaSP Q345F transfer to (rac)-naringehin A) Lineweaver-Burk lot B) residual analysis of the Lineweaver Burk plot C) Hanes-Woolf Plot D) residual analysis of the Hanes-Woolf plot

Table S 13 Kinetic Parameters of BaSP Q345F, transfer to (rac)-naringenin, linear plots

Method	k_{cat} [s^{-1}]	K_M [mM]
direct linear plot	0.022	0.085
Lineweaver-Burk plot	0.022	0,078
Hanes-Woolf plot	0.022	0,078

3.1.7 Glucose BaSP Q345F

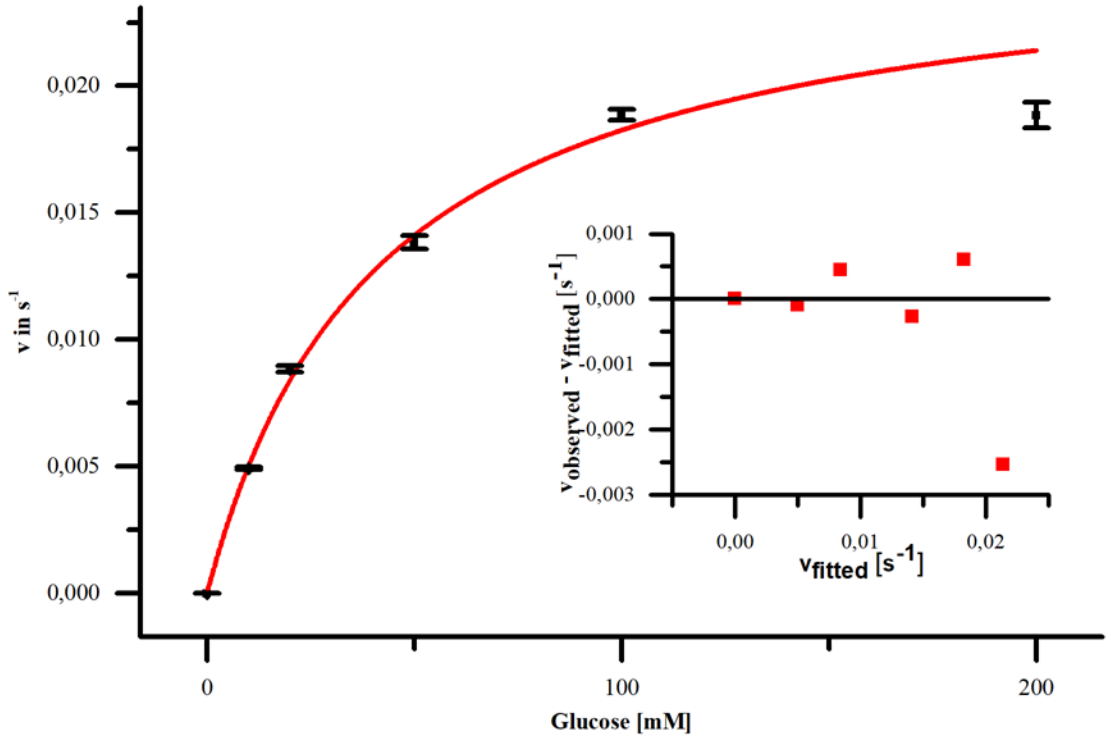

Fig. S 17 Michaelis Menten Fit and and residual analysis of BaSP Q345F transfer to glucose

Table S 14 Kinetic Parameters of BaSP Q345F, transfer to glucose derived via Michaelis-Menten fit

k_{cat} [s^{-1}]	standard deviation k_{cat} [s^{-1}]	K_M [mM]	standard deviation K_M [mM]	Kor. R^2
0.02583	0.00143	41,52203	3,77837	0.99766

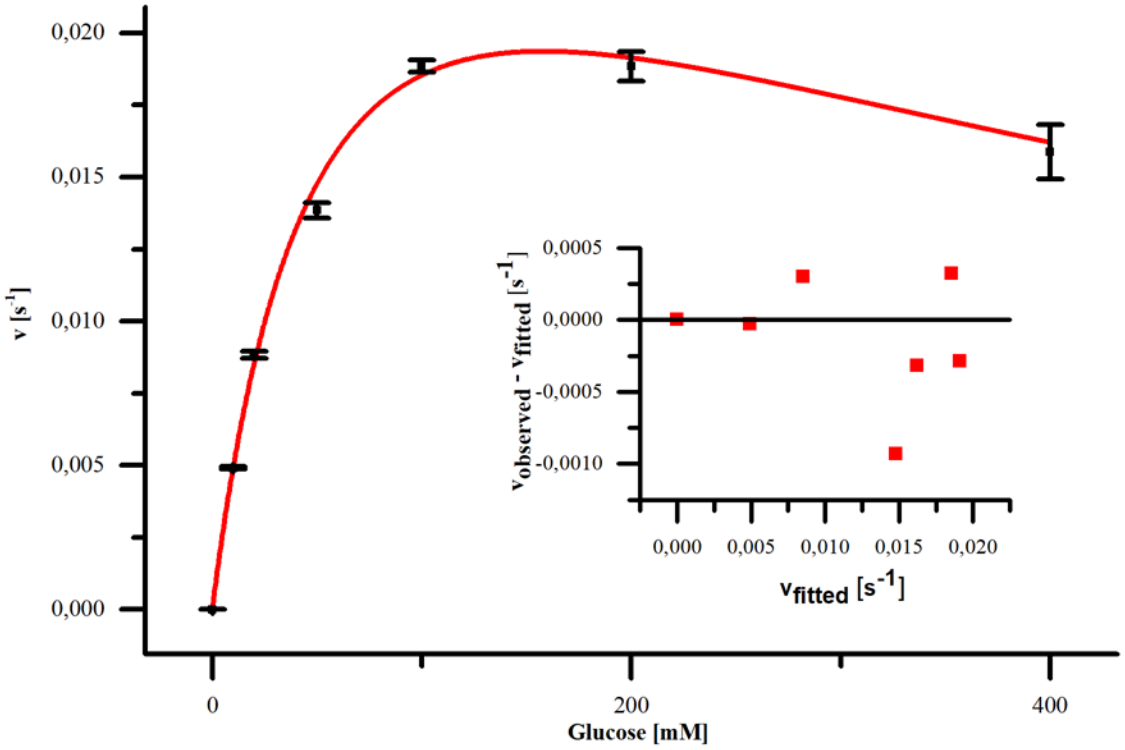

Fig. S 18 Michaelis Menten Fit with substrate inhibition and and residual analysis of BaSP Q345F transfer to glucose

Table S 15 Kinetic Parameters of BaSP Q345F, transfer to glucose derived via Michaelis-Menten fit with substrate inhibition

k_{cat} [s^{-1}]	standard deviation k_{cat} [s^{-1}]	K_M [mM]	standard deviation K_M [mM]	K_I [mM]	standard deviation K_M [mM]	Kor. R^2
0.02583	0.00143	41,52203	3,77837	435	174	0.99766

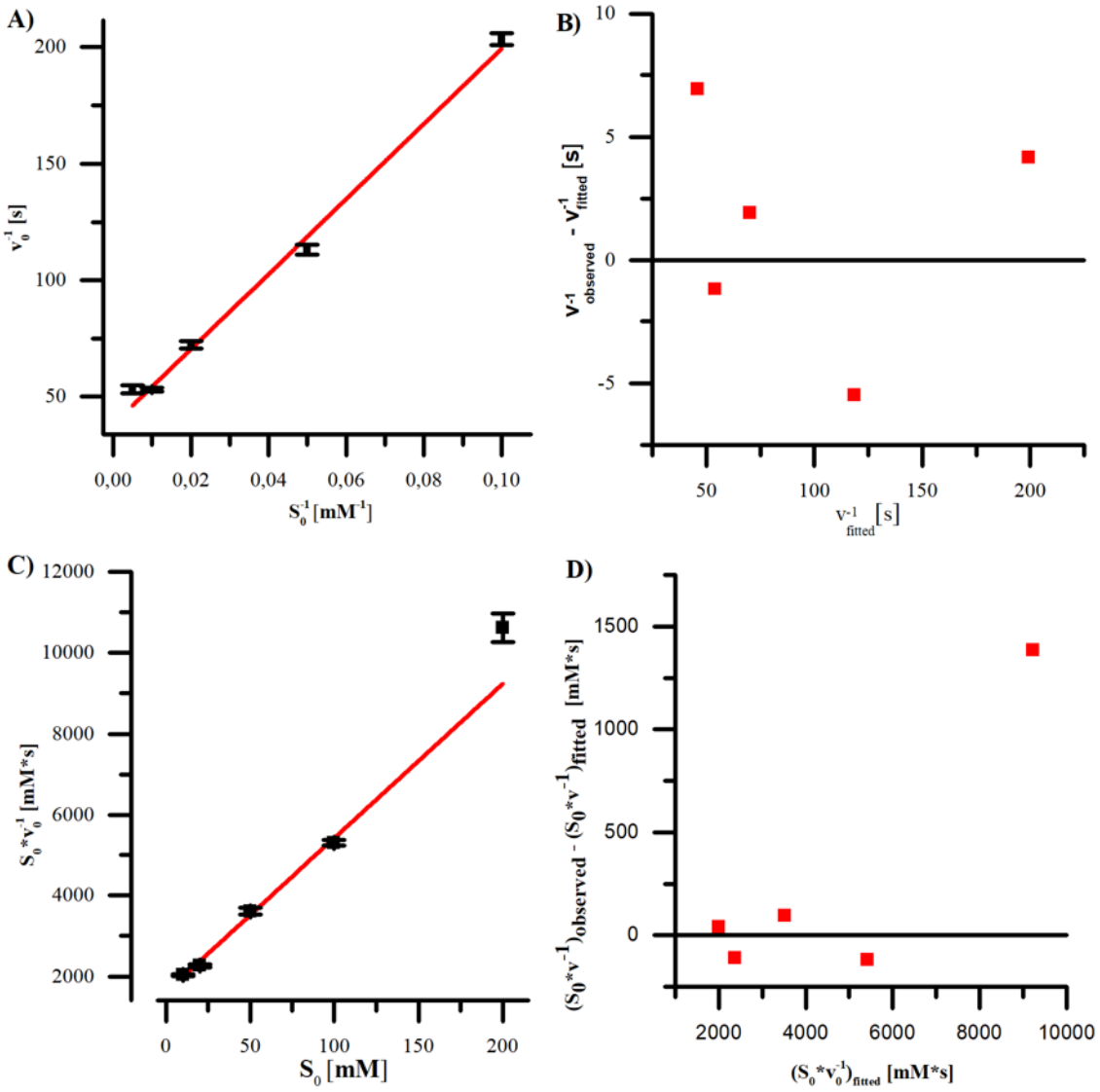

Fig. S 19 Linear plots of BaSP Q345F transfer to glucose A) Lineweaver-Burk lot B) residual analysis of the Lineweaver Burk plot C) Hanes-Woolf Plot D) residual analysis of the Hanes-Woolf plot

Table S 16 Kinetic Parameters of BaSP Q345F, transfer to glucose, linear plots

Method	k_{cat} [s^{-1}]	K_M [mM]
direct linear plot	0.024	37.3
Lineweaver-Burk plot	0.026	42.3
Hanes-Woolf plot	0.026	42.3

3.1.8 Phosphate BaSP Q345F

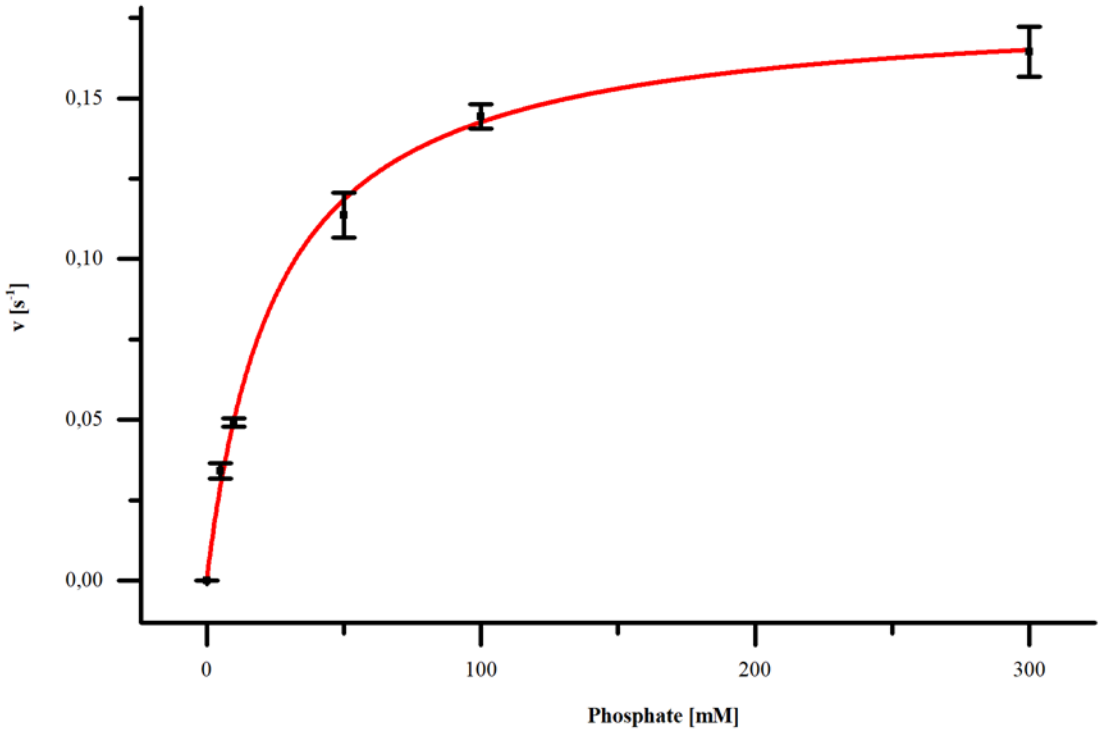

Fig. S 20 Michaelis Menten Fit and and residual analysis of BaSP Q345F transfer to phosphate

Table S 17 Kinetic Parameters of BaSP Q345F, transfer to phosphate derived via Michaelis-Menten fit

k_{cat} [s^{-1}]	standard deviation k_{cat} [s^{-1}]	K_M [mM]	standard deviation K_M [mM]	Kor. R^2
0.179	0.0066	25,7	1,86	0.9981

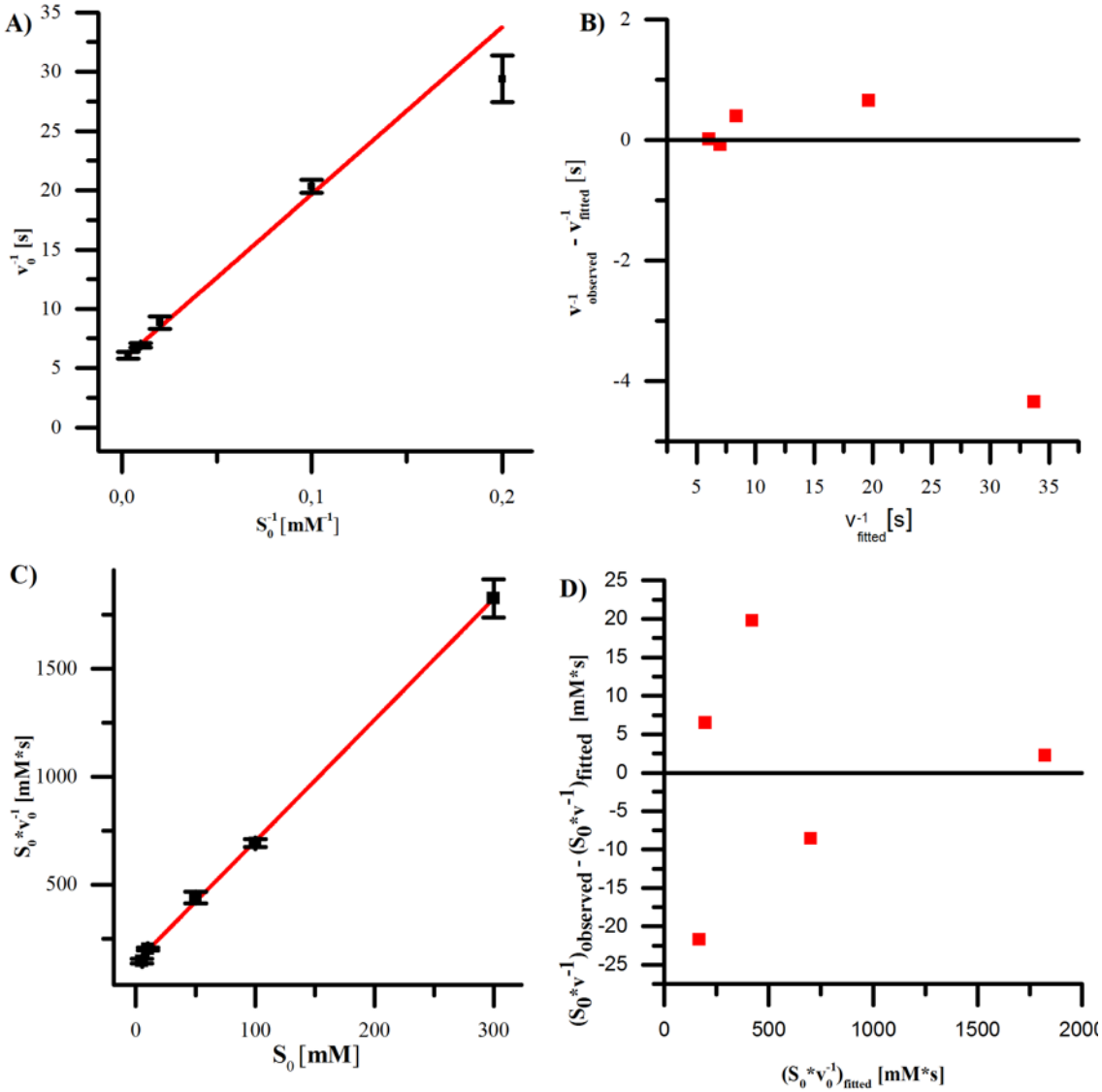

Fig. S 21 Linear plots of BaSP Q345F transfer to glucose A) Lineweaver-Burk lot B) residual analysis of the Lineweaver Burk plot C) Hanes-Woolf Plot D) residual analysis of the Hanes-Woolf plot

Table S 18 Kinetic Parameters of BaSP Q345F, transfer to phosphate, linear plots

Method	k_{cat} [s^{-1}]	K_M [mM]
direct linear plot	0.176	23.5
Lineweaver-Burk plot	0.178	25.1
Hanes-Woolf plot	0.178	25.1

3.1.9 Sucrose BaSP Q345F

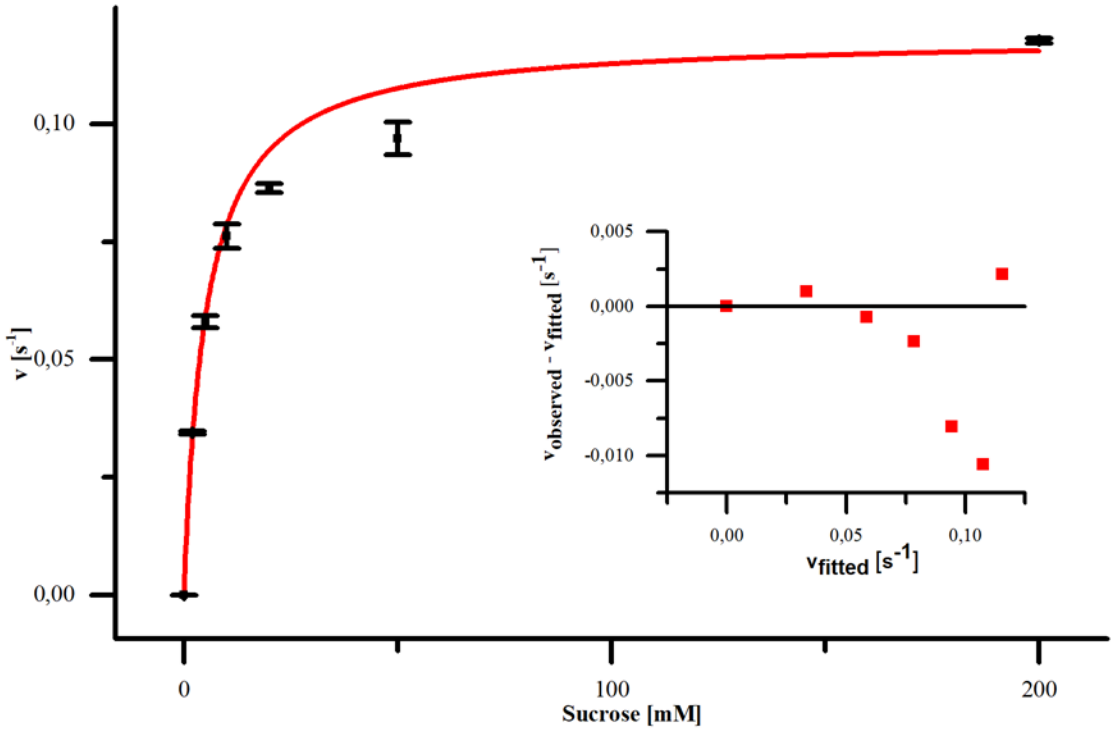

Fig. S 22 Fig. S 23 Michaelis Menten Fit and and residual analysis of BaSP Q345F transfer of glucose from sucrose to 20 mM resveratrol

Table S 19 Kinetic Parameters of BaSP Q345F, transfer of glucose from sucrose to 20 mM resveratrol derived via Michaelis-Menten fit

k_{cat} [s^{-1}]	standard deviation k_{cat} [s^{-1}]	K_M [mM]	standard deviation K_M [mM]	Kor. R^2
0.1183	0.00293	5,41	0.512	0.9979

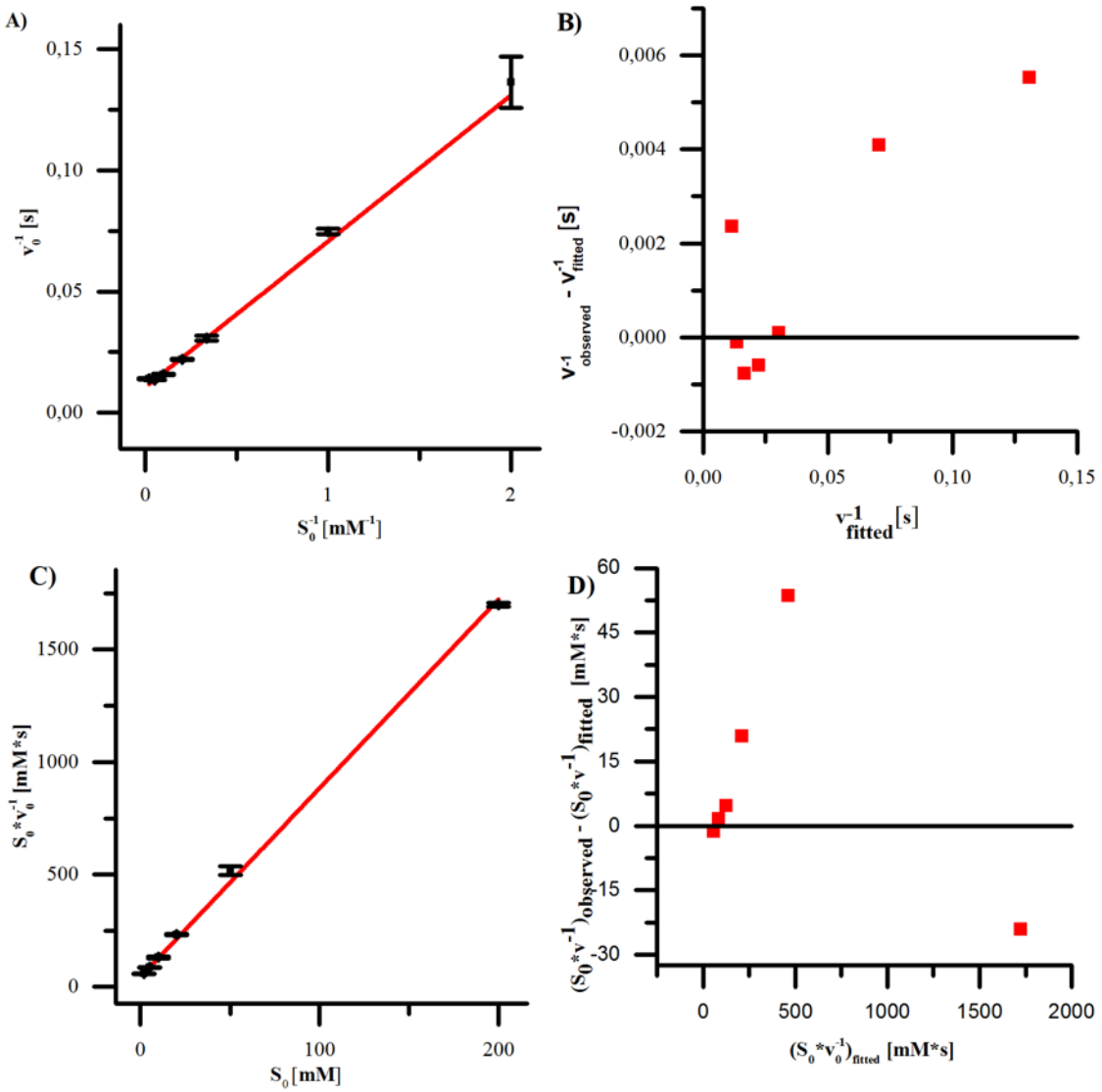

Fig. S 24 Linear plots of BaSP Q345F transfer of glucose from sucrose to 20 mM resveratrol A) Lineweaver-Burk lot B) residual analysis of the Lineweaver Burk plot C) Hanes-Woolf Plot D) residual analysis of the Hanes-Woolf plot

Table S 20 Kinetic Parameters of BaSP Q345F, transfer of glucose from sucrose to 20 mM resveratrol, linear plots

Method	k_{cat} [s^{-1}]	K_M [mM]
direct linear plot	0.107	4.35
Lineweaver-Burk plot	0.119	5.07
Hanes-Woolf plot	0.119	5.07

3.1.10 Sucrose BaSP wild type

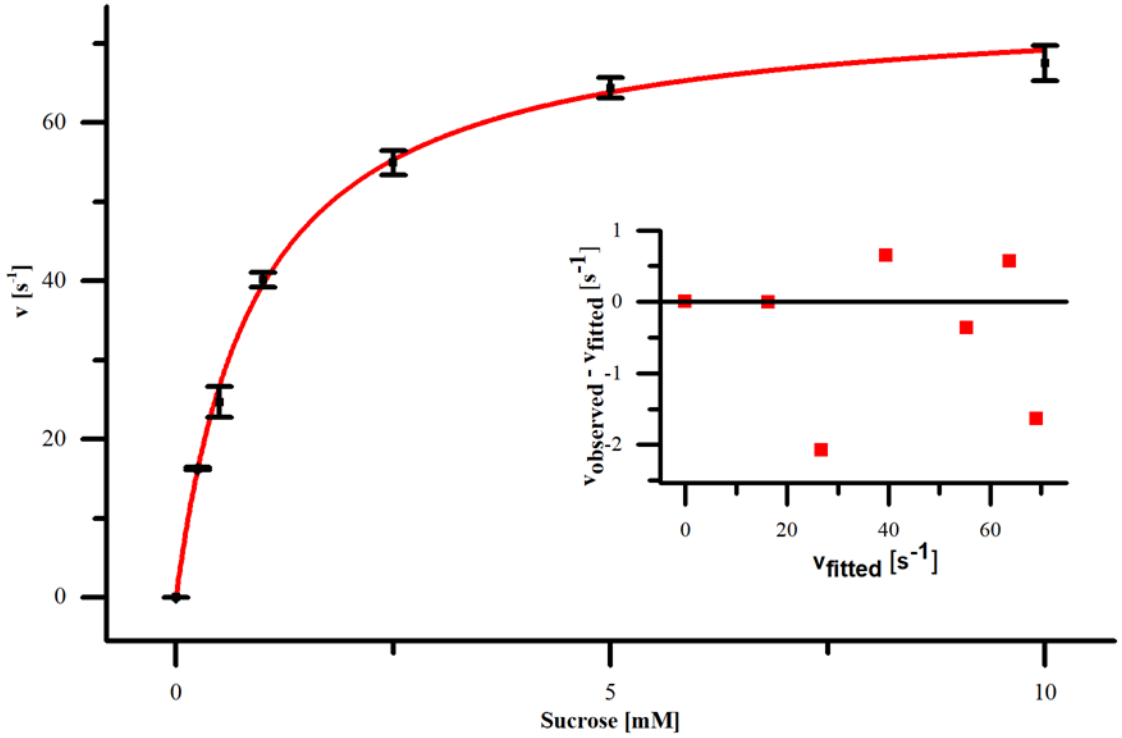

Fig. S 25 Michaelis Menten Fit and and residual analysis of BaSP wild type transfer of glucose from sucrose to 50 mM phosphate

Table S 21 Kinetic Parameters of BaSP wild type transfer of glucose from sucrose to 50 mM phosphate derived via Michaelis-Menten fit

k_{cat} [s^{-1}]	standard deviation k_{cat} [s^{-1}]	K_M [mM]	standard deviation K_M [mM]	Kor. R^2
75,4	0.95	0.908	0.019	0.9998

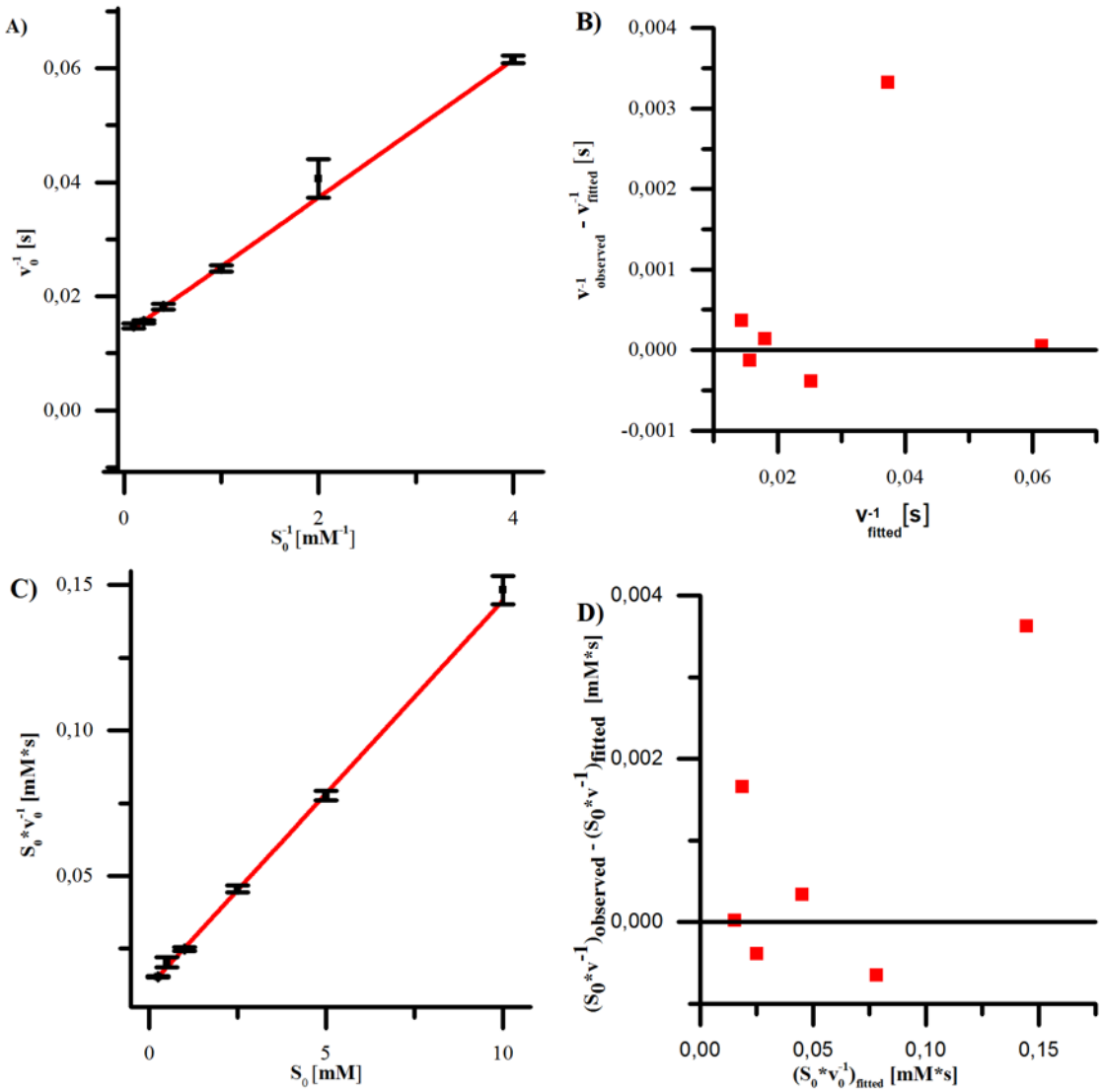

Fig. S 26 Linear plots of BaSP wild type transfer of glucose from sucrose to 50 mM phosphate A) Lineweaver-Burk lot B) residual analysis of the Lineweaver Burk plot C) Hanes-Woolf Plot D) residual analysis of the Hanes-Woolf plot

Table S 22 Kinetic Parameters of BaSP wild type transfer of glucose from sucrose to 50 mM phosphate, linear plots

Method	k_{cat} [s^{-1}]	K_M [mM]
direct linear plot	74.7	0.898
Lineweaver-Burk plot	75.4	0.908
Hanes-Woolf plot	75.4	0.908

3.1.11 Sucrose BaSP wild type

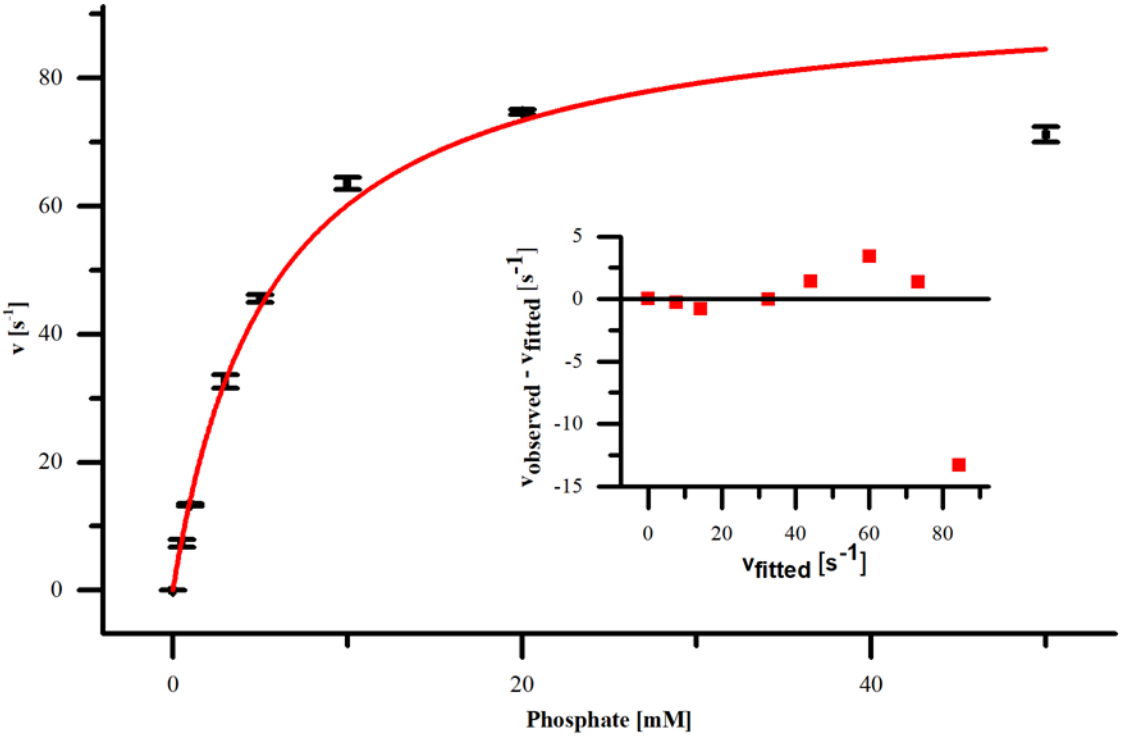

Fig. S 27 Fig. S 28 Michaelis Menten Fit and and residual analysis of BaSP wild type transfer of phosphate

Table S 23 Kinetic Parameters of BaSP Q345F, BaSP wild type transfer to phosphate derived via Michaelis-Menten fit

k_{cat} [s^{-1}]	standard deviation k_{cat} [s^{-1}]	K_M [mM]	standard deviation K_M [mM]	Kor. R^2
94,0	3,82	5,63	0.611	0.9967

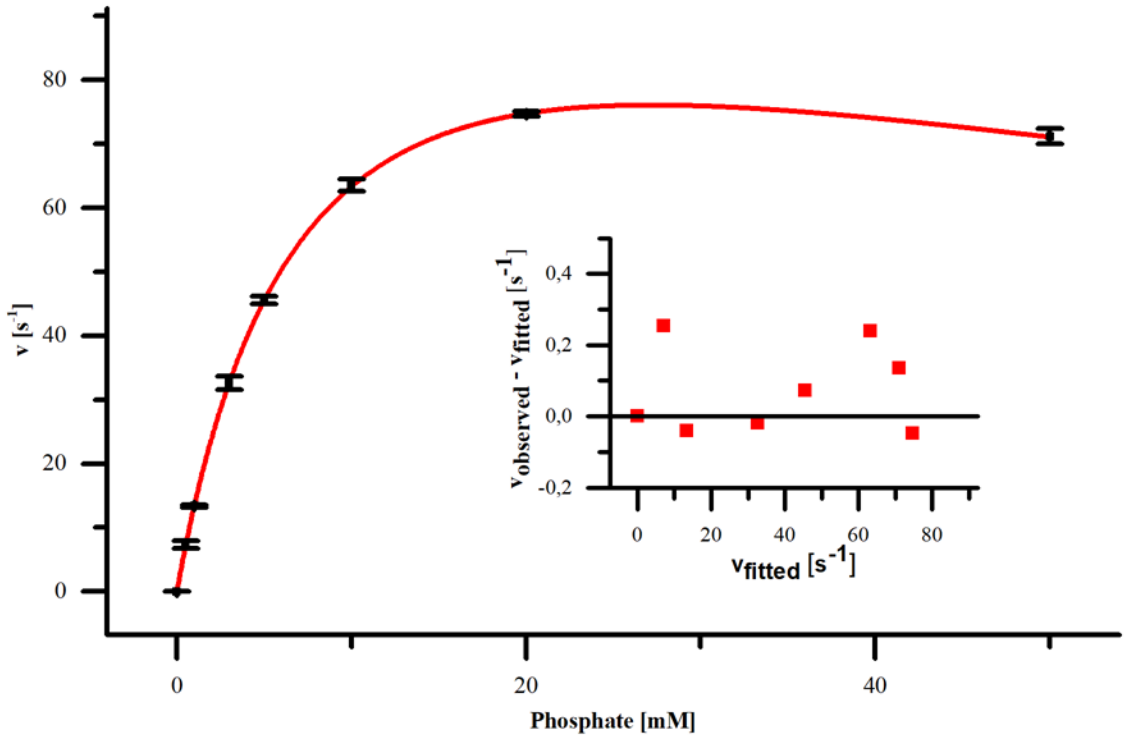

Fig. S 29 Michaelis Menten Fit with substrate inhibition and and residual analysis of BaSP wild type transfer to phosphate

Table S 24 Kinetic Parameters of BaSP Q345F, transfer to glucose derived via Michaelis-Menten fit with substrate inhibition

k_{cat} [s^{-1}]	standard deviation k_{cat} [s^{-1}]	K_M [mM]	standard deviation K_M [mM]	K_I [mM]	standard deviation K_M [mM]	Kor. R^2
121	0,78	7,99	0,078	92,7	2,6	0,99999

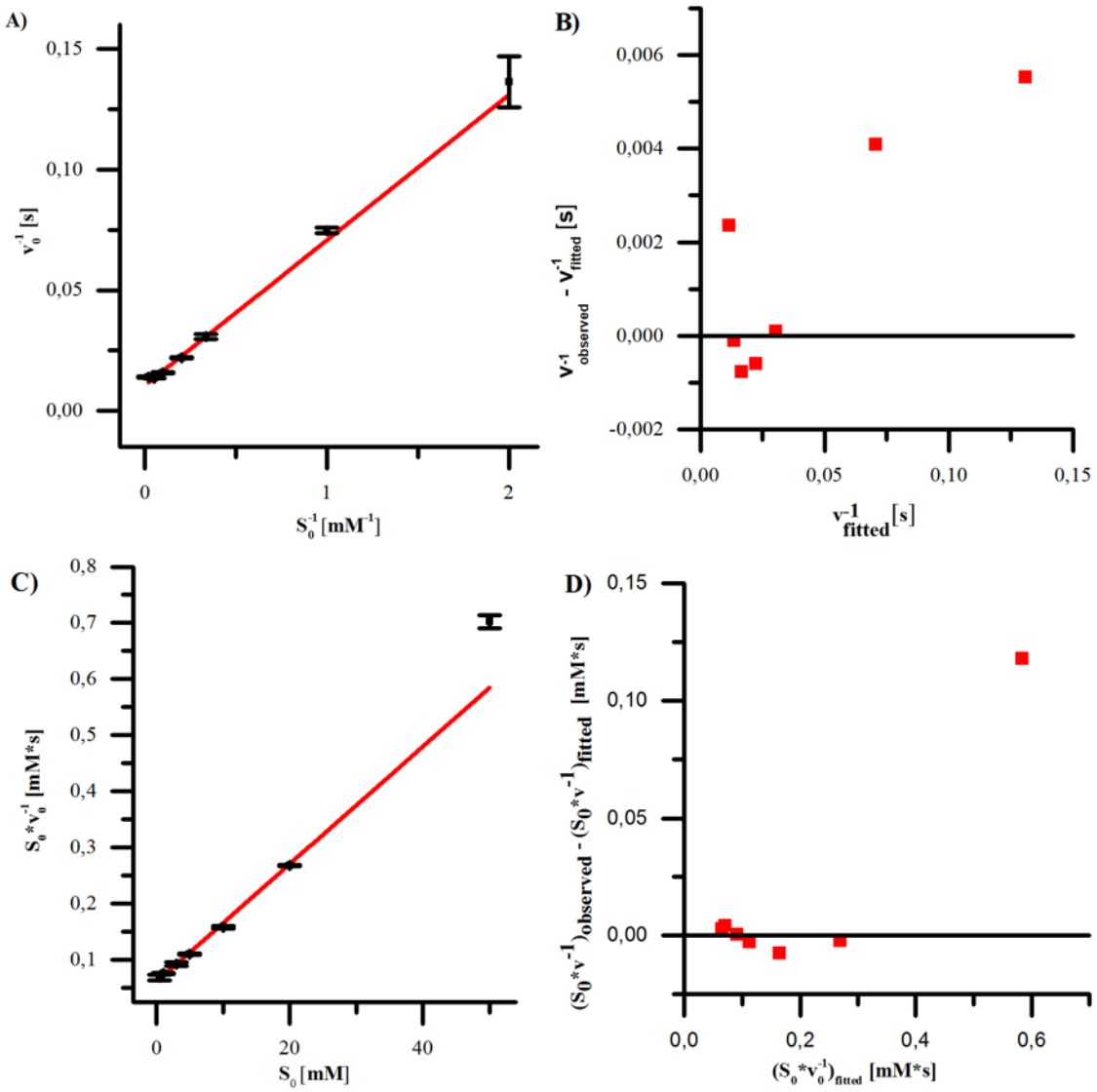

Fig. S 30 Linear plots of BaSP wild type transfer to phosphate A) Lineweaver-Burk lot B) residual analysis of the Lineweaver Burk plot C) Hanes-Woolf Plot D) residual analysis of the Hanes-Woolf plot

Table S 25 Kinetic Parameters of BaSP Q345F, BaSP wild type transfer phosphate, linear plots

Method	k_{cat} [s^{-1}]	K_M [mM]
direct linear plot	97.6	6.12
Lineweaver-Burk plot	95.3	5.74
Hanes-Woolf plot	95.3	5.74

3.2 Product distribution of BaSP Q345F

Table S 26 Maximum yields observed for glucosylation products of BaSP Q345F

	3'-monoglucosid	*5-monoglucosid*	*7-monoglucosid*	*3'-5 or 3'-7 diglucosid*	*maximum total glucosylation*
(-)-epicatechin	28%	25%		67%	97%
(+)-catechin	75%	15%		32%	89%
quercetin	61%		21%	40%	94%
fisetin	82%				90%
naringenin			57%		57%
resveratrol			3-glucosid		
			95%		95%

Conditions: 600 mM Sucrose, 30% (v/v) DMSO, 50 °C, acceptor concentrations: (-)-epicatechin, (+)-catechin: 100 mM, quercetin, fisetin: 50 mM, naringenin: 25 mM, resveratrol 75 mM.

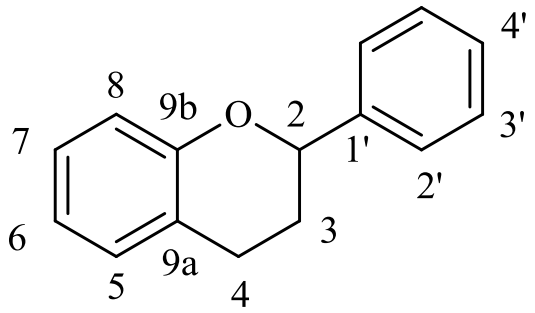

Fig. S 31 Numbering of positions in flavonoids

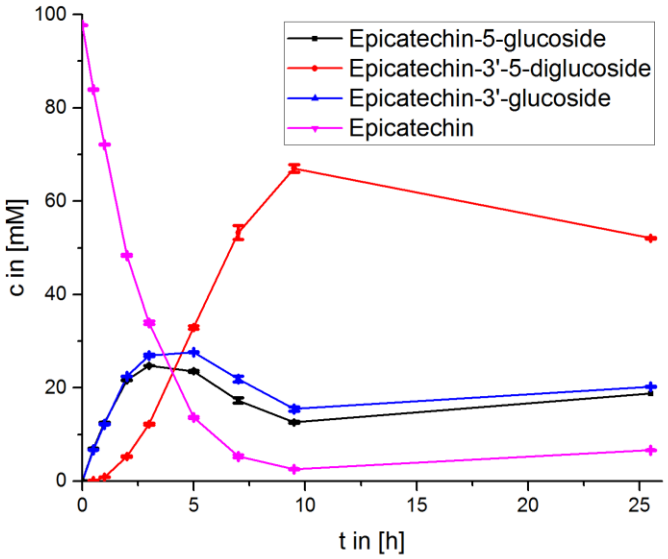

Fig. S 32 Product profile of BaSP Q345F with epicatechin as acceptor

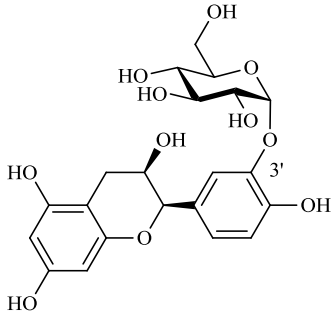

(-)-epicatechin-3’-glucosid

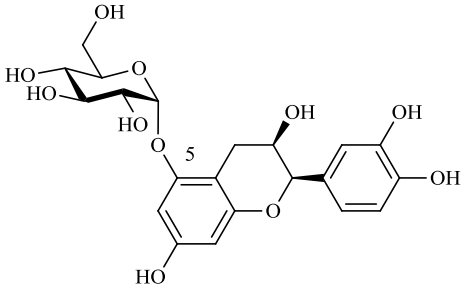

(-)-epicatechin-5-glucosid

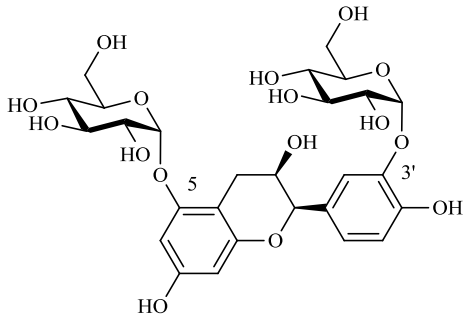

(-)-epicatechin-3’-5-diglucosid

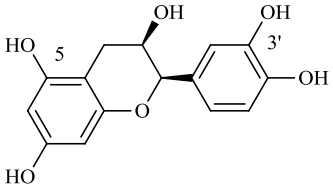

(-)-epicatechin

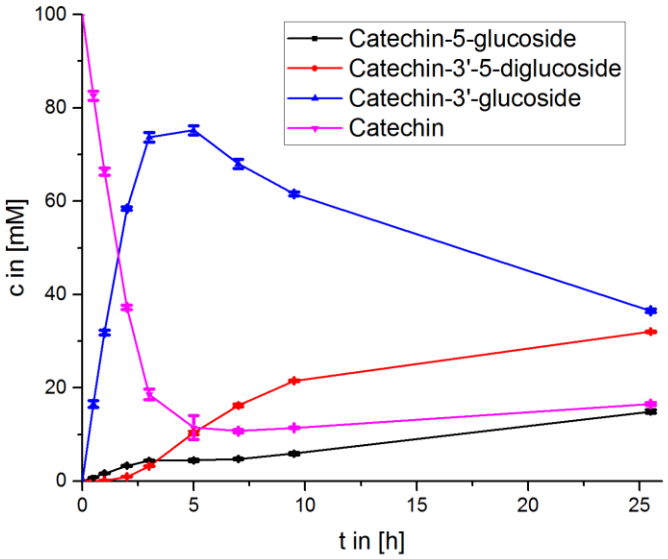

Fig. S 33 Product profile of BaSP Q345F with catechin as acceptor

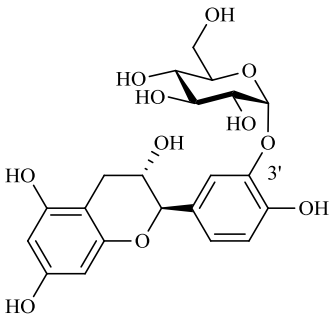

(+)-catechin-3'-glucosid

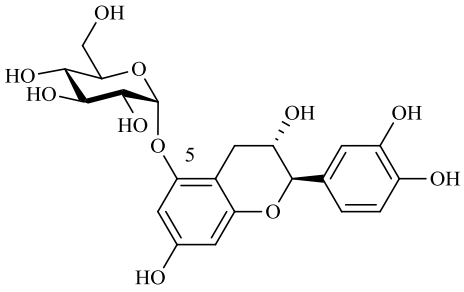

(+)-catechin-5-glucosid

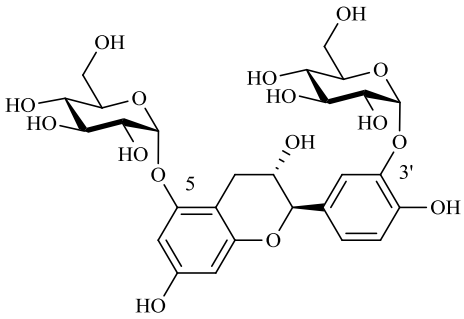

(+)-catechin-3'-5-diglucosid

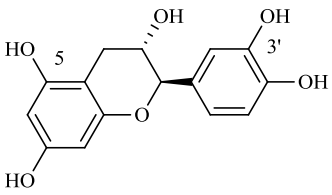

(+)-catechin

An peak of an uncharacterized product was detected and assigned to (+)-catechin-5-glucosid as it displays similar retention times as (-)-epicatechin-5-glucosid and the Q345F variant is known to produce (+)-catechin-3'-5-diglucosid.

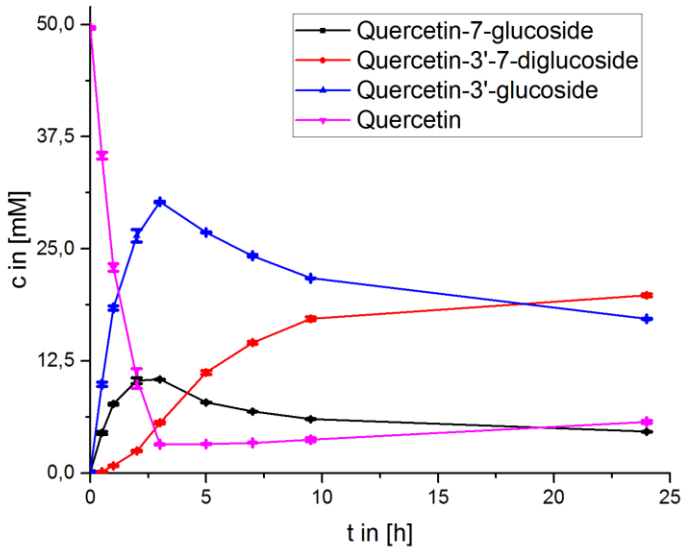

Fig. S 34: Product profile of BaSP Q345F with quercetin as acceptor.

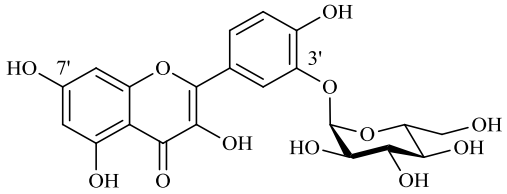

quercetin-3'-glucosid

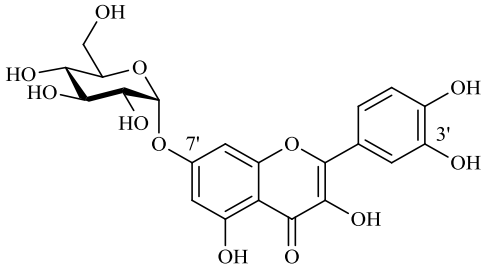

quercetin-5-glucosid

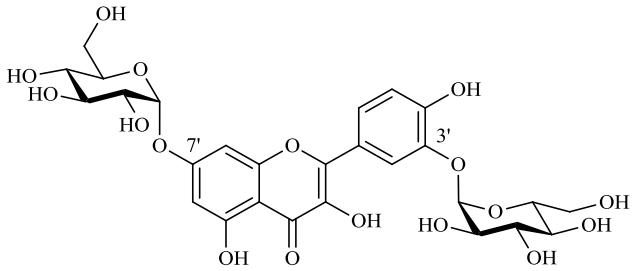

quercetin-3'-5-diglucosid

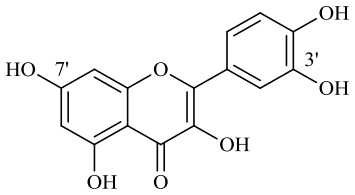

quercetin

Quercetin-3'-glucosid and quercetin -3'-5-diglucosid were isolated, the third component was not obtained in sufficient purity to allow NMR-characterisation. Its chromatographic behaviour corresponds to a monoglucoside and as the diglucoside is glucosylated in 3'- and 5-position we assumed the third product to be quercetin -5-glucosid.

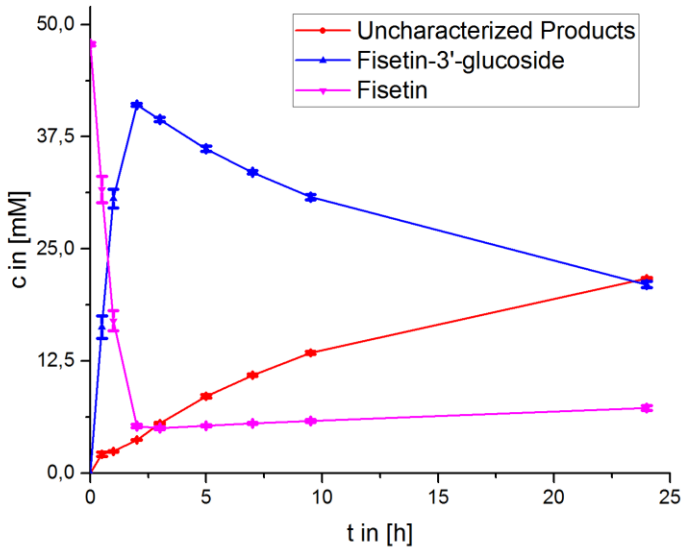

Fig. S 35 Product profile of BaSP Q345F with fisetin as acceptor

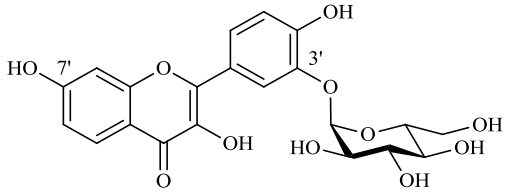

fisetin-3'-glucosid

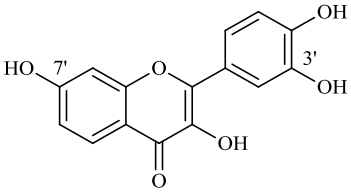

fisetin

Two peaks of uncharacterized products were detected. Most likely this compounds are fisetin-7-glucoside and fisetin 3'-7-diglucoside similar to the reaction products found in quercetin.

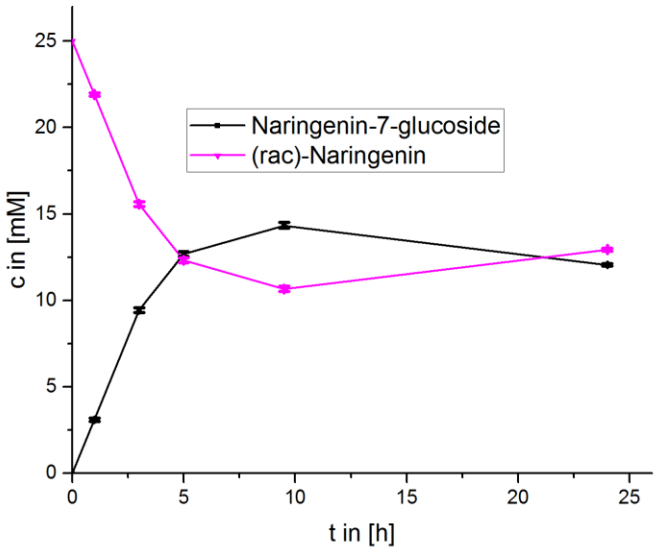

Fig. S 36 Product profile of BaSP Q345F with naringenin as acceptor

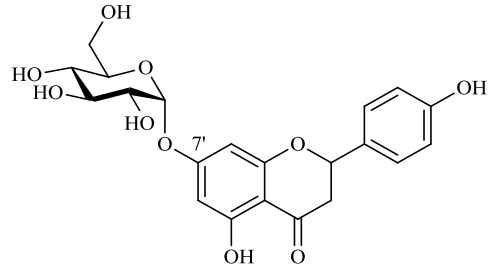

naringennin-7-glucosid

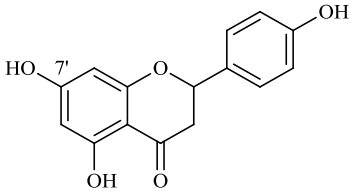

naringenin

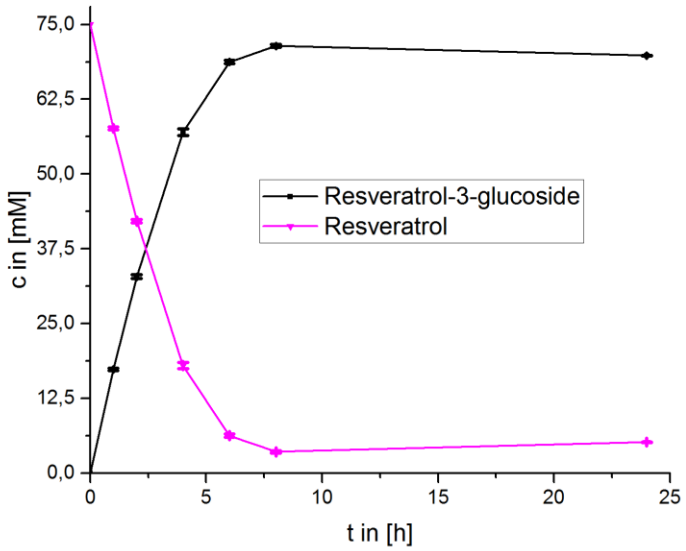

Fig. S 37 Product profile of BaSP Q345F with resveratrol as acceptor

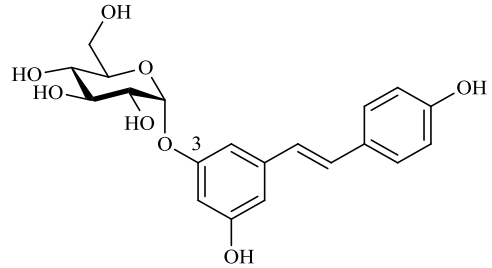

resveratrol-3-glucosid

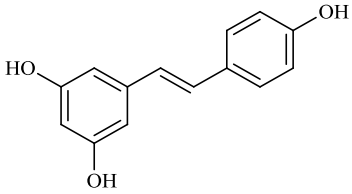

resveratrol

4 NMR- and MS-Data

4.1 NMR- and MS-Data of novel compounds

Naringenin-7-α-D-glucoside

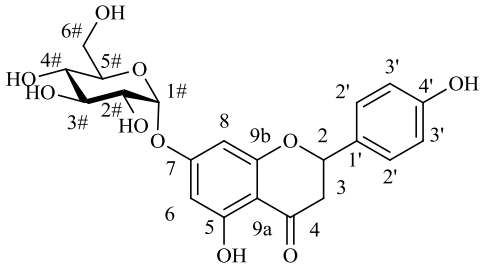

1:1: mixture of diastereomers

^{1}H-NMR (400 MHz; CD_3OD): δ= 7.33-7.31 (m, 2H, *H*-2‘), 6.83-6.81 (m, 2H, *J* = 2.0 Hz, *H*-3‘),6.30-6.27 (m, 2H, *H*-6, *H*-8), 5.59-5.56 (d, 1H, *J* = 3.5 Hz, *H*-1#), 5.40-5.36 (dd, 1H, *J* = 13.2, 2.9 Hz, *H*-2), 3.83-3.78 (dd, 1H, *J* = 9.3, 9.2 Hz, *H*-3#), 3.75-3.66 (m, 2H, *H*-6#), 3.58-3.55 (dd, 1H, *J* = 9.7, 3.8 Hz, *H*-2#), 3.55-3.51 (m, 1H, *H*-5#) 3.45-3.40 (dd, 1H, *J* = 9.4, 9.5 Hz, *H*-4#) 3.20-3.13 (dd, 1H, *J*= 17.2, 13.3 Hz, *H*-3) 2.77-2.72 (m, 1H, *H*-3) ppm.

^{13}C-NMR (100 MHz; CD_3OD): δ= 198.6 (*C*-4), 166.6, 165.0 164.6 (*C*-5, *C*-7, *C*-9b), 159.1 (*C*-4‘), 131.8 (*C*-1‘), 129.1 (*C*-2‘), 116.3 (*C*-3‘), 104.9 (*C*-9a), 98.6 (*C*-1#), 98.1, 97.1 (*C*-6, *C*-8), 80.6 (*C*-2) 74.9 (*C*-5#), 74.7 (*C*-3#), 73.0 (*C*-2#), 71.1 (*C*-4#), 62.1 (*C*-6#), 44.1 (*C*-3) ppm.

MS (ESI positive):

Ion Formula:	$C_{21}H_{22}O_{10}Na^+$ $[M+Na]^+$
m/z calculated:	457.11052
m/z experimental:	457.11057
error [ppm]:	-0.11

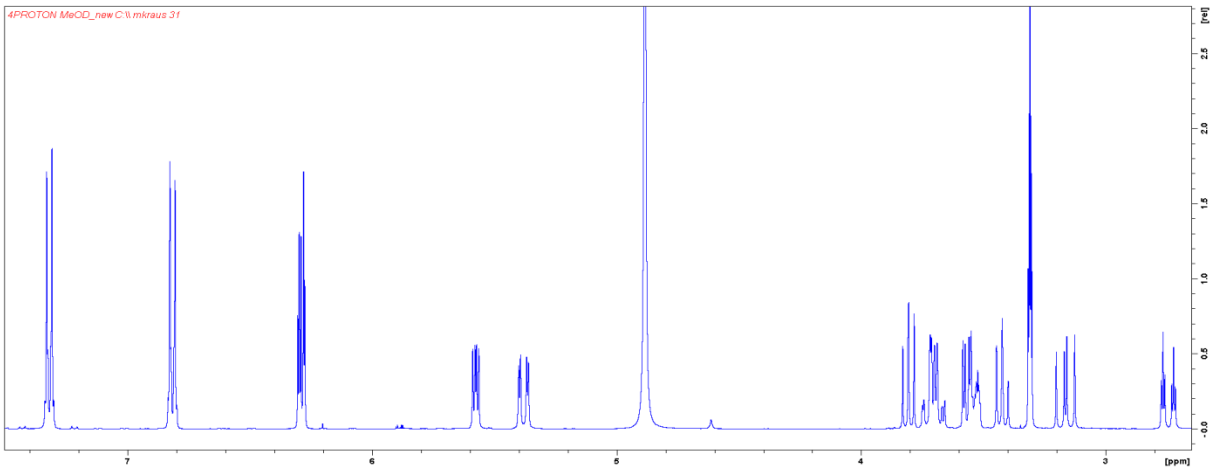

Fig. S 38 ^{1}H-NMR of Naringenin-7-α-D-glucoside

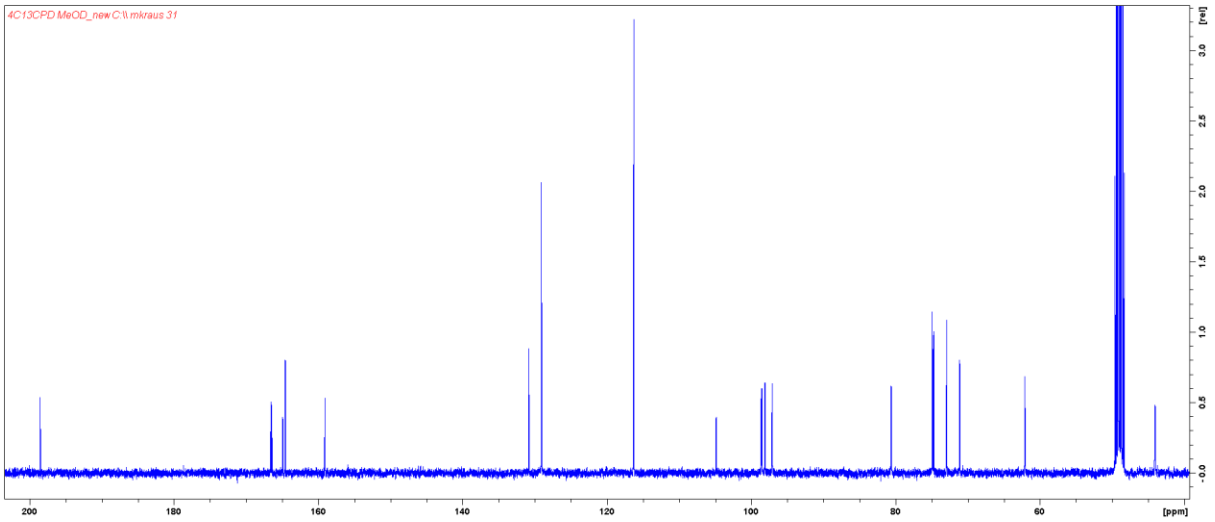

Fig. S 39 ^{13}C-NMR of Naringenin-7-α-D-glucoside

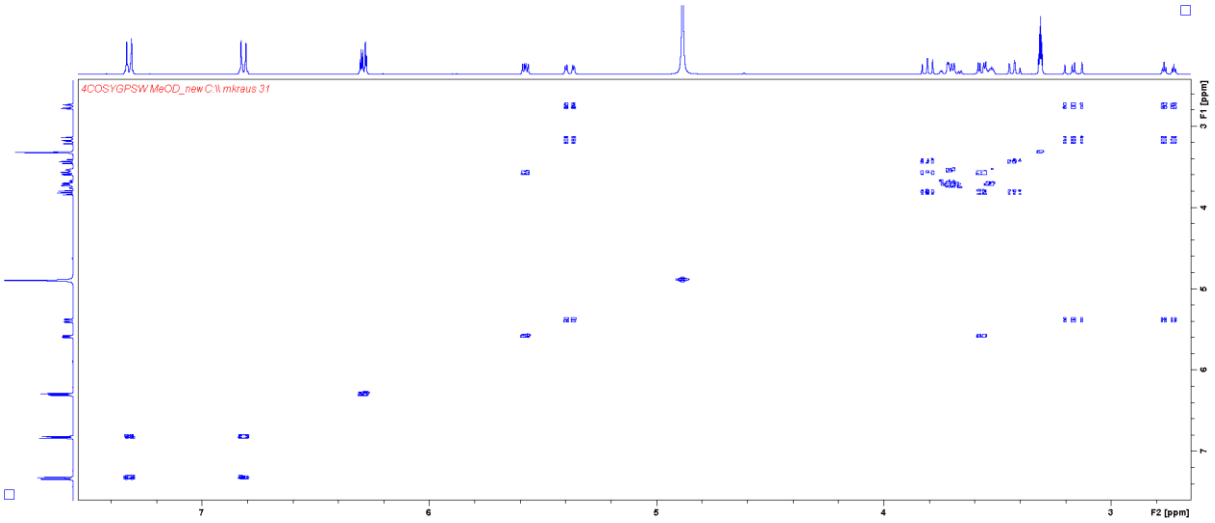

Fig. S 40 COSY of Naringenin-7-α-D-glucoside

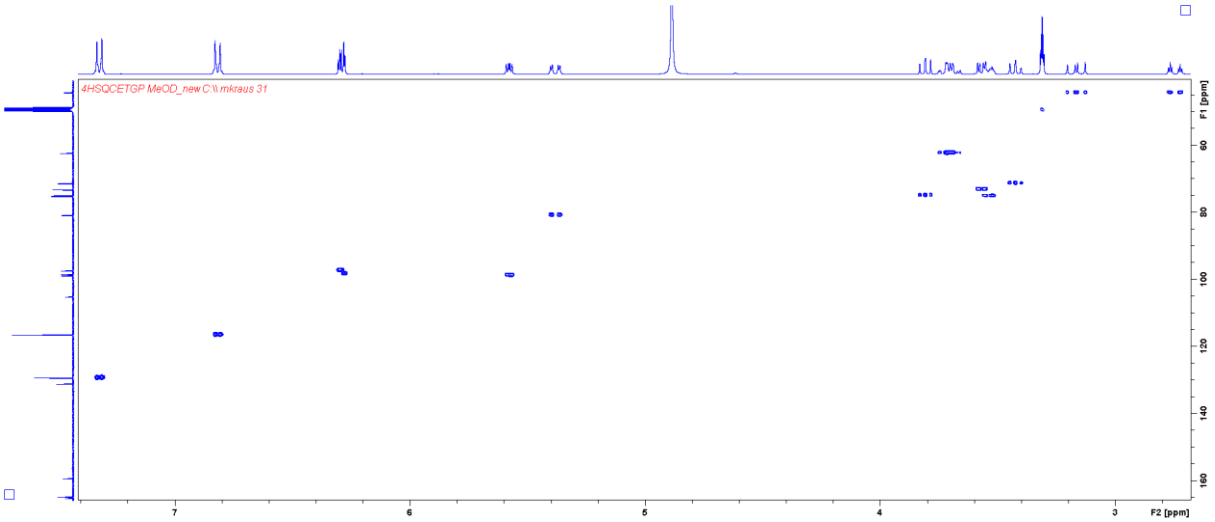

Fig. S 41 HSQC of Naringenin-7-α-D-glucoside

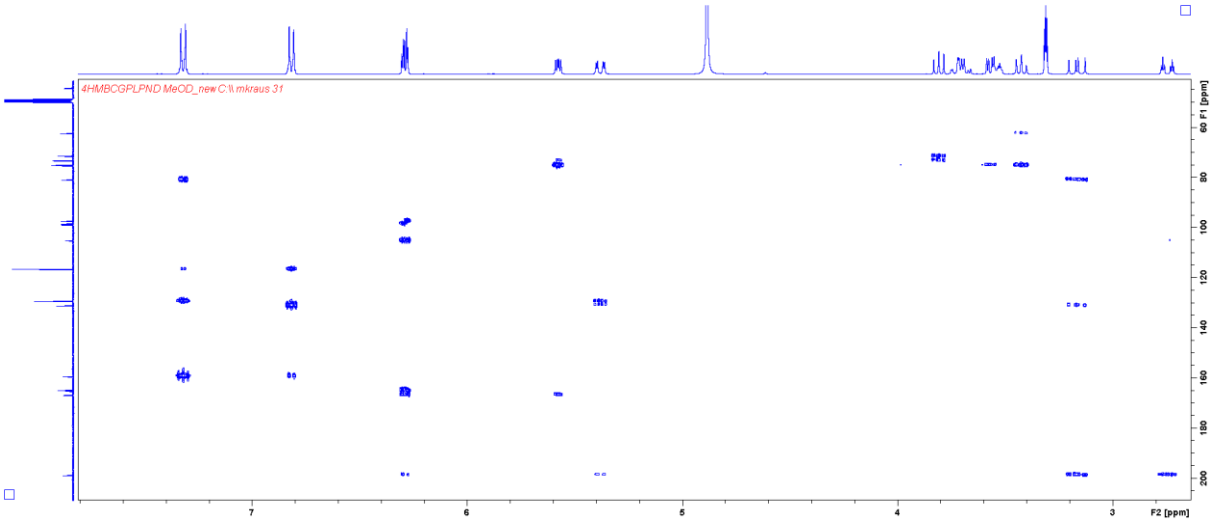

Fig. S 42 HMBC of Naringenin-7-α-D-glucoside

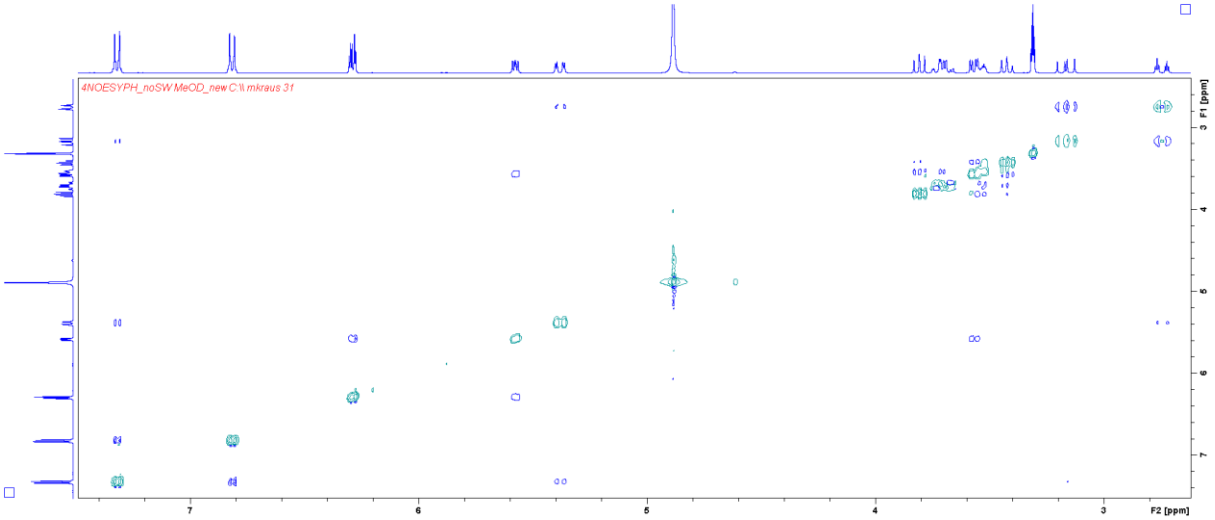

Fig. S 43 NOESY of Naringenin-7-α-D-glucoside

Quercetin-3'-α-D-glucoside

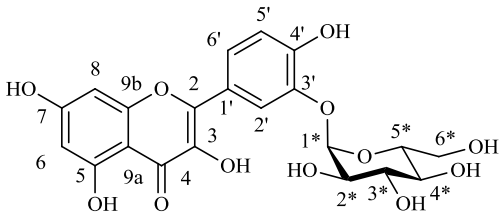

^{1}H-NMR (400 MHz; CD_3OD): δ= 8.16 (d, 1H, *J* = 2.1 Hz, *H*-2‘), 7.86-7.83 (dd, 1H, *J* = 8.5, 2.2 Hz, *H*-6‘), 6.98-6.96 (d, 1H, *J* = 8.7 Hz, *H*-5‘), 6.41 (d, 1H, *J* = 2.0 Hz, *H*-8), 6.18 (d, 1H, *J* = 2.1 Hz, *H*-6), 5.41-5.40 (d, 1H, *J* = 3.7 Hz, *H*-1*), 3.93-3.89 (dd, 1H, *J* = 9.0 Hz, *H*-3*), 3.88-3.79 (m 3H, *H*-5*, *H*-6*), 3.65-3.61 (dd, 1H, *J* = 9.7, 3.7 Hz, *H*-2*), 3.54-3.49 (d, 1H, *J* = 9.0 Hz, *H*-4*) ppm.

^{13}C-NMR (100 MHz CD_3OD): δ= 177.4 (*C*-4), 165.6 (*C*-7), 162.5 (*C*-5), 158.2 (*C*-9b), 151.0 (*C*-4‘), 147.5 (*C*-2),146.3 (*C*-3‘), 137.4 (*C*-3), 125.3 (*C*-6‘), 124.3 (*C*-1‘), 119.1 (*C*-2‘), 117.2 (*C*-5‘), 104.5 (*C*-9a), 101.8 (C-1*), 99.3 (*C*-6), 94.6 (*C*-8), 74.9 (*C*-3*),74.6 (*C*-5*), 73.4 (*C*-2*), 71.1 (*C*-4*), 62.2 (*C*-6*) ppm.

MS (ESI positive):

Ion Formula:	$C_{21}H_{20}O_{12}Na^+$ $[M+Na]^+$
m/z calculated:	487.08470
m/z experimental:	487.08486
error [ppm]:	-0.34

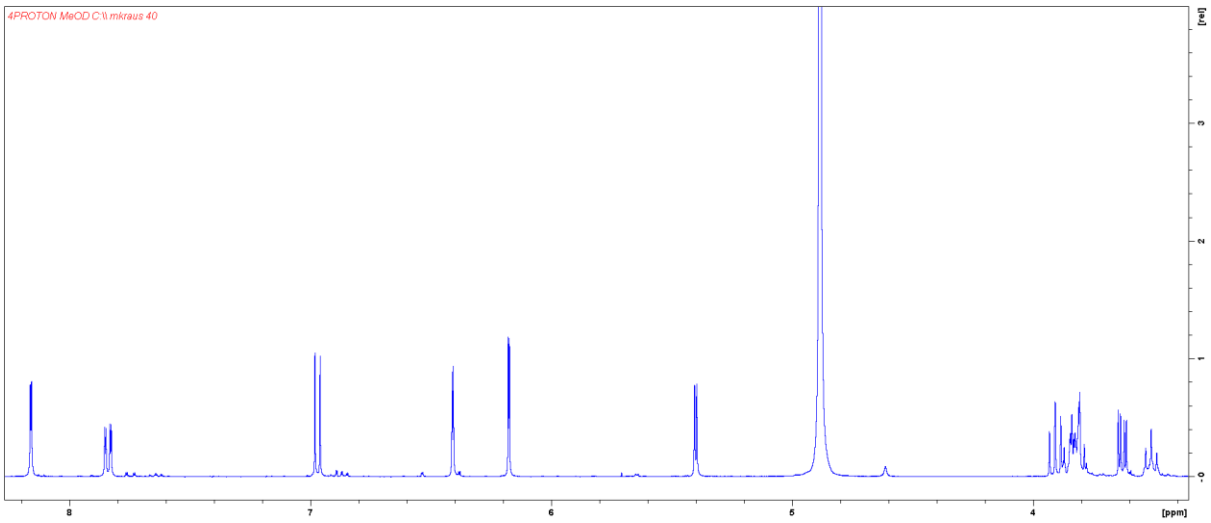

Fig. S 44 ^{1}H-NMR of Quercetin-3'-α-D-glucoside

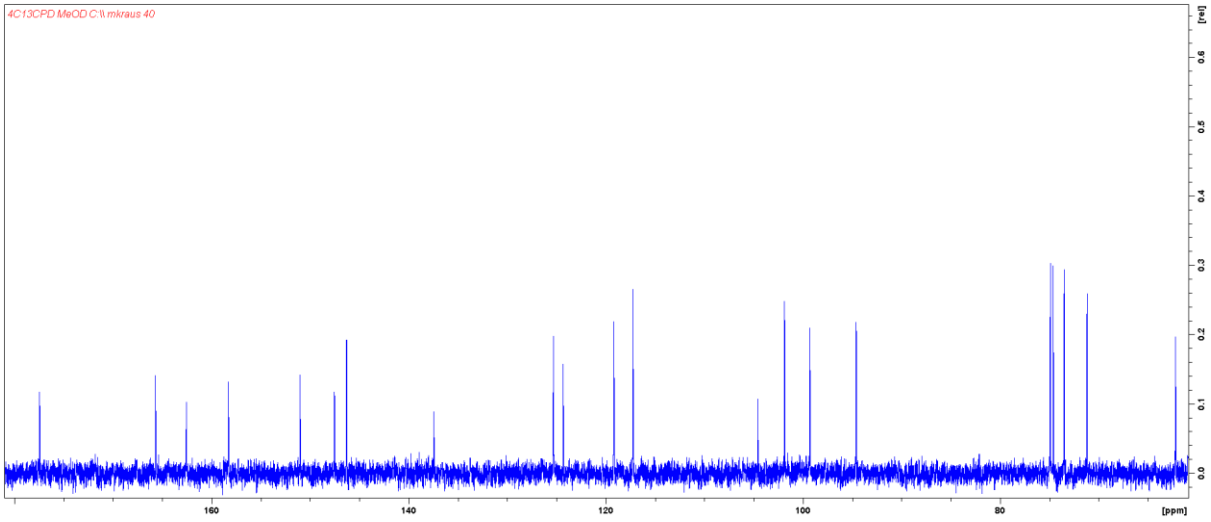

Fig. S 45 ^{13}C-NMR of Quercetin-3'-α-D-glucoside

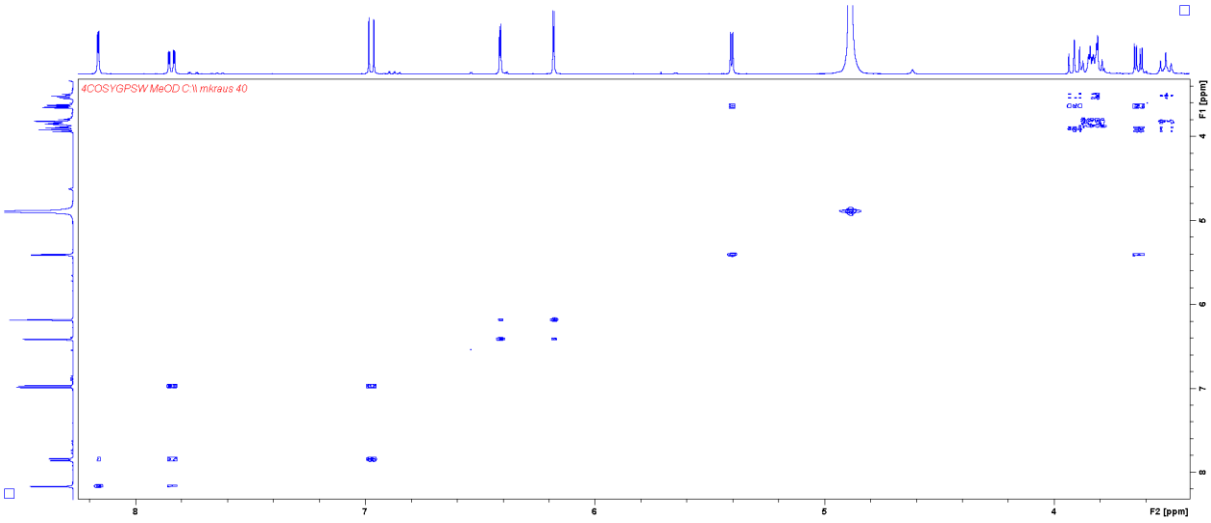

Fig. S 46 COSY of Quercetin-3'-α-D-glucoside

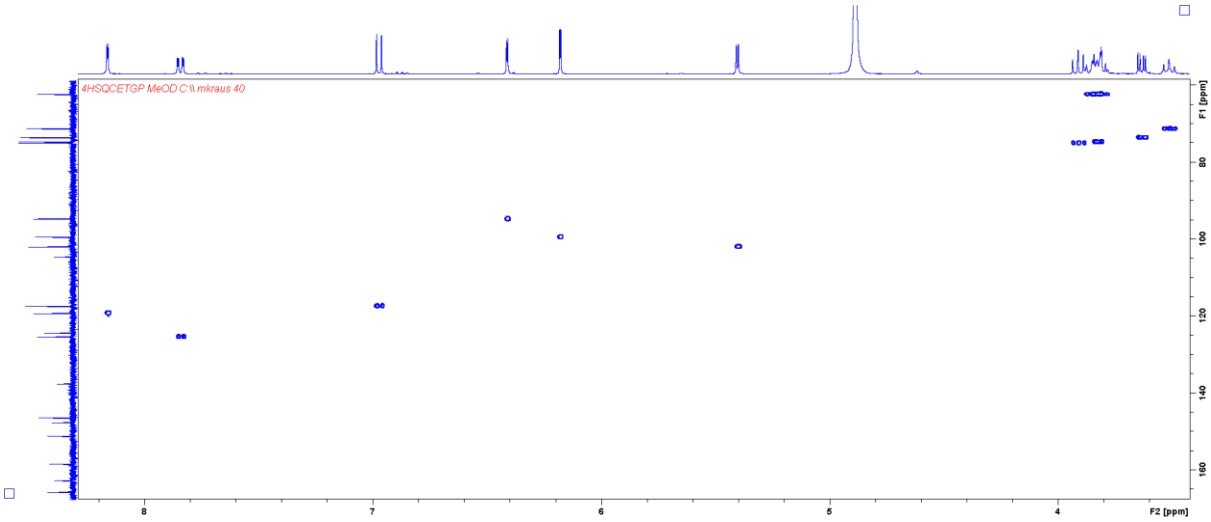

Fig. S 47 HSQC of Quercetin-3'-α-D-glucoside

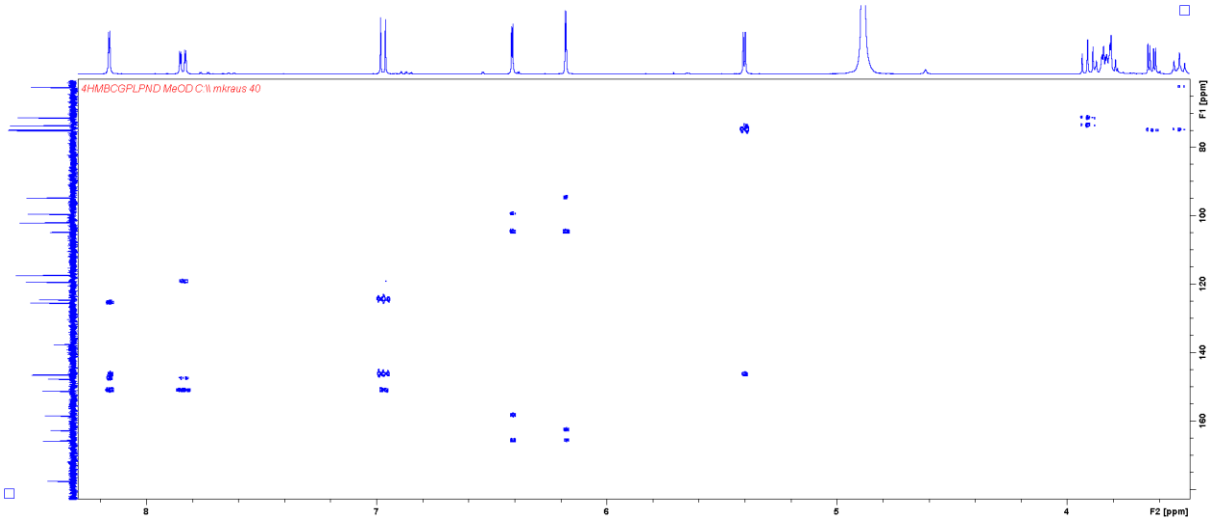

Fig. S 48 HMBC of Quercetin-3'-α-D-glucoside

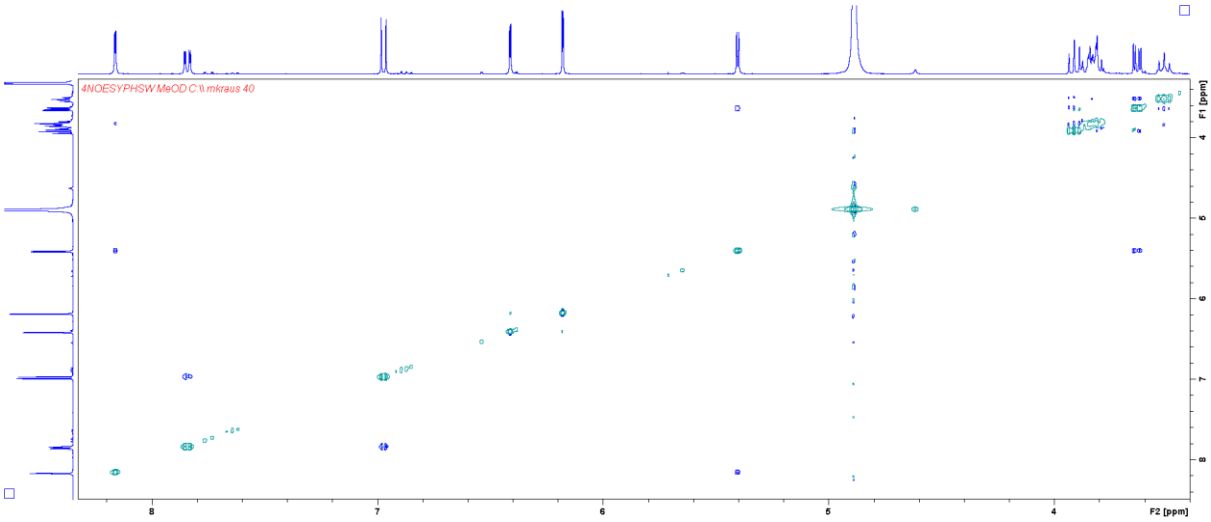

Fig. S 49 NOESY of Quercetin-3'-α-D-glucoside

Quercetin-3',7-α-D-diglucoside-undecaacetate

To determine the linkage of the second (#) glucose moiety quercetin-3',7-α-D-diglucosid was acetylated in order to allow identification of *H-6* and *H-8*

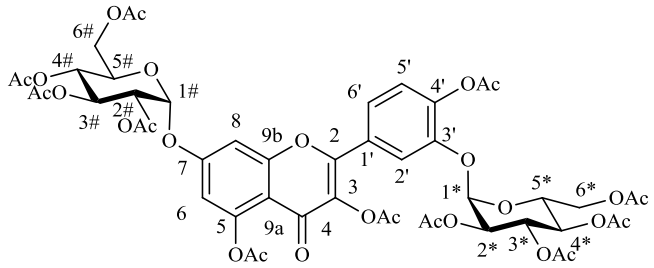

^{1}H-NMR (400 MHz; $CDCl_3$): δ= 7.73 (d, 1H, *J* = 2.0 Hz, *H*-2'), 7.58 (dd, 1H, *J* = 8.4, 2.0 Hz, *H*-6'), 7.22 (d, 1H, *J* = 8.4 Hz, *H*-5'), 7.18 (d, 1H, *J* = 2.4 Hz, *H*-6), 6.84 (d, 1H, *J* = 2.4 Hz, *H*-8), 5.89 (d, 1H, *J* = 3.6 Hz, *H*-1#), 5.81 (d, 1H, *J* = 3.5 Hz, *H*-1*), 5.69-5.62 (m, 2H, *H*-3#, *H*-3*), 5.22-5.16 (m, 2H, *H*-4#, *H*-4*), 5.11-5.08 (dd, 1H, *J* = 10.3, 3.6 Hz, *H*-2#), 5.02 (dd, 1H, *J* = 10.4, 3.5 Hz, *H*-2*), 4.31-4.21 (m, 2H, *H*-6#, *H*-6*), 4.12-4.02 (m, 4H, *H*-5#, *H*-6#, *H*-5*, *H*-6*), 2.43 (s, 3H, COC*H*$_3$), 2.43 (s, 3H, COC*H*$_3$), 2.33 (s, 3H, COC*H*$_3$), 2.09 (s, 3H, COC*H*$_3$), 2.08 (s, 3H, COC*H*$_3$), 2.06 (s, 3H, COC*H*$_3$), 2.055 (s, 3H, COC*H*$_3$), 2.05 (s, 3H, COC*H*$_3$), 2.04 (2s, 6H, COC*H*$_3$), 2.00 (s, 3H, COC*H*$_3$);

^{13}C-NMR (100 MHz; $CDCl_3$): δ =170.7, 170.6 170.3 170.2 170.2 170.2 170.0. 169.6, 169.6 169.6 168.8 167.9 (H_3*C*O, *C*-4), 159.9 (*C*-7), 157.8 (*C*-5), 153.6 (*C*-2), 151.1 (*C*-9b), 147.8 (*C*-3') 142.8 (*C*-4') 134.1 (*C*-3) 128.5 (*C*-1'), 123.5 123.4 (*C*-5' und *C*-6') 115.0 (*C*-2'), 112.7 (*C*-9a), 109.8 (*C*-8), 102.4 (*C*-6), 94.8 (*C*-1*) 94.4 (*C*-1#), 70.5 (*C*-2*), 70.0 (*C*-2#), 69.8, 69.5 (*C*-3*, *C*-3#), 69.0. 68,9 (*C*-5*, *C*-5#); 68.0. 67.7 (*C*-4*, *C*-4#), 61.4, 61.3 (*C*-6*, *C*-6#), 21.2, 20.8, 20.8 20.8, 20.7, 20.7, 20.7, 20.7 20.7, 20.7, 20.5 (*C*H_3CO) ppm.

MS (ESI positive, of the non-acetylated compound):

Ion Formula:	$C_{27}H_{30}O_{17}Na^+$ $[M+Na]^+$
m/z calculated:	649.13752
m/z experimental:	649.13675
error [ppm]:	1.19

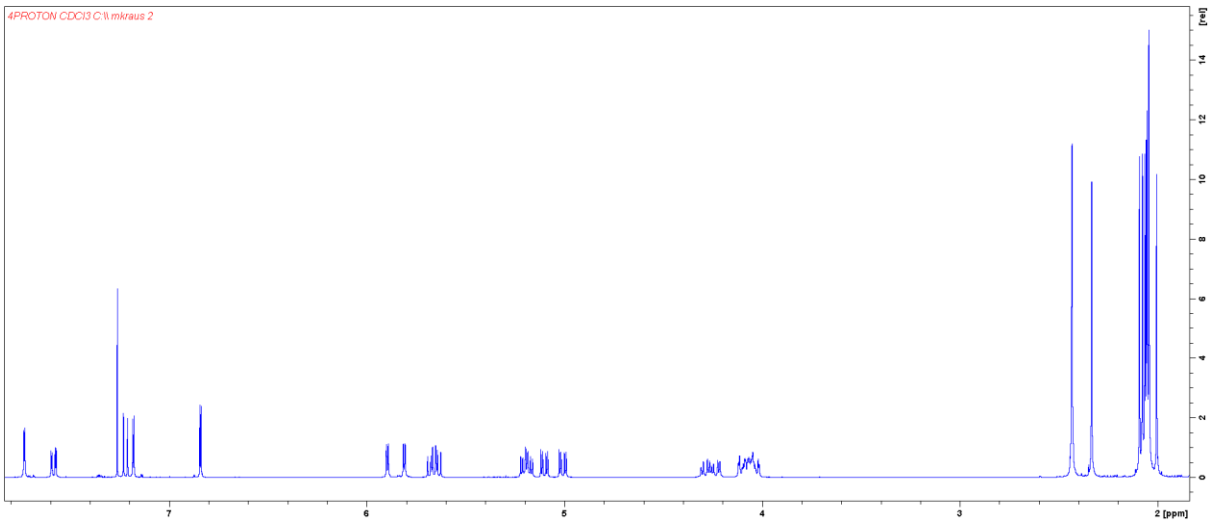

Fig. S 50 ^{1}H-NMR of Quercetin-3',7-α-D-diglucoside-undecaacetate

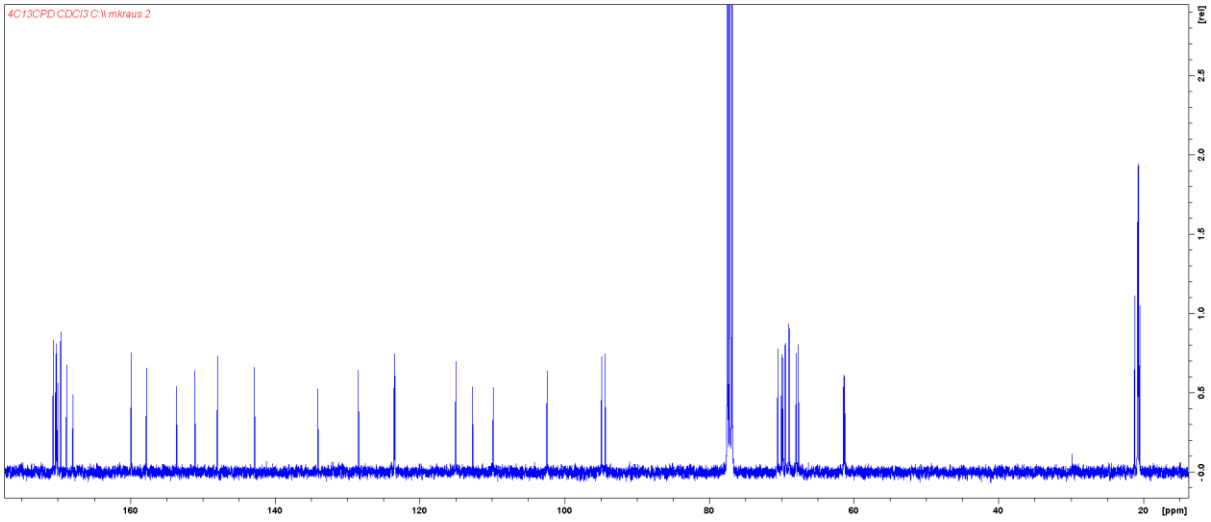

Fig. S 51 ^{13}C-NMR of Quercetin-3',7-α-D-diglucoside-undecaacetate

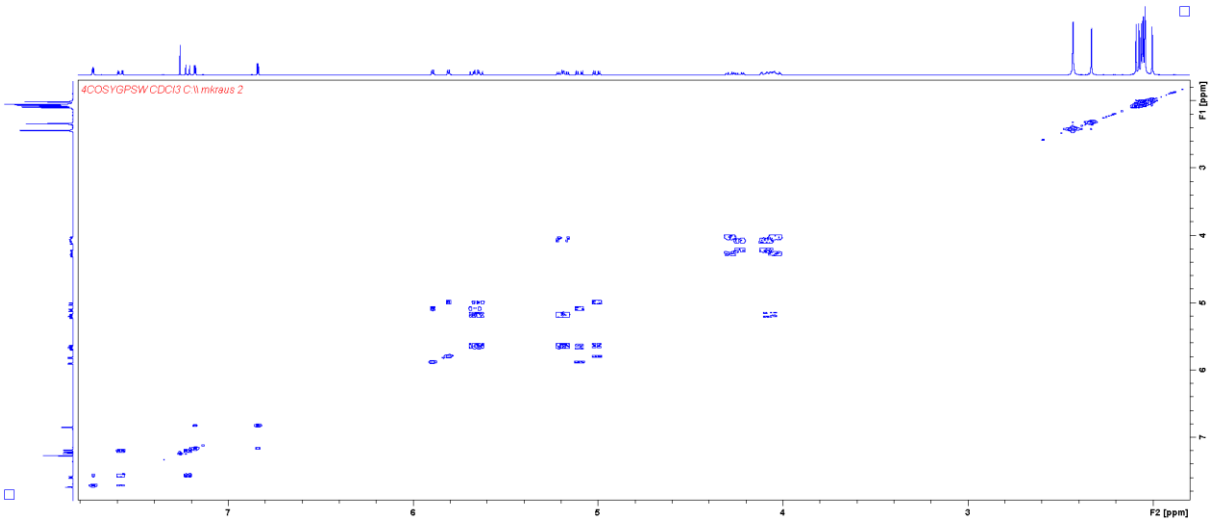

Fig. S 52 COSY of Quercetin-3',7-α-D-diglucoside-undecaacetate

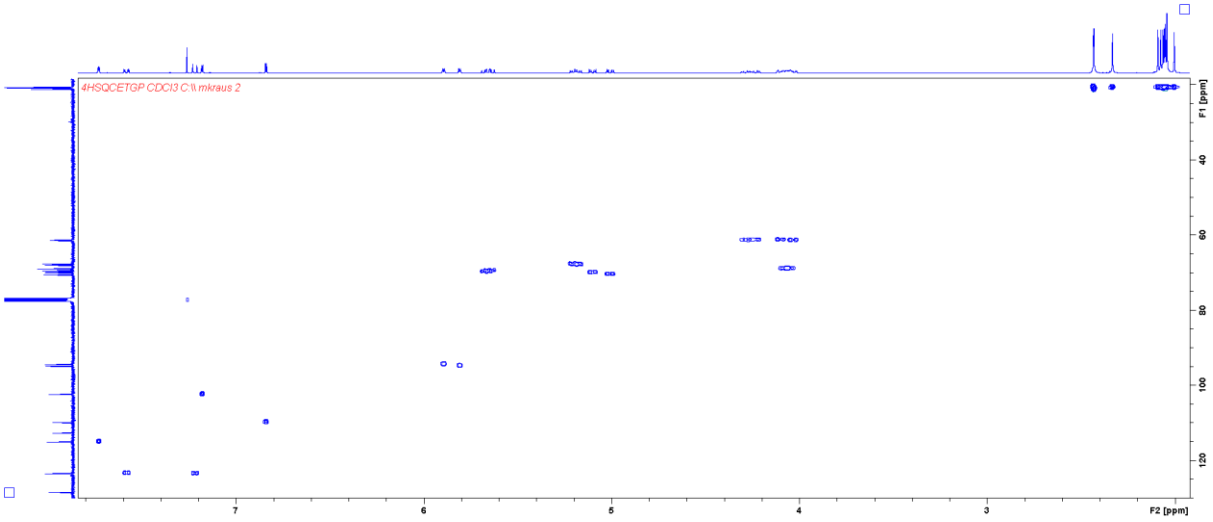

Fig. S 53 HSQC of Quercetin-3',7-α-D-diglucoside-undecaacetate

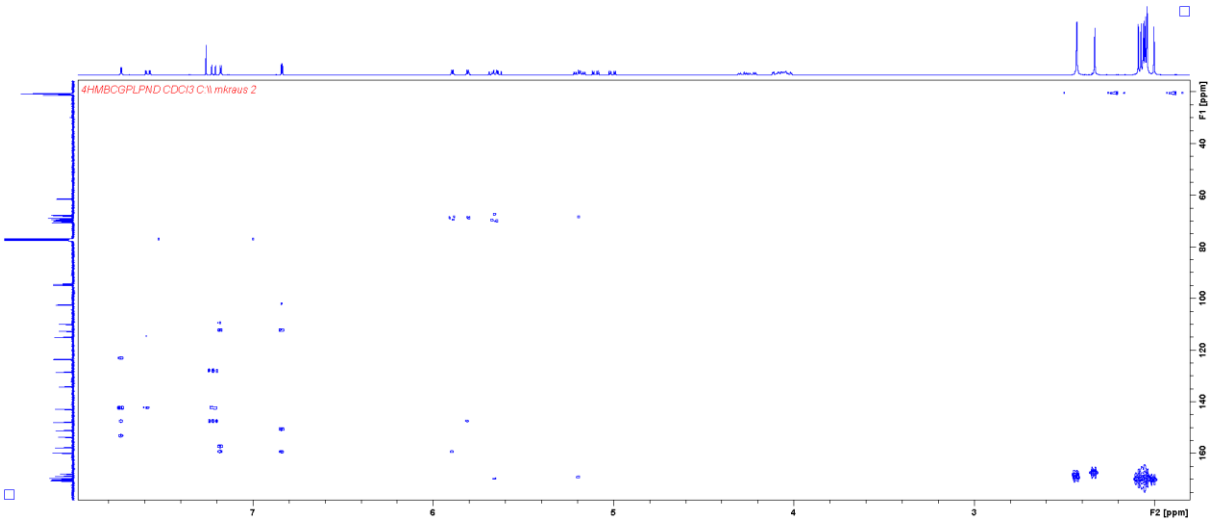

Fig. S 54 HMBC of Quercetin-3',7-α-D-diglucoside-undecaacetate

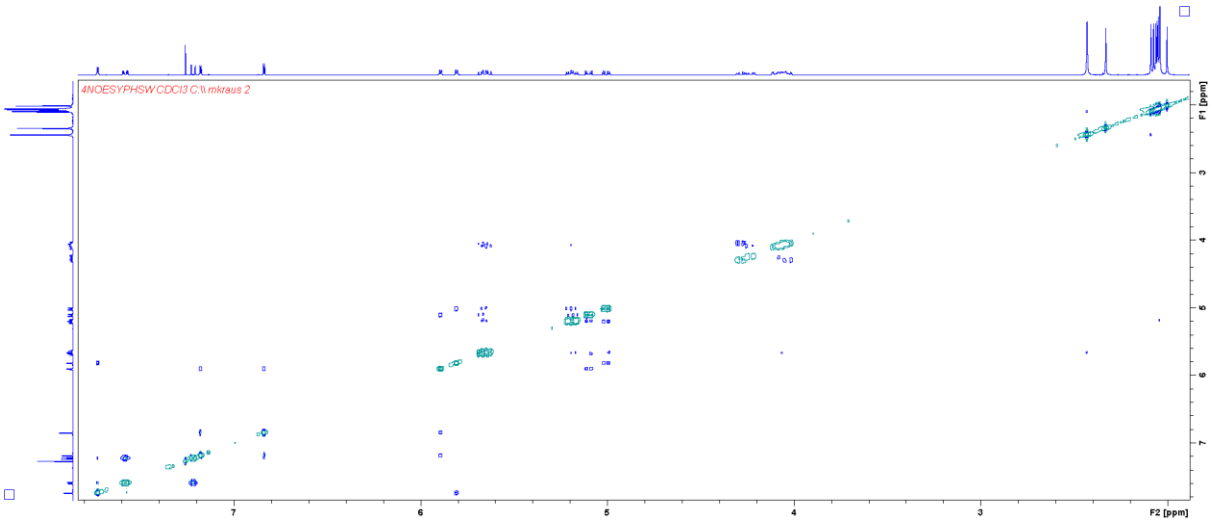

Fig. S 55 NOESY of Quercetin-3',7-α-D-diglucoside-undecaacetate

Fisetin-3'-α-D-glucoside

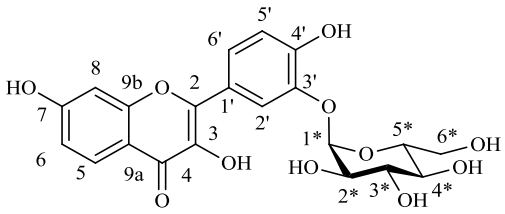

[1]H-NMR (400 MHz; CD_3OD): δ= 8.21-8.20 (d, 1H, *J* = 2.1 Hz, *H*-2'), 8.00-7.97 (d, 1H, *J* = 8.5 Hz, *H*-5), 7.90-7.87 (dd, 1H, *J* = 8.6, 2.1 Hz, *H*-6'), 7.00-6.98 (d, 1H, *J* = 8.6 Hz, *H*-5'), 6.95-6.94 (d, 1H, *J* = 2.1 Hz, *H*-8) 6.93-6.90 (dd, 1H, *J* = 8.7, 2.1 Hz, *H*-6), 5.41-5.40 (d, 1H, *J* = 3.7 Hz, *H*-1*), 3.94-3.89 (dd, 1H, *J*= 9.3, 9.3 Hz, *H*-3*), 3.88-3.79 (m, 3H, *H*-5*, *H*-6*), 3.65-3.62 (dd, 1H, *J* = 9.5, 3.8 Hz, *H*-2*),3.53-3.49 (dd, 1H, *J* = 9.0. 9.0 Hz, *H*-4*) ppm.

[13]C-NMR (100 MHz CD_3OD): δ= 174.4 (*C*-4), 164.3 (*C*-7), 158.6 (*C*-9b), 150.9 (*C*-4'), 147.0 (*C*-2), 146.3 (*C*-3'), 138.7 (*C*-3), 127.5 (*C*-5), 125.3 (*C*-6'), 124.5 (*C*-1') 119.2 (*C*-2'), 117.2 (*C*-5'), 116.0 (*C*-6), 115.5 (*C*-9a) 103.1 (*C*-8), 101.9 (*C*-1*), 74.9 (*C*-3*), 74.6 (*C*-5*), 73.5 (*C*-2*), 71.2 (*C*-4*), 62.2 (*C*-6*) ppm.

MS (ESI positive):

Ion Formula:	$C_{21}H_{20}O_{11}Na^+$ $[M+Na]^+$
m/z calculated:	471.08978
m/z experimental:	471.08839
error [ppm]:	2.95

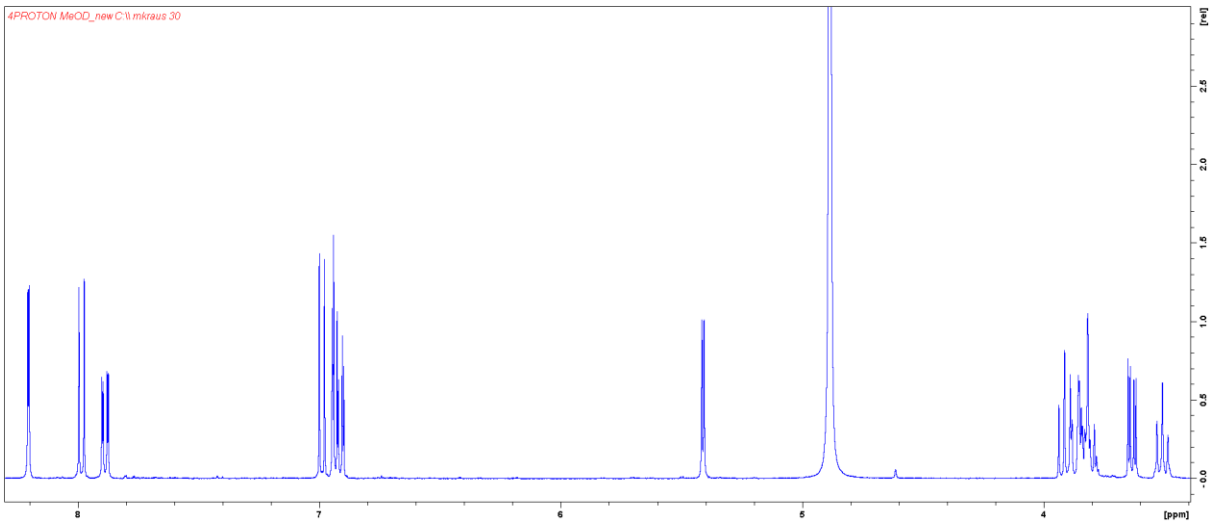

Fig. S 56 ^{1}H-NMR of Fisetin-3'-α-D-glucoside

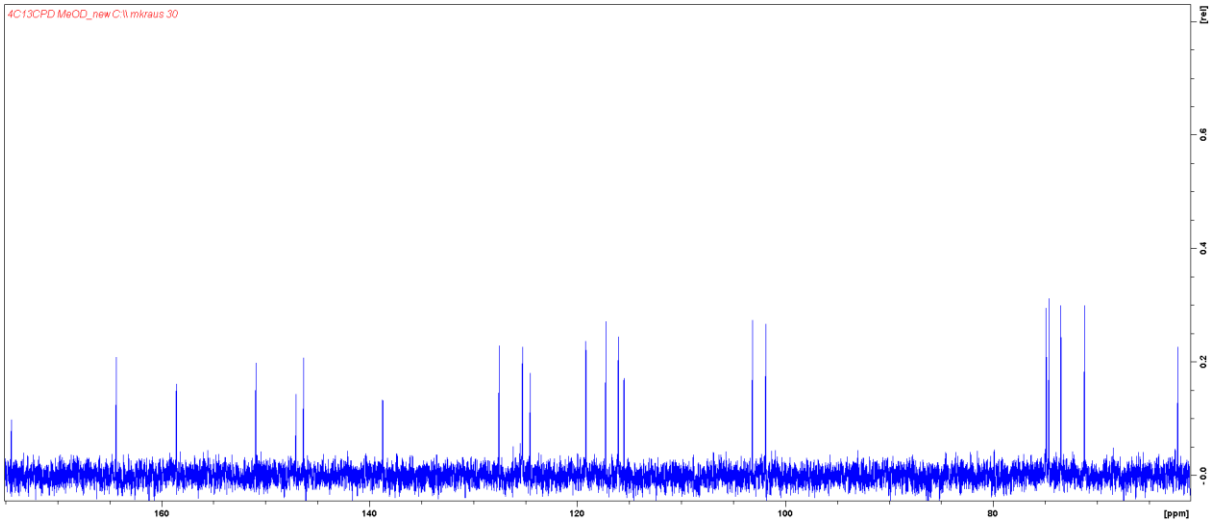

Fig. S 57 ^{13}C-NMR of Fisetin-3'-α-D-glucoside

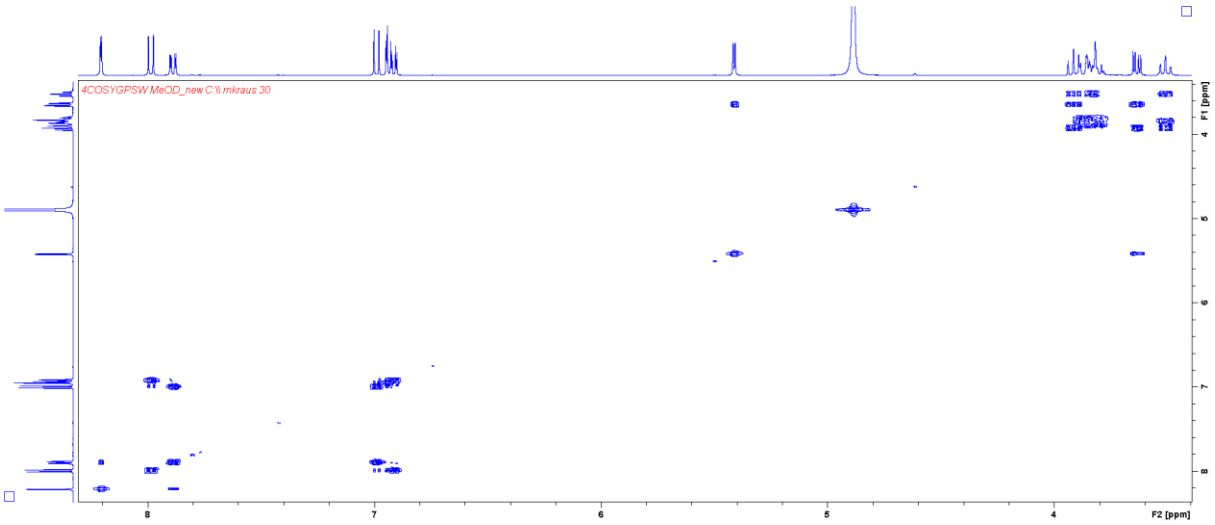

Fig. S 58 COSY of Fisetin-3'-α-D-glucoside

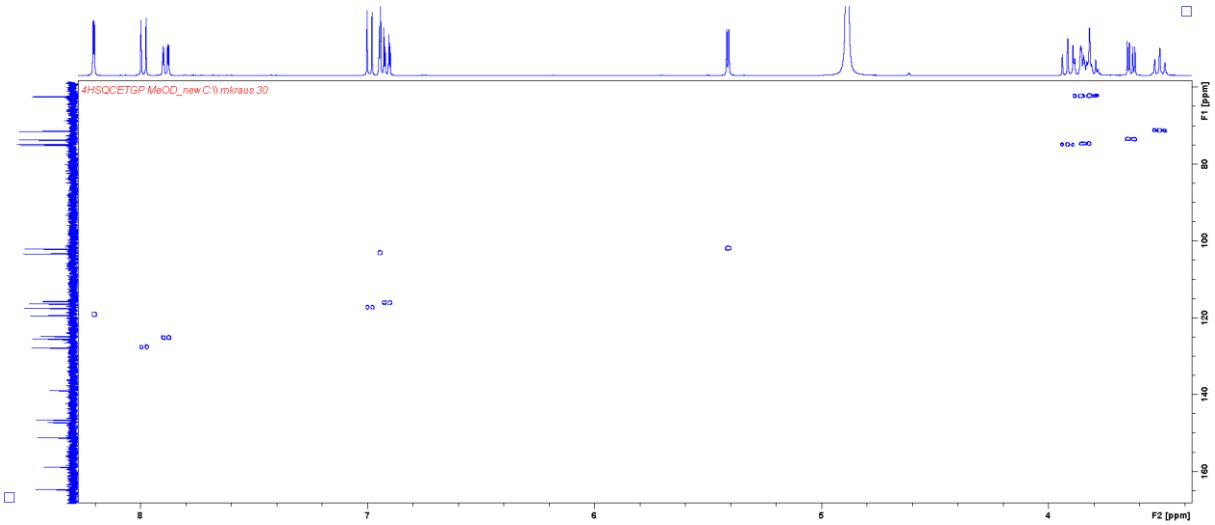

Fig. S 59 HSQC of Fisetin-3'-α-D-glucoside

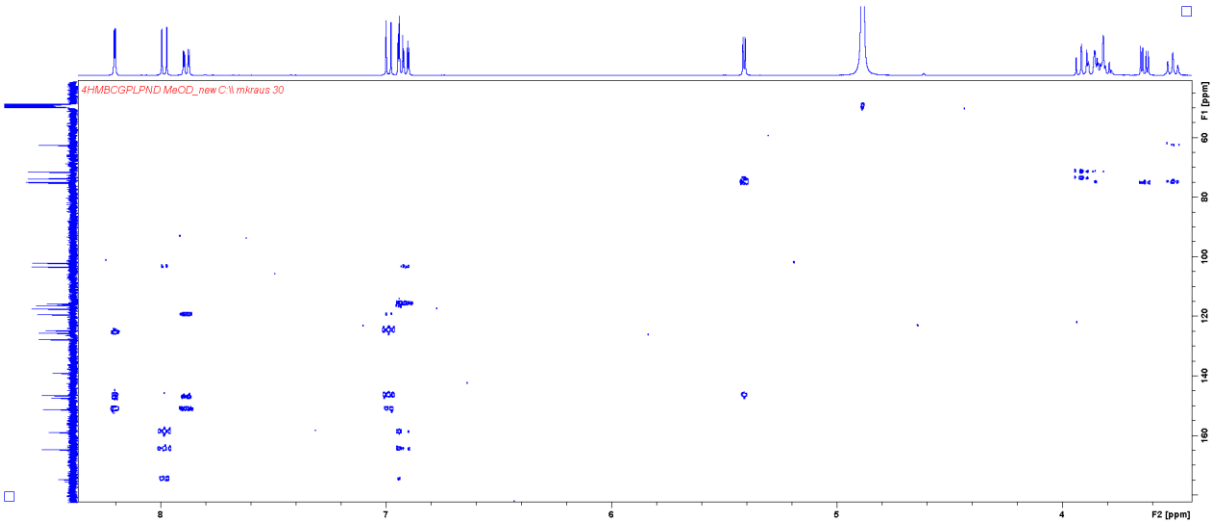

Fig. S 60 HMBC of Fisetin-3'-α-D-glucoside

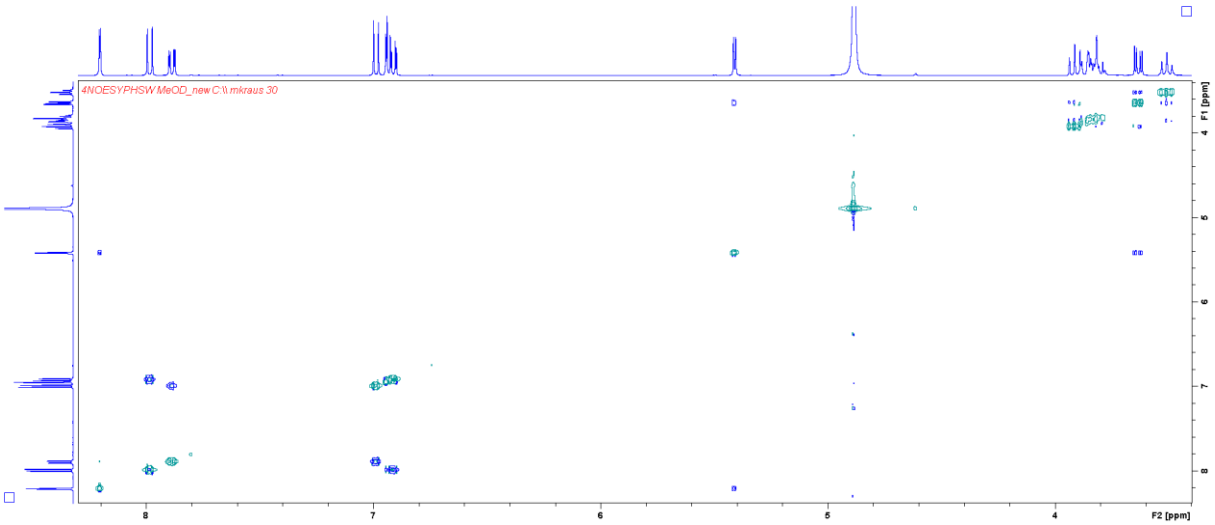

Fig. S 61 NOESY of Fisetin-3'-α-D-glucoside

4.2 NMR- and MS-Data of previously reported compounds:

Nigerose:[2]

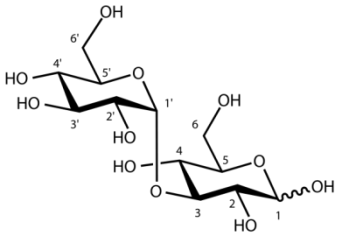

α-anomer (40%):

^{1}H NMR (600 MHz, D_2O) δ 5.37 (d, *J* = 3.9 Hz, 1H, H-1'), 5.23 (d, *J* = 3.8 Hz, 1H, H-1), 4.02 (m, 1H, H-5'), 3.87-3.81 (m, 4H, H-3, H-5, H-6a, H-6'a), 3.80-3.73 (m, 2H, H-6'b, H-6b), 3.75 (dd, *J* = 9.5, 9.5 Hz, 1H, H-3'), 3.64 (dd, *J* = 9.5, 7.0 Hz, 1H, H-4), 3.62 (dd, *J* = 9.8, 3.9 Hz, 1H, H-2), 3.57 (dd, *J* = 9.9, 5.1 Hz, 1H, H-2'), 3.46 (dd, *J* = 9.2, 10.2 Hz, 1H, H-4') ppm.

^{13}C NMR (150 MHz, D_2O) δ 100.25 (C-1'), 93.43 (C-1), 80.73 (C-3), 74.05 (C-3'), 72.93 (C-5'), 72.89 (C-2'), 72.38 (C-5), 71.29, 71.22 (C-2, C-4), 70.60 (C-4'), 61.56, 61.53 (C-6, C-6') ppm.

ß-anomer (60%):

^{1}H NMR (600 MHz, D_2O) δ 5.36 (d, *J* = 3.9 Hz, 1H, H-1'), 4.66 (d, *J* = 8.0 Hz, 1H, H-1), 4.02 (m, 1H, H-5'), 3.89 (dd, *J* = 2.2, 12.3 Hz, 1H, H-6a), 3.84 (dd, *J* = 12.7, 2.2 Hz, 1H, H-6'a), 3.78 (ddd, *J* = 12.7, 8.4, 4.0 Hz, 1H, H-6'b), 3.74 (dd, *J* = 9.6, 9.6 Hz, 1H, H-3'), 3.72 (dd, *J* = 12.4, 5.9 Hz, 1H, H-6b), 3.64 (dd, *J* = 9.5, 7.0 Hz, 1H, H-3), 3.63 (m, 1H, H-4), 3.56 (dd, *J* = 9.8, 4.1 Hz, 1H, H-2'), 3.47 (ddd, 9.7, 5.4, 2.8, 1H, H-5), 3.44 (dd, *J* = 10.6, 9.5 Hz, 1H, H-4'), 3.33 (dd, *J* = 9.3, 8.0 Hz, 1H, H-2) ppm.

^{13}C NMR (150 MHz, D_2O) δ 100.21 (C-1'), 97.16 (C-1), 83.25 (C-3), 76.84 (C-5), 74.08 (C-3'), 74.03 (C-2), 72.90 (C-5'), 72.82 (C-2'), 71.25 (C-4), 70.47 (C-4'), 61.74 (C-6), 61.37 (C-6') ppm.

Resveratrol-3-*O*-α-D-glucoside[1]

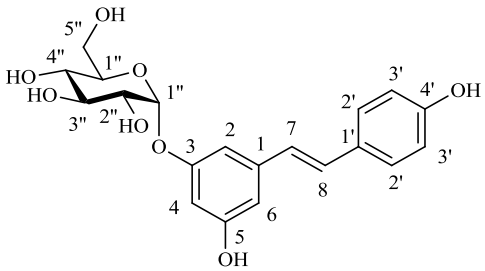

^{1}H-NMR (400 MHz; CD_3OD): δ= 7.38-7.36 (m, 2H, *J*= *8.2* Hz, *H*-2'), 7.03-6.99 (d, 1H, *J*= 16.4 Hz, *H*-8), 6.87-6.83 (m, 2H, *H*-2, *H*-7), 6.78 -6.76 (m, 2H, *J*= 8.7 Hz, *H*-3'), 6.63-6.62 (dd, 1H, *H*-6), 6.52-6.51 (dd, 1H, *H*-4), 5.48-5.47 (d, 1H, *J*= 3.7 Hz, *H*-1''), 3.88 (dd, 1H, *J*=9.7Hz 9.0 Hz, *H*-3''), 3.80-3.67 (m, 3H, *H*-5'', *H*-6''), 3.59-3.55 (dd, 1H, *J*= 9.8, *J*=3.7 Hz, *H*-2''), 3.47-3.42 (dd, 1H, *J*= 9.7 Hz, *J*= 8.2 Hz, *H*-4) ppm.

^{13}C-NMR (100 MHz; CD_3OD): δ= 159.9 (*C*-3), 159.6 (*C*-5), 158.5 (*C*-4'), 141.4 (*C*-1), 130.3 (*C*-8), 129.9 (*C*-1'), 128.9 (*C*-2'), 126.7 (*C*-7), 116.5 (*C*-3'), 108.3 (*C*-6), 107.4 (*C*-4), 104.5 (*C*-2), 99.3 (*C*-1''), 75.0 (C-5''), 74.3 (C-3''), 73.3 (*C*-2'') 71.5 (*C*-4''), 62.3 (*C*-6'') ppm.

MS (ESI positive):

Ion Formula:	$C_{20}H_{22}O_8Na^+$ $[M+Na]^+$
m/z calculated:	413.12069
m/z experimental:	413.12034
error [ppm]:	0.84

(+)-catechin-3‘-*O*-α-D-glucopyranoside[1]

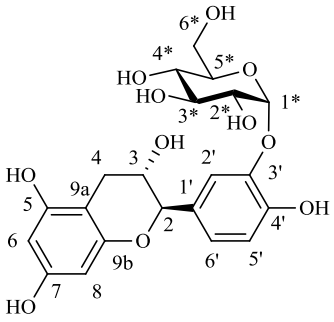

^{1}H-NMR (400 MHz; CD_3OD): δ= 7.32-7.31 (d, 1H, *J*= 2.0 Hz, *H*-2‘),7.00-6.97 (d, 1H, *J*= 8.6 Hz, 2.0 Hz, *H*-6‘), 6.86-6.84 (d, 1H, *J*= 8.3 Hz, *H*-5‘), 5.93-5.84 (d, 1H, *J*= 2.4 Hz, *H*-6), 5.85-5.84 (d, 1H, *J*= 2.2 Hz, *H*-8),5.34-5.33 (d, 1H, *J*= 3.7 Hz, *H*-1#), 4.58-4.56 (d, 1H, *J*= 8.0 Hz, *H*-2), 4.02-3.96 (m, 1H, *H*-3), 3.90-3.85 (dd, 1H, *J*= 9.3 Hz, *H*-3*), 3.82 – 3.72 (m, 3H, *H*-5*, *H*-6*), 3.60-3.56 (dd, 1H, *J*= 9.7 Hz 3.7 Hz, *H*-2*), 3.47-3.43 (d, 1H, *J*= 9.1 Hz, *H*-4*), 2.92-2.87 (dd, 1H, *J*= 16.2 Hz 5.6 Hz, *H*-4a), 2.53-2.47 (dd, 1H, *J*= 16.2 Hz, *H*-4b) ppm.

^{13}C-NMR (100 MHz; CD_3OD): δ= 157.9 (C7), 157.6 (C5), 156.9 (C9a), 148.7 (C4’) 146.3 (C3’), 132.3 (C1’) 124.0 (C6’), 118.6 (C2’), 116.9 (C5’) 101.6 (C1*), 100.9 (C9b), 96.3 (C6), 95.5 (C8), 82.8 (C2), 74.9 (C3*), 74.5 (C5*), 73.5 (C2*), 71.2 (C4*), 68.8 (C3), 62.2 (C6*), 29.0 (C4) ppm.

MS (ESI positive):

Ion Formula:	$C_{21}H_{24}O_{11}Na^+$ $[M+Na]^+$
m/z calculated:	475.12108
m/z experimental:	475.12102
error [ppm]:	0.14

(+)-catechin-3‘,5-*O*-α-D-diglucoside[1]

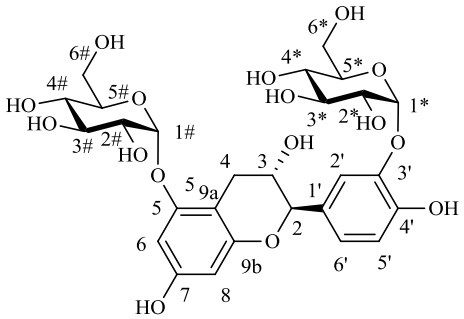

^{1}H-NMR (600 MHz; CD_3OD): δ= 7.30 (d, 1H, *J*= 2.0 Hz, *H*-2‘), 7.00-6.96 (dd, 1H, *J*= 8.3 Hz 2.2 Hz, *H*-6‘),6.86-6.84 (d, 1H, *J*= 8.1 Hz, *H*-5‘), 6.34-6.33 (d, 1H, *J*= 2.3 Hz, *H*-6), 6.01 (d, 1H, *J*= 2.3 Hz, *H*-8), 5.50 (d, 1H, *J*= 3.4 Hz, *H*-1#), 5.32 (d, 1H, *J*= 3.6 Hz, *H*-1*), 4.65-4-64 (d, 1H, *J*= 7.7 Hz, *H*-2), 4.05-4.01 (m, 1H, *H*-3), 3.89-3.87 (m, 2H, *H*-3*, *H*-3#), 3.80-3.70 (m, 5H, *H*-6*, *H*-6#, *H*-2*), 3.60-3.57 (m, 3H, *H*-4*, *H*-4#, *H*-

2#), 3.47-3.43 (m, 2H, *H*-5*, *H*-5#), 2.92-2.89 (dd, 1H, *J*= 16.2 Hz 5.4 Hz, *H*-4a), 2.72-2.68 (dd, 1H, *J*= 16.4 Hz, 7.9 Hz, *H*-4b) ppm.

^{13}C-NMR (150 MHz; CD_3OD): δ= 158.1 (C7), 157.2 (C5), 156.6 (C9a), 148.7 (C4‘), 146.3 (C3‘), 132.2 (C1’) 123.8 (C6’) 118.4 (C2’), 116.9 (C5’), 103.2 (C9b), 101.6 (C1*), 98.7 (C1#), 97.9 (C8) 96.8 (C6) 82.6 (C2), 74.9 74.86 (C3*, C3#), 74.5, 74.5 (C2*, C2#), 73.4 73.3 (C4*, C4#), 71.3 71.2 (C5*, C5#), 68.5 (C3), 62.2 62.18 (C6*, C6#) 28.5 (C4) ppm.

The spectra reveal the presence of a second, uncharacterized product, possibly a regioisomer.

MS (ESI positive):

Ion Formula:	$C_{27}H_{34}O_{16}Na^+$ $[M+Na]^+$
m/z calculated:	637.17391
m/z experimental:	637.17462
error [ppm]:	-1.12

(-)-epicatechin-3‘-*O*-α-D-glucopyranoside[1]

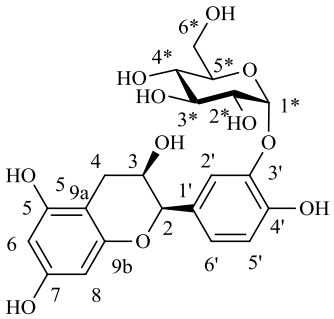

^{1}H-NMR (400 MHz; CD_3OD): δ= 7.43 (d, 1H, *J*= 2.2 Hz, *H*-2‘), 7.08-7.05 (dd, 1H, *J*= 8.2 Hz, 2.0 Hz, *H*-6‘), 6.85-6,83 (d, 1H, *J*= 8.2 Hz, *H*-5‘), 5.94-5.92 (m, 2H, *H*-6, *H*-8), 5.36-5.35 (d, 1H, *J*= 3.8 Hz, *H*-1*), 4.86 (s, 1H, *H*-2), 4.20-4.18 (m, 1H, *H*-3), 3.90-3.85 (dd, 1H, *J*= 9.2 Hz, *H*-3*), 3.84-3.80 (m, 1H, *H*-6*a), 3.80-3.76 (m, 1H, *H*-5*), 3.76-3.70 (m, 1H, *H*-6*b), 3.59-3.56 (dd, 1H, *J*= 9.7 Hz, 3.8 Hz, *H*-2*), 3.44-3.40 (dd, 1H, *J*= 9.6 Hz, 9.1 Hz, *H*-4*), 2.90-2.89 (dd, 1H, *J*= 16.8 Hz, 4.6 Hz, *H*-4a), 2.77-2.72 (dd, 1H, *J*= 16.9 Hz, 2.7 Hz, *H*-4b) ppm.

^{13}C-NMR (100 MHz; CD_3OD): δ= 158.0 157.7 157.3 (C9a, C7, C5), 148.1 (C4‘), 146.1 (C3‘), 132.5 (C1’), 123.2 (C6’), 118.1 (C2’), 116.6 (C5’), 101.4 C1*), 100.0 (C9b), 96.4 95.9 (C6, C8), 79.7 (C2), 74.9 (C3*), 74.5 (C5*), 73.5 (C2*), 71.4 (C4*), 67.4 (C3), 62.5 (C6*), 29.4 (C4) ppm.

MS (ESI positive):

Ion Formula:	$C_{21}H_{24}O_{11}Na^+$ $[M+Na]^+$
m/z calculated:	475.12108
m/z experimental:	475.12224
error [ppm]:	-2.45

(-)-epicatechin-5-*O*-α-D-glucopyranoside[1]

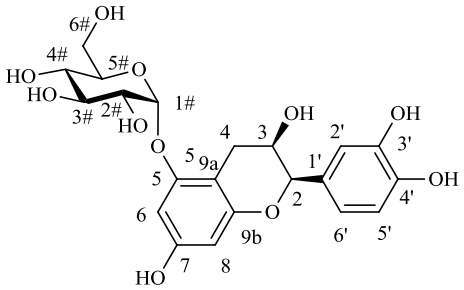

^{1}H-NMR (400 MHz; CD_3OD): δ= 6.97 (d, 1H, *J*= 1.92 Hz, *H*-2‘), 6.81-6.75 (m, 2H, *H*-5‘, *H*-6‘),6.34-6.33 (d, 1H, *J*= 2.32 Hz, *H*-6), 6.07 (d, 1H, *J*= 2.3 Hz, *H*-8), 5.51 (d, 1H, *J*= 3.6 Hz, *H*-1#), 4.83 (s, 1H, *H*-2), 4.19-4.17 (m, 1H, *H*-3), 3.91-3.86 (dd, 1H, *J*= 9.7 Hz 9.1Hz, *H*-3#), 3.72-3.71 (d, 2H, *J*= 3.5 Hz, *H*-6#), 3.63-3.58 (m, 2H, *H*-2#, *H*-5#), 3.50-3.45 (dd, 1H, *J*= 9.9 Hz, 8.8 Hz, *H*-4#), 3.06-3.00 (dd, 1H, *J*= 17.0 Hz 4.6 Hz, *H*-4a), 2.82-2.77 (,m, 1H, *J*= 17.1 Hz, 2.9 Hz, *H*-4b) ppm.

^{13}C-NMR (100 MHz; CD_3OD): δ= 157.8 (C7), 157.5 (C5), 157.1 (C9a), 146.0. 145.8 (C3’, C4‘), 132.1 (C1’), 119.4 (C6’), 115.9 (C5’), 115.3 (C2’), 102.5 (C9b), 98.4 (C1#), 98.2 (C8), 96.7 (C6), 80.0 (C2), 75.0 (C3#) 74.4 C2#) 73.4 (C5#), 71.3 (C4#), 67.3 (C3), 62.1 (C6#), 29.4 (C4) ppm.

MS (ESI positive):

Ion Formula:	$C_{21}H_{24}O_{11}Na^{+}$ $[M+Na]^{+}$
m/z calculated:	475.12108
m/z experimental:	475.12005
error [ppm]:	2.17

(-)-epicatechin-3‘,5-*O*-α-D-diglucoside[1]

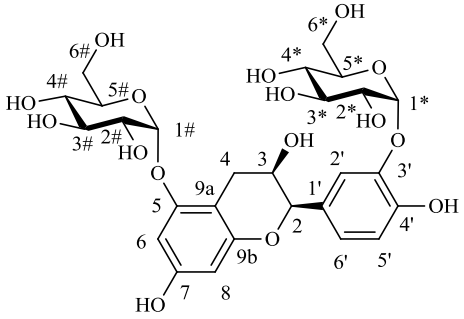

^{1}H-NMR (600 MHz; CD_3OD): δ= 7.43 (d, 1H, *J*= 1.92 Hz, *H*-2‘), 7.07-7.05 (dd, 1H, *J*= 8.31, 1.99 Hz, *H*-6‘), 6.86-6.84 (d, 1H, *J*= 8.24 Hz, *H*-5’) 6.34-6.33 (d, 1H, *J*= 2.28 Hz, *H*-6), 6.08 (d, 1H, *J*= 2.24 Hz, *H*-8), 5.51 (d, 1H, *J*= 3.6 Hz, *H*-1#), 5.35 (d, 1H, *J*= 3.64 Hz, *H*-1*), 4.88 (under Water) (1H, *H*-2), 4.20 (m, 1H, *H*-3), 3.91-3.71 (m, 7H, *H*-3#, *H*-3*, *H*-4*or#, 2*H*-6*, 2*H*-6#), 3.63-3.56 (m, 3H, *H*-2#, *H*-2*, *H*-4*or#,), 3.50-3.42 (m, 2H, *H*-5*, *H*-5#), 3.06-3.05 (dd, 1H, *J*= 17 Hz, 4.6 Hz *H*-4), 2.83-2.78 (dd, 1H, *J*= 17 Hz, 2.8 Hz *H*-4) ppm.

^{13}C-NMR (150 MHz; CD_3OD): δ= 157.9 (C7), 157.5 (C5), 157.1 (C9a), 148.2(C4‘), 146.1 (C3‘), 132.3 (C1’) 123.2 (C5’), 118.1 (C2’), 116.6 (C6’), 102.5 (C9b) 101.4 (C1*), 98.5 (C1#) 98.3 (C8), 96.8 (C6), 79.8 (C2), 75.0. 74.9, 74.4, 74.4 (C3#, C3*, C4#, C4*) 73.5, 73.4 (C2*, C2#) 71.5, 71.4, (C5*, C5#), 67.3 (C3), 62.5, 62.1 (C6*, C6#), 29.5 (C4) ppm.

The spectra reveal the presence of a second, uncharacterized product, possibly a regioisomer.

5 A little tool to perform the direct linear plot analysis

Regrettably we did not come up with a smart sounding acronym.

Notes: The programm is written in Python 3.4.

The input file is a .txt file. Each line contains a pair of values separated by at least one space: The first value is the starting concentration, the second value the observed initial reaction velocity. The values need to contain a comma: eg.: 0,23 or 10,00. The tool is started by entering the directory of the input file, and generates an output file in the same directory with the median K_M and v_{max} value at the end.

```
import os
from shutil import copyfile
in_dir1 = os.path.normpath(input("Enter input file directory. column A [S0], column B [Vini]"))
# Make sure your numbers all contain a comma!! Else it crashes during float conversion
f_in1 = open(in_dir1, "r")
rename1 = in_dir1.split(".")
f_out1 = open(rename1[0]+"_out."+rename1[1], "a")

f_out1.write("[S0]          [V0]" + "\n")
ln = 1

raw = []
num = []

parameters ={}
for line in f_in1:
        f_out1.write(line)
        raw = line.split()
        a = 0
        print (raw)

        for thing in raw:
                num = thing.split(",")
                if a == 0:
                        s_out = float(num[0]+"."+num[1])
                        a = 1
                else:
                        v_out = float(num[0]+"."+num[1])
        parameter = [ln, s_out, v_out]
        #print (parameter)
        parameters.update({ln : parameter})
        ln = ln + 1
print (parameters)
para_count = 0
for parameter_set in parameters:
        para_count = para_count +1
print (para_count)

count = 0
base = 0
s = 1
```

```
v = 2
list_of_all_KM = []
list_of_all_Vmax = []
while base < para_count:
        base = base + 1
        count = 0
        while count + base < para_count:
                count = count + 1
                set_a = parameters[base]
                bc = base + count
                #print (bc)
                set_b = parameters[bc]
                #print (set_a)
                #print (set_b)
                KM = (set_b[v]-set_a[v])/( (set_a[v]/set_a[s]) - (set_b[v]/set_b[s]) )
                Vmax = KM*(set_a[v]/set_a[s]) + set_a[v]
                print (str(base)+","+str(bc))
                print (KM)
                print (Vmax)
                f_out1.write(str(base)+","+str(bc)+"\n"+"KM:  "+str(KM)+"\n"+"Vmax:  "+str(Vmax)+"\n")
                list_of_all_KM.append(KM)
                list_of_all_Vmax.append(Vmax)
print ("KM-values:")
print (list_of_all_KM)
f_out1.write("KM-values:" + "\n")
for value in list_of_all_KM:
        f_out1.write(str(value)+"   ")
#f_out1.write(list_of_all_KM)
f_out1.write("  "+ "\n")
print ("Vmax-values:")
print (list_of_all_Vmax)
f_out1.write("Vmax-values:" +"\n")
for value in list_of_all_Vmax:
        f_out1.write(str(value)+"   ")

f_out1.write("  "+ "\n")
list_of_all_KM.sort()
print ("KM-values sorted:")
print (list_of_all_KM)
f_out1.write("KM-values sorted:" + "\n")
for value in list_of_all_KM:
        f_out1.write(str(value)+"   ")
f_out1.write("  "+ "\n")
list_of_all_Vmax.sort()
print ("Vmax-values sorted:")
print (list_of_all_Vmax)
f_out1.write("Vmax-values sorted:" +"\n")
for value in list_of_all_Vmax:
        f_out1.write(str(value)+"   ")

f_out1.write("  "+ "\n")

print (len(list_of_all_KM))
f_out1.write("  "+ "\n")

if len(list_of_all_KM)%2==0:
```

```
        print ("even")
        n = (len(list_of_all_KM))/2
        med_km = (list_of_all_KM[int(n)]+list_of_all_KM[int(n-1)])/2
        print ("Median KM:")
        print (med_km)
        f_out1.writelines("Median KM:"+"\n")

        f_out1.writelines(str(med_km)+"\n")

else :
        print ("odd")
        n = ((len(list_of_all_KM))+1)/2 - 1
        n = int(n)
        med_km = (list_of_all_KM[n])
        print ("Median KM:")
        print (med_km)
        f_out1.writelines("Median KM:"+"\n")

        f_out1.writelines(str(med_km)+"\n")

f_out1.write("  "+ "\n")

if len(list_of_all_Vmax)%2==0:
        print ("even")
        n = len(list_of_all_Vmax)/2
        med_Vmax = (list_of_all_Vmax[int(n)]+list_of_all_Vmax[int(n-1)])/2
        print ("Median Vmax:")
        print (med_Vmax)
        f_out1.writelines("Median Vmax:"+"\n")

        f_out1.writelines(str(med_Vmax)+"\n")

else :
        print ("odd")
        n = ((len(list_of_all_Vmax))+1)/2-1
        n = int(n)
        med_Vmax = (list_of_all_Vmax[n])
        print ("Median Vmax:")
        print (med_Vmax)
        f_out1.writelines("Median Vmax:"+"\n")

        f_out1.writelines(str(med_Vmax)+"\n")

f_out1.write("  "+ "\n")

f_in1.close()
f_out1.close()
```

6 References

1. M. Kraus, C. Grimm and J. Seibel, *Chembiochem*, 2016, **17**, 33-36.
2. M. Kraus, J. Gorl, M. Timm and J. Seibel, *Chem Commun (Camb)*, 2016, **52**, 4625-4627.
3. A. J. McCoy, R. W. Grosse-Kunstleve, P. D. Adams, M. D. Winn, L. C. Storoni and R. J. Read, *Journal of applied crystallography*, 2007, **40**, 658-674.
4. P. D. Adams, P. V. Afonine, G. Bunkoczi, V. B. Chen, I. W. Davis, N. Echols, J. J. Headd, L. W. Hung, G. J. Kapral, R. W. Grosse-Kunstleve, A. J. McCoy, N. W. Moriarty, R. Oeffner, R. J. Read, D. C. Richardson, J. S. Richardson, T. C. Terwilliger and P. H. Zwart, *Acta Crystallogr D*, 2010, **66**, 213-221.
5. P. Emsley, B. Lohkamp, W. G. Scott and K. Cowtan, *Acta crystallographica. Section D, Biological crystallography*, 2010, **66**, 486-501.
6. R. Eisenthal and A. Cornish-Bowden, *Biochemical Journal*, 1974, **139**, 715-720.